



Introduction to Electron Backscatter Diffraction

**Electron Backscatter Diffraction
(EBSD) is a technique which allows
crystallographic information to be
obtained from the samples in the
Scanning Electron Microscope
(SEM)**



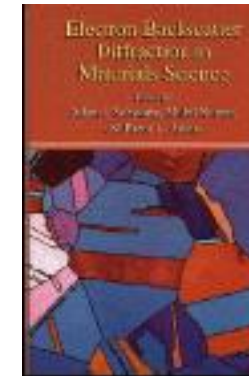
Electron Backscatter Diffraction in Materials Science

Edited by Adam J. Schwartz - *Lawrence Livermore National Laboratory, CA, USA*

Mukul Kumar - *Lawrence Livermore National Laboratory, CA, USA*

Brent L. Adams - *Brigham Young University, Provo, UT, USA*

Kluwer Academic/Plenum Publishers, 2000

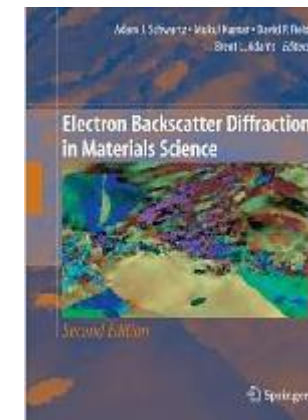


Electron Backscatter Diffraction in Materials Science

Editors:

Adam J. Schwartz, Mukul Kumar, Brent L. Adams, David P. Field

Springer, 2009





European
Funds
Knowledge Education Development

European Union
European Social Fund



MAREK FARYNA

**DYFRAKCYA ELEKTRONÓW
WSTECZNIE ROZPROSZONYCH
W SKANINGOWYM MIKROSKOPIE
ELEKTRONOWYM**

ELEMENTY TEORII I PRAKTYKI

 **AGH**
Akademia Górniczo-Hutnicza im. Stanisława Staszica w Krakowie

KATOWICE 2012



Outline

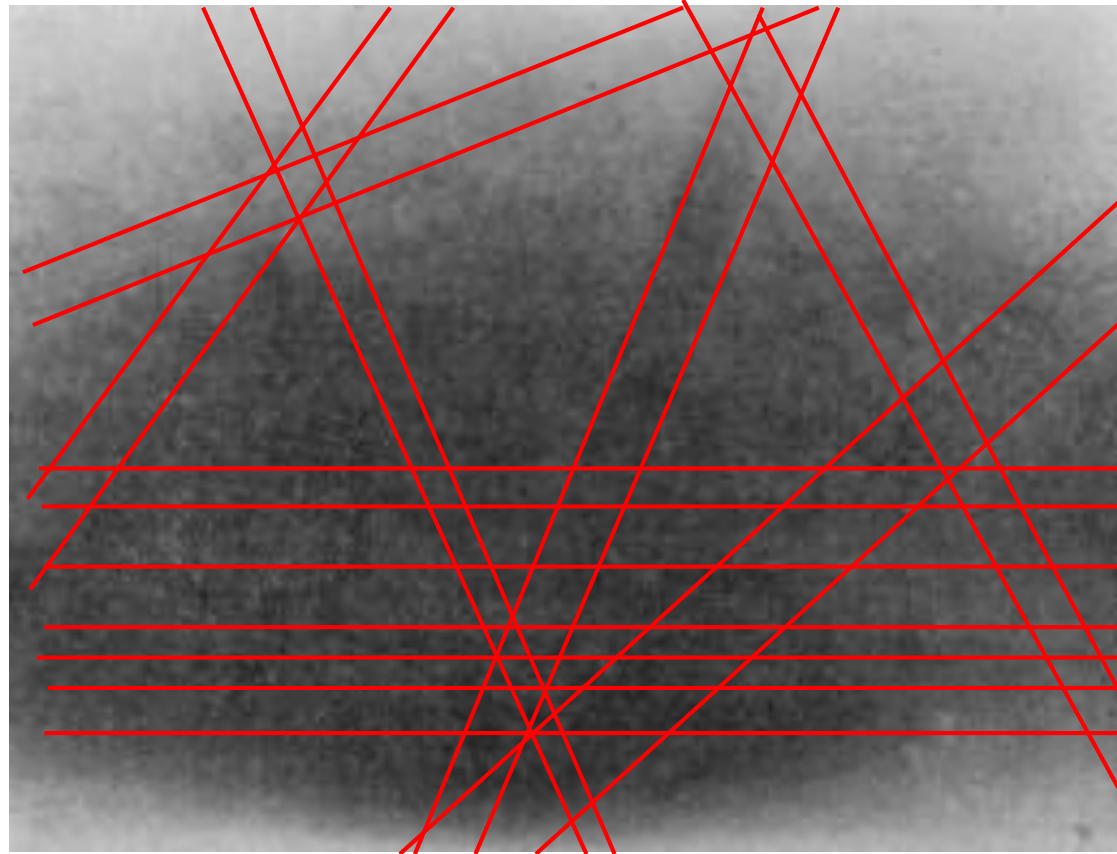
- 1. Introduction – a little bit of history**
- 2. EBSD – the basics**
- 3. EBSD – solving the pattern**
- 4. Information available from EBSD**
- 5. A few examples**
- 6. Conclusions**



1. Introduction – a little bit of history



A gas discharge beam of 50 keV electrons was directed onto a cleavage face of calcite at a grazing incidence of 6° . Patterns were also obtained from cleavage faces of mica, topaz, zinc blende and a natural face of quartz.



**Shoji Nishikawa
and Seishi
Kikuchi
*The Diffraction of
Cathode Rays by
Calcite***

***Proc. Imperial Academy (of
Japan) 4 (1928!!!) 475-477***



Point analysis

EBSD - Electron Backscatter Diffraction

EBSP - Electron Backscatter Pattern (J.A.Venables)

BKP - Backscatter Kikuchi Pattern

Scan analysis

COM - Crystal Orientation Mapping

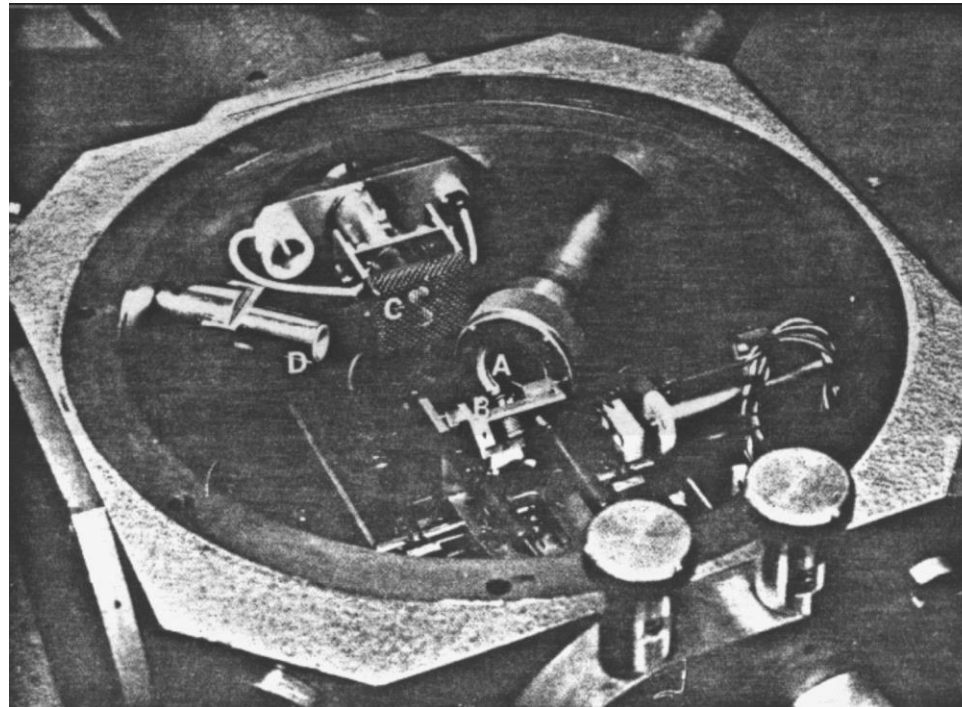
ACOM - Automatic Crystal Orientation Mapping (R.Schwarzer)

OIM[®] - Orientation Imaging Microscopy (TexSEM Laboratories trademark)



Introduction of the EBSD technique to the SEM

J. A. Venables and C. J. Harland (1973) „Electron Back Scattering Patterns – A New Technique for Obtaining Crystallographic Information in the Scanning Electron Microscope”, *Philosophical Magazine*, **2**, 1193-1200.



**Arrangement of the specimen chamber in the Cambridge Stereoscan:
A – Screen, B – Specimen, C – Electron detector, D – X-ray detector**

Project WND-POWR.03.02.00-00-1043/16

International interdisciplinary PhD Studies in Materials Science with English as the language of instruction

Project co-financed by the European Union within the European Social Funds



EBSP in the SEM recorded on film

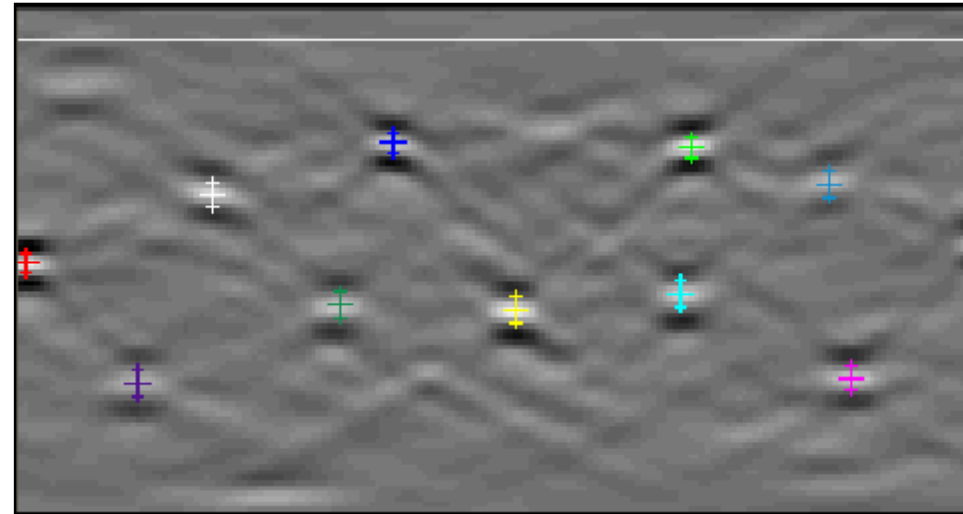
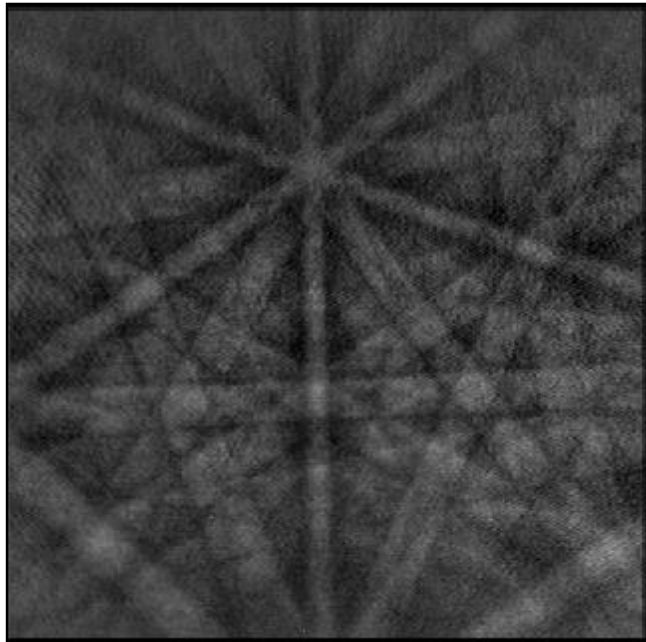
D. J. Dingley (1984) „Diffraction From Sub-Micron Areas Using Electron Backscattering In A Scanning Electron Microscope”, *Scanning Electron Microscopy*, **11**, 569-575

Film replaced by TV camera

D. J. Dingley, M. Longdon, J. Wienbren and J. Alderman (1987) „On-line Analysis of Electron Backscatter Diffraction Patterns, Texture Analysis of Polysilicon”, *Scanning Electron Microscopy* , **11**, 451-456.



N. C. Krieger-Lassen, K. Conradsen and D. Juul-Jensen (1992)
„Image Processing Procedures for Analysis of Electron Back
Scattering Patterns”, *Scanning Microscopy*, 6, 115-121.



Hough Transform



Full automation

K. Kunze, S. I. Wright, B. L. Adams, and D. J. Dingley, 1993
„Advances in Automatic EBSP Single Orientation Measurements”,
Textures Microstructures, 20, 41-54.

Phase ID

D. J. Dingley and K. Baba-Kishi (1986) „Use of Electron Backscatter Diffraction Patterns for Determination of Crystal Symmetry Elements”, *Scanning Electron Microscopy*, II, 383-391.

D. J. Dingley, R. Mackenzie and K. Baba-Kishi (1989) „Application of Backscatter Kikuchi Diffraction for Phase Identification and Crystal Orientation Measurements in Materials”, *Microbeam Analysis*, ed. P.E.Russell, San Francisco Press, 435-436.

J. R. Michael and R. P. Goehner (1993) „Crystallographic Phase Identification in the Scanning Electron Microscope: Backscattered Electron Kikuchi Patterns Imaged with a CCD-Based Detector”, *MSA Bulletin*, **23**, 168-175.

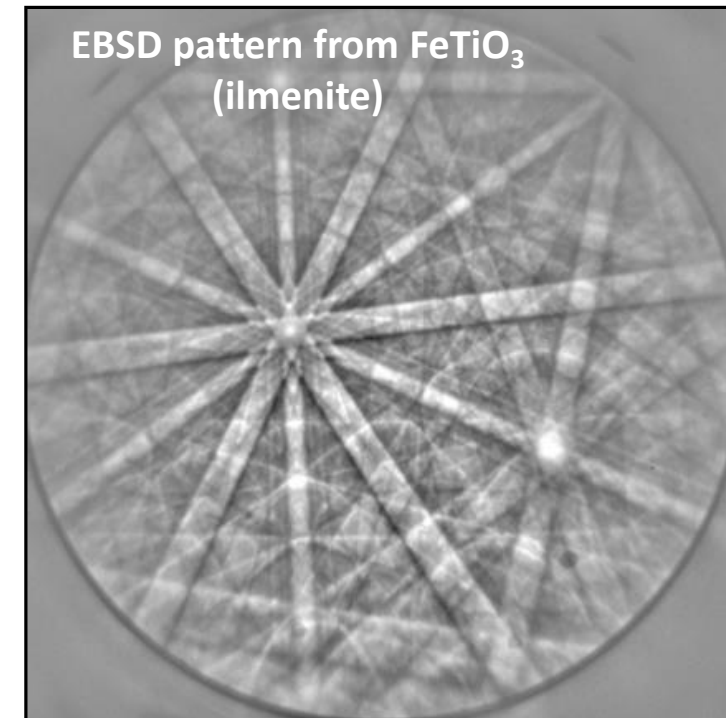
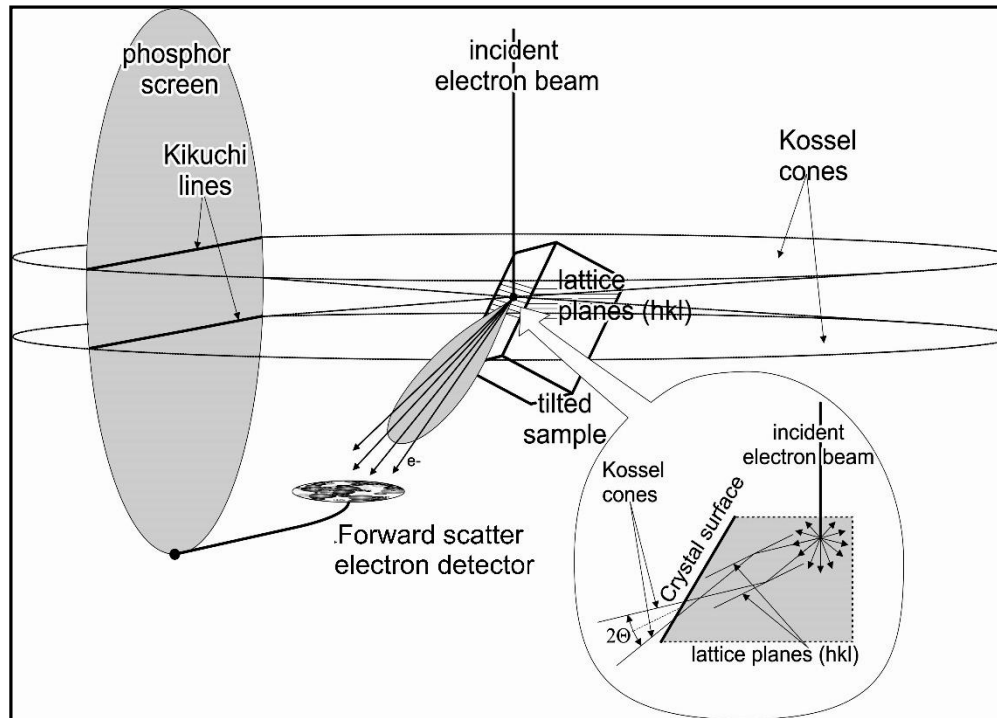


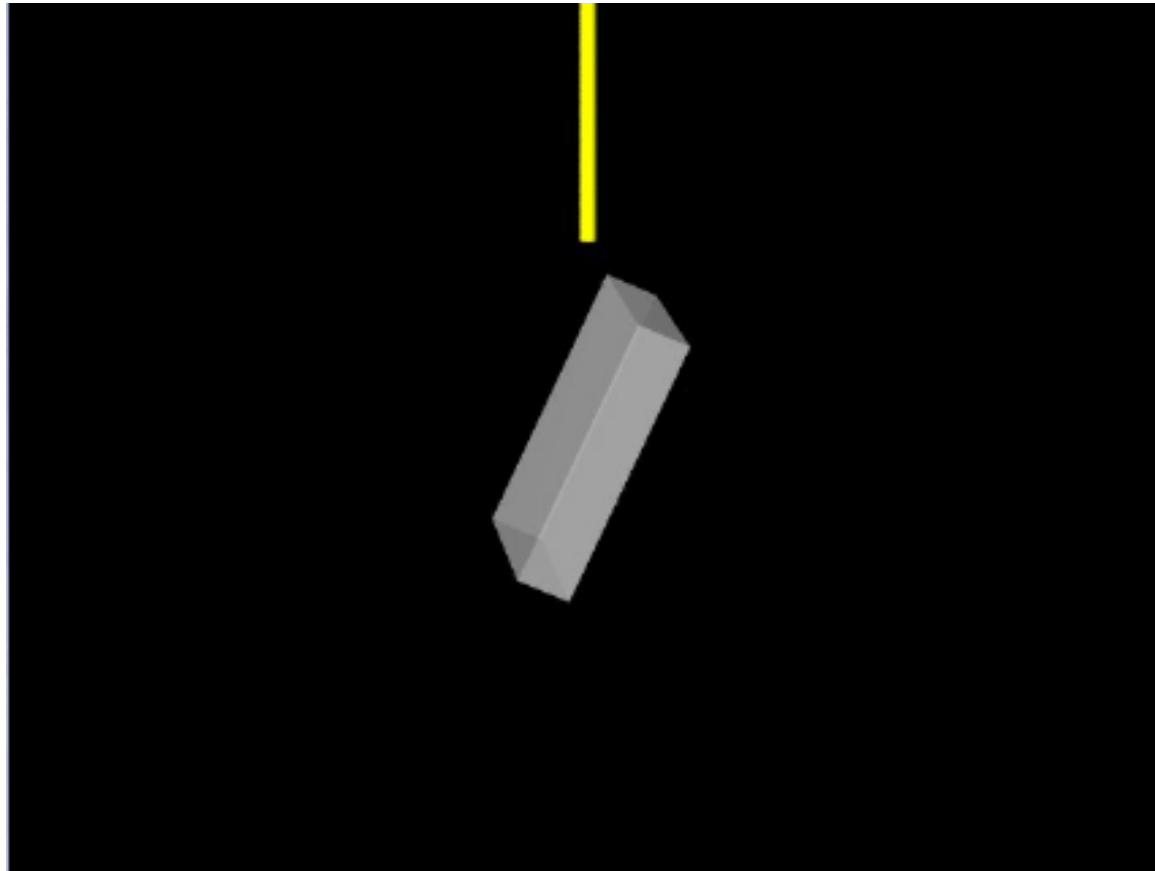
2. EBSD – the basics



Electron Backscatter Diffraction

- Backscatter electrons interact with the crystal and form for each lattice plane two diffraction cones (so called „Kossel cones” with VERY large conical angles)
- Intersections of diffraction cones with the phosphor screen become visible as a pair of parallel lines – the „Kikuchi bands”

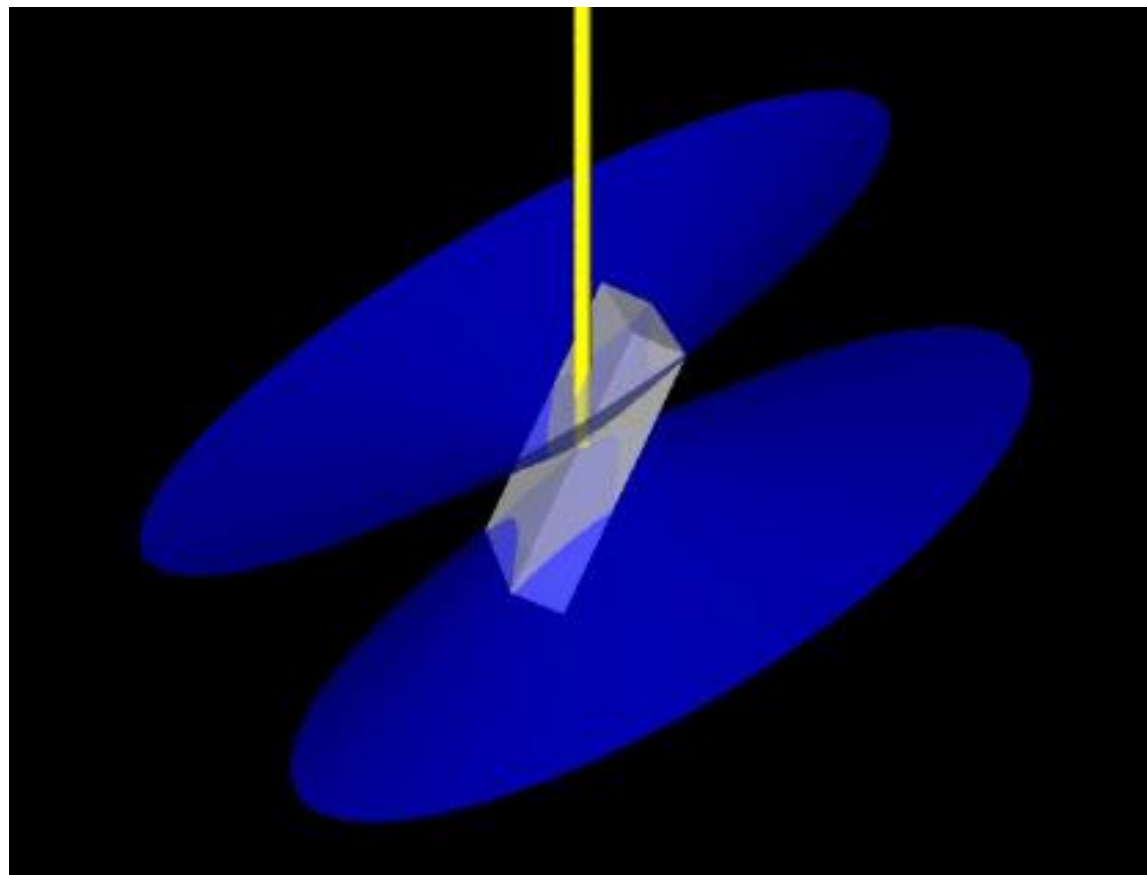
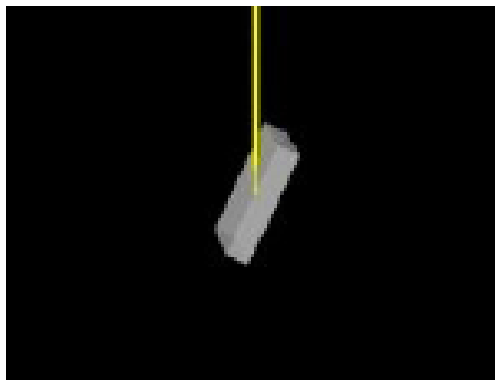


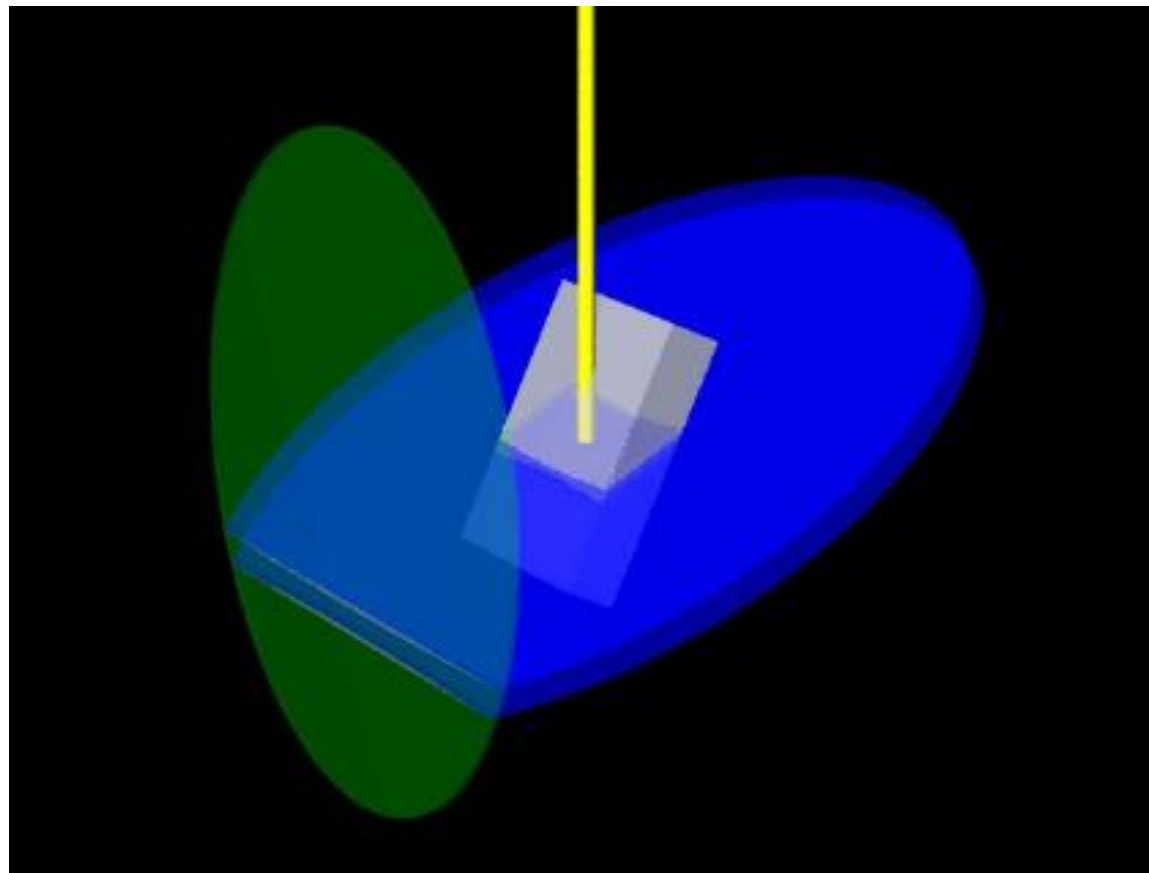
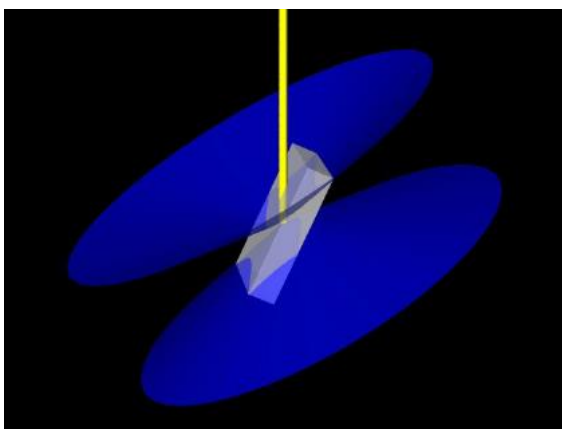
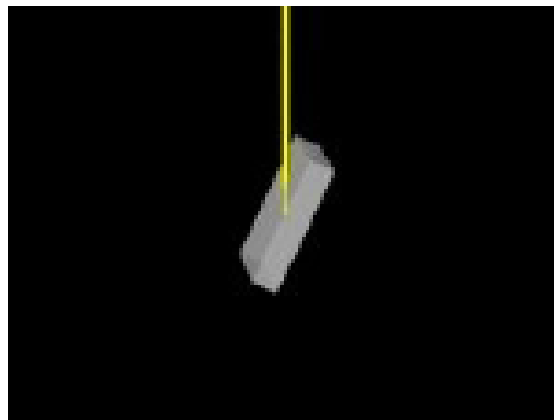


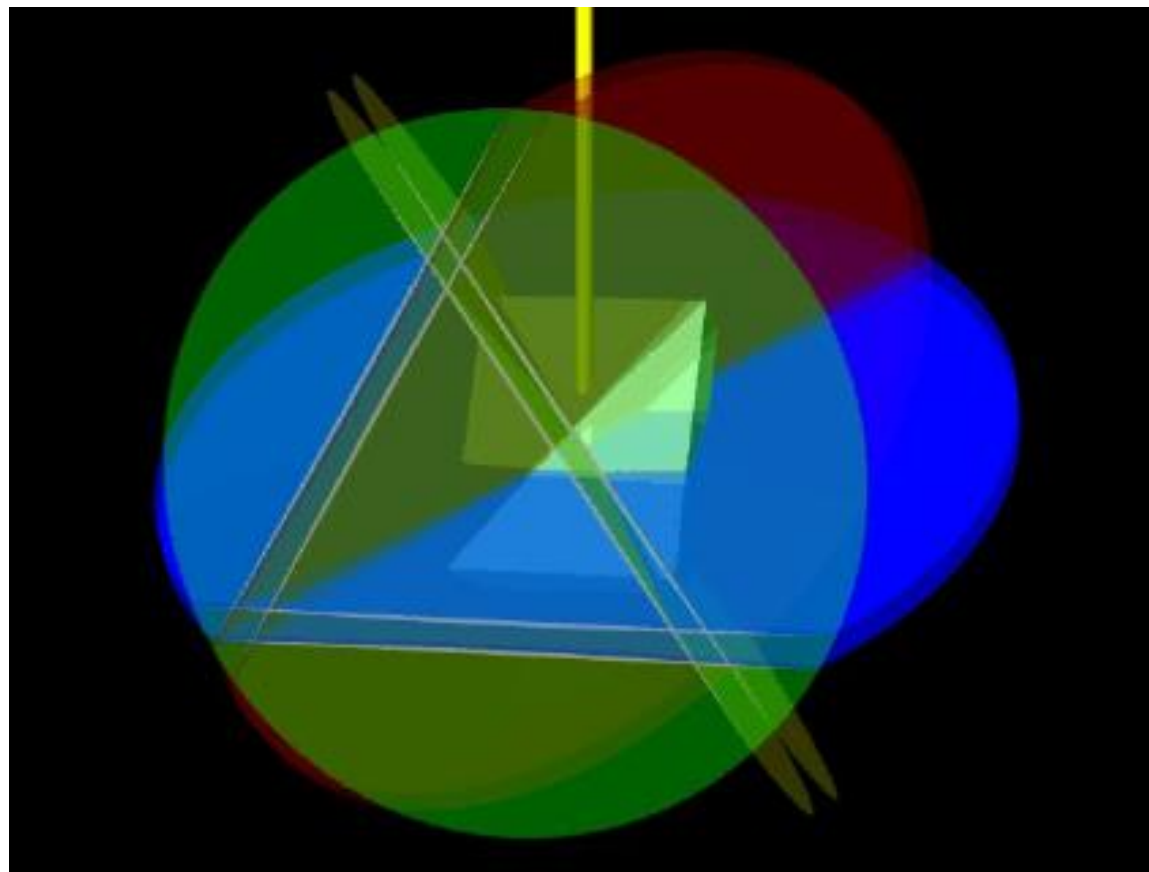
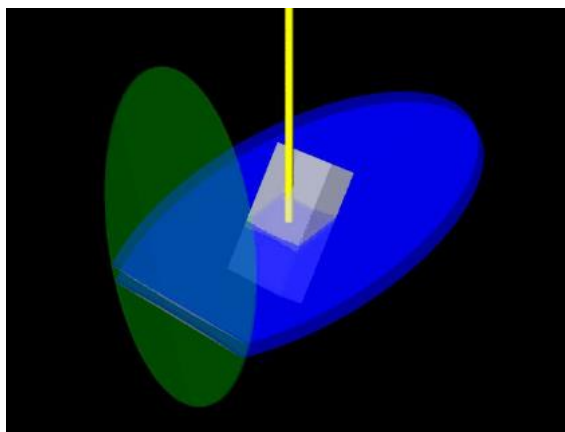
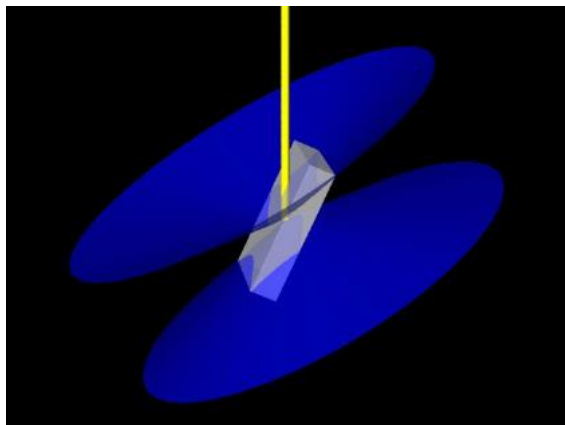
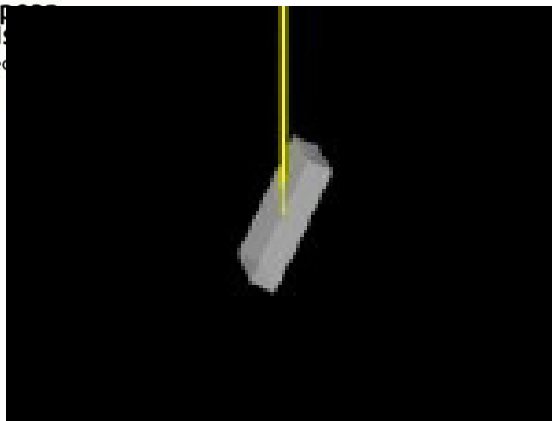
Project WND-POWR.03.02.00-00-1043/16

International interdisciplinary PhD Studies in Materials Science with English as the language of instruction

Project co-financed by the European Union within the European Social Funds



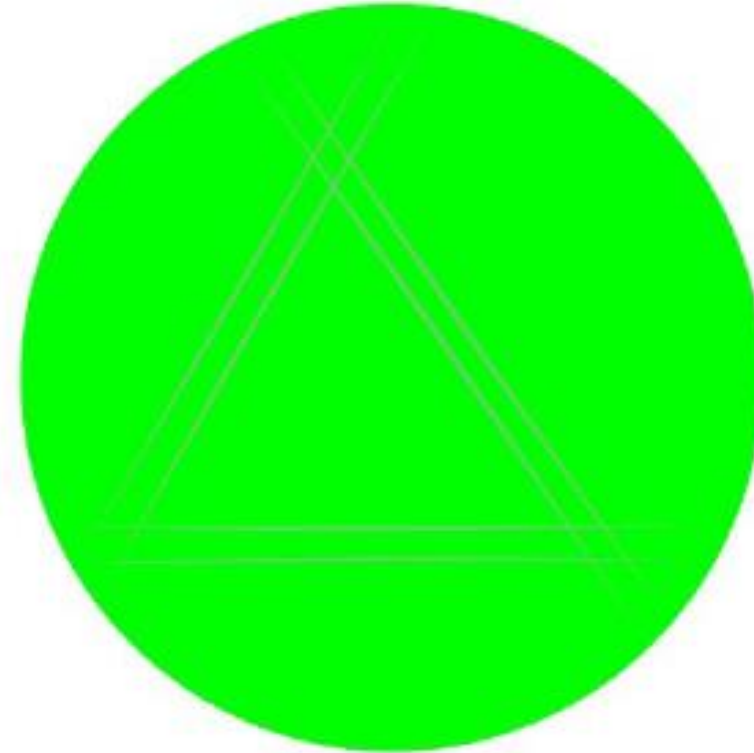
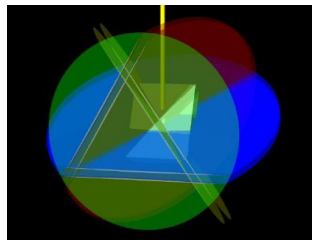
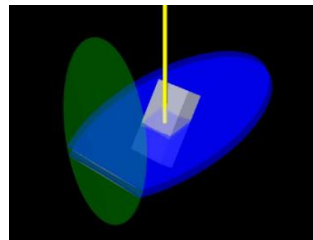
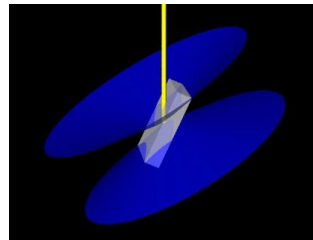
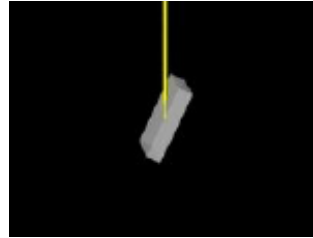




Project WND-POWR.03.02.00-00-1043/16

Interdisciplinary PhD Studies in Materials Science with English as the language of instruction

Project co-financed by the European Union within the European Social Funds



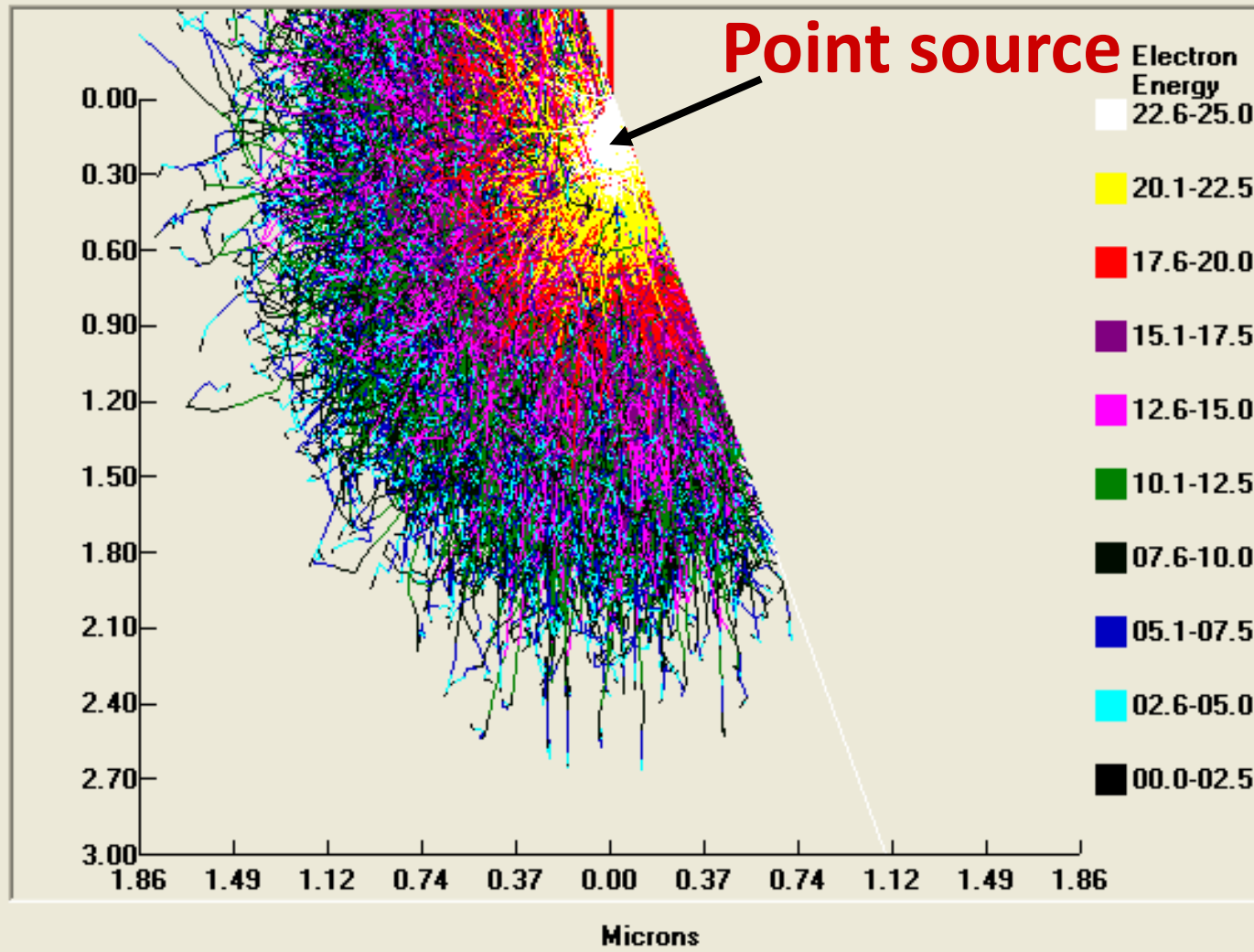
Project WND-POWR.03.02.00-00-1043/16

Interdisciplinary PhD Studies in Materials Science with English as the language of instruction

Project co-financed by the European Union within the European Social Funds



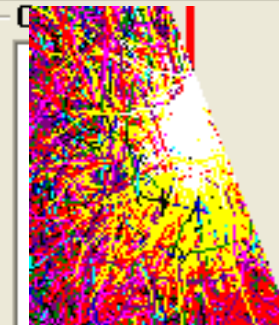
Interaction Volume Simulation



Sample Conditions

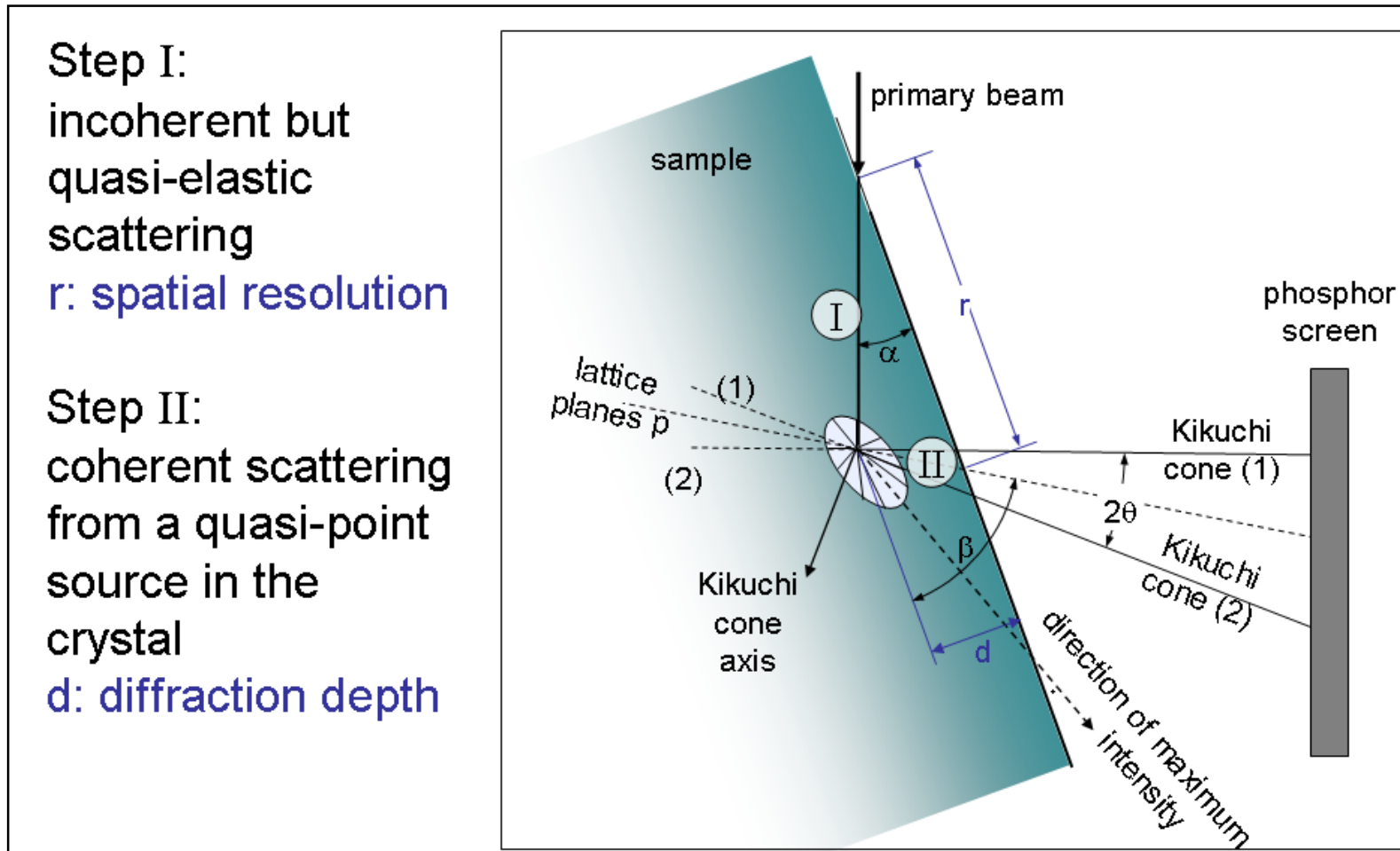
kV: 25.0 Tilt: 70
No. Trajectories: 30000
B.S. Coefficient: 0.5182

Bulk Ni





Spatial resolution of EBSD

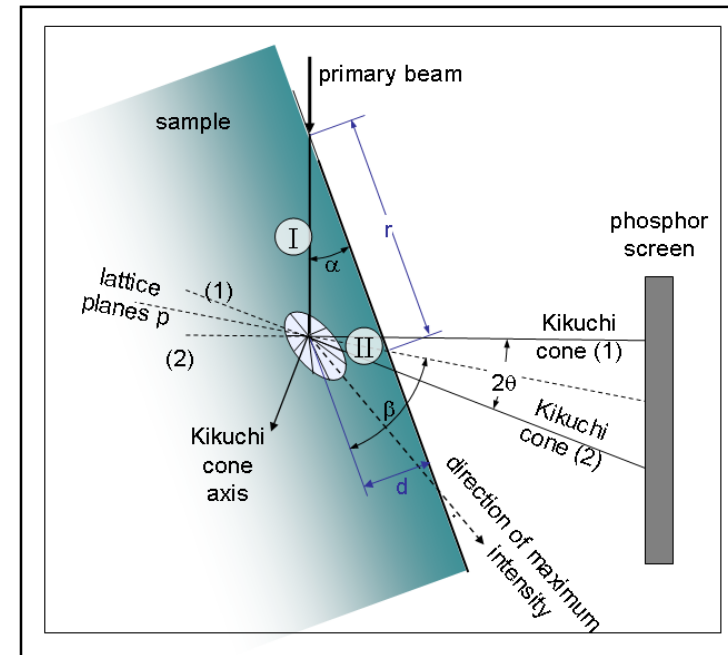
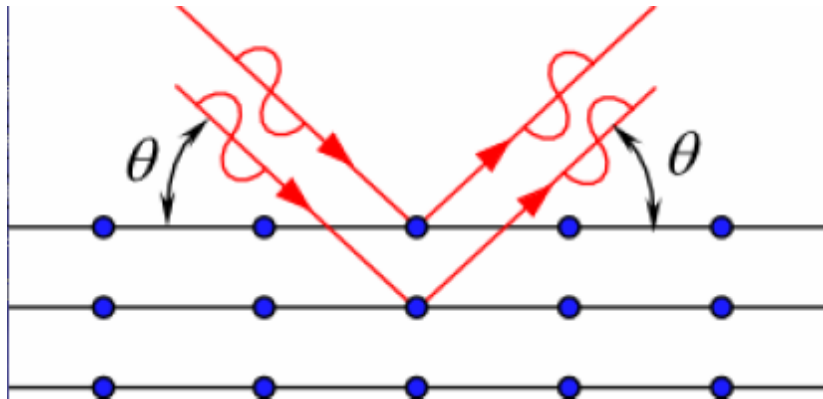




Step 1: electrons enter the material and are quasi-elastically but incoherently scattered. This leads to a wide directional distribution of electrons emerging from a very small volume in the crystal.

This process can be regarded as the formation of an electron source inside the crystal („a point source”). These electrons may now be diffracted according to the Bragg equation.

$$\lambda = 2d_{hkl} \sin \theta$$



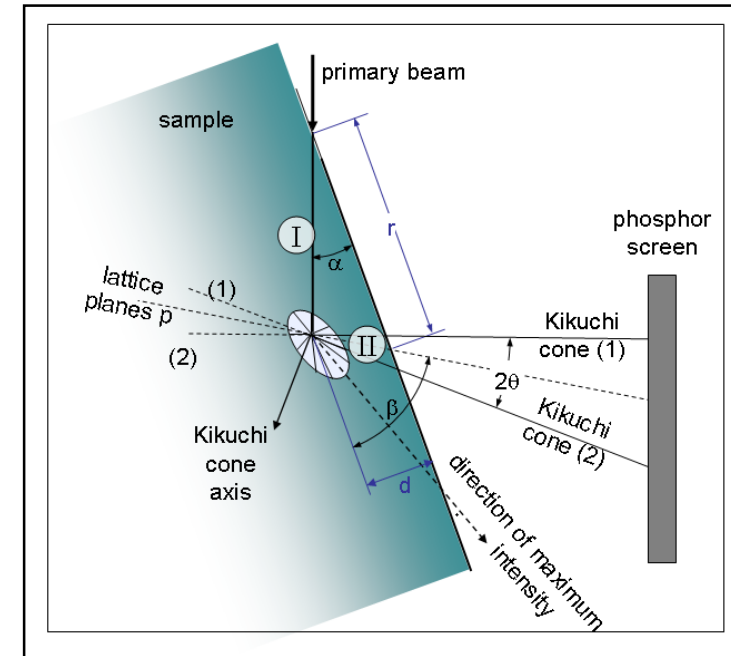


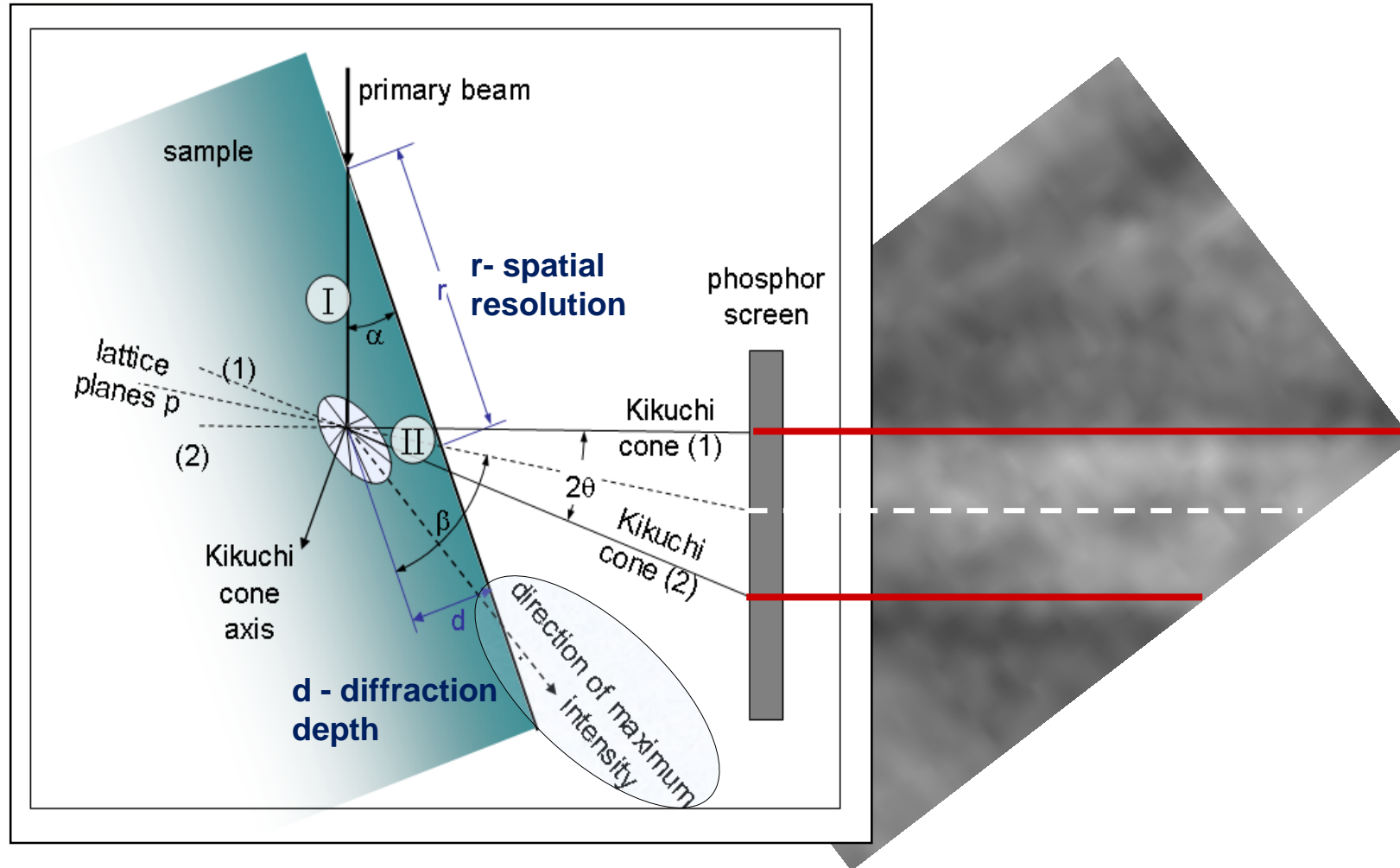
Step 2: diffracted electrons emerging from „the point source” inside of the crystal are coherently scattered (diffracted) by the crystal lattice.

They form **pairs of cones centred about the lattice plane normal vectors with the operating angle $180^\circ - 2\theta$ and the angle of 2θ between them.**

Since the Bragg angle is rather small (in order of 1° for 15 kV accelerating voltage) – the cones are very large. Each pair of cones intersects phosphor screen in almost straight and parallel lines.

The distance between the two lines is approximately proportional to $\tan(\theta)$, while the position of the centre line can be understood as the **gnomonic projection** of the diffraction plane onto the observation screen.





A very surface sensitive technique

Project WND-POWR.03.02.00-00-1043/16

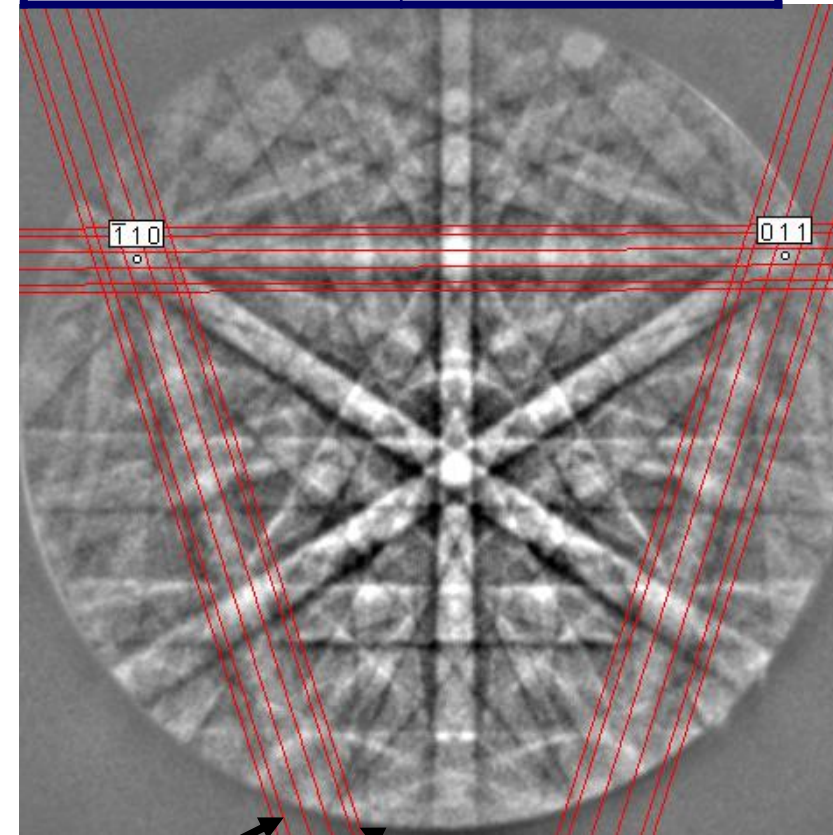
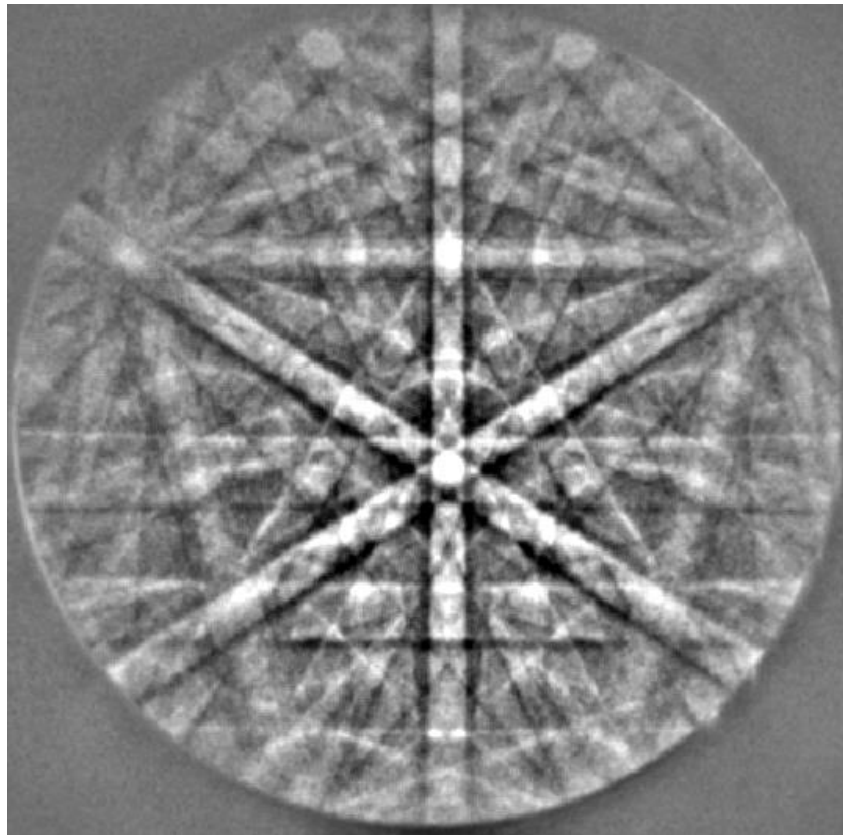
International interdisciplinary PhD Studies in Materials Science with English as the language of instruction

Project co-financed by the European Union within the European Social Funds



Band width is inversely proportional to d-spacing

| | |
|-----------------|----------------|
| Si 1-1-1 | 3,135 A |
| Si 3-3-3 | 1,045 A |
| Si 4-4-4 | 0,784 A |

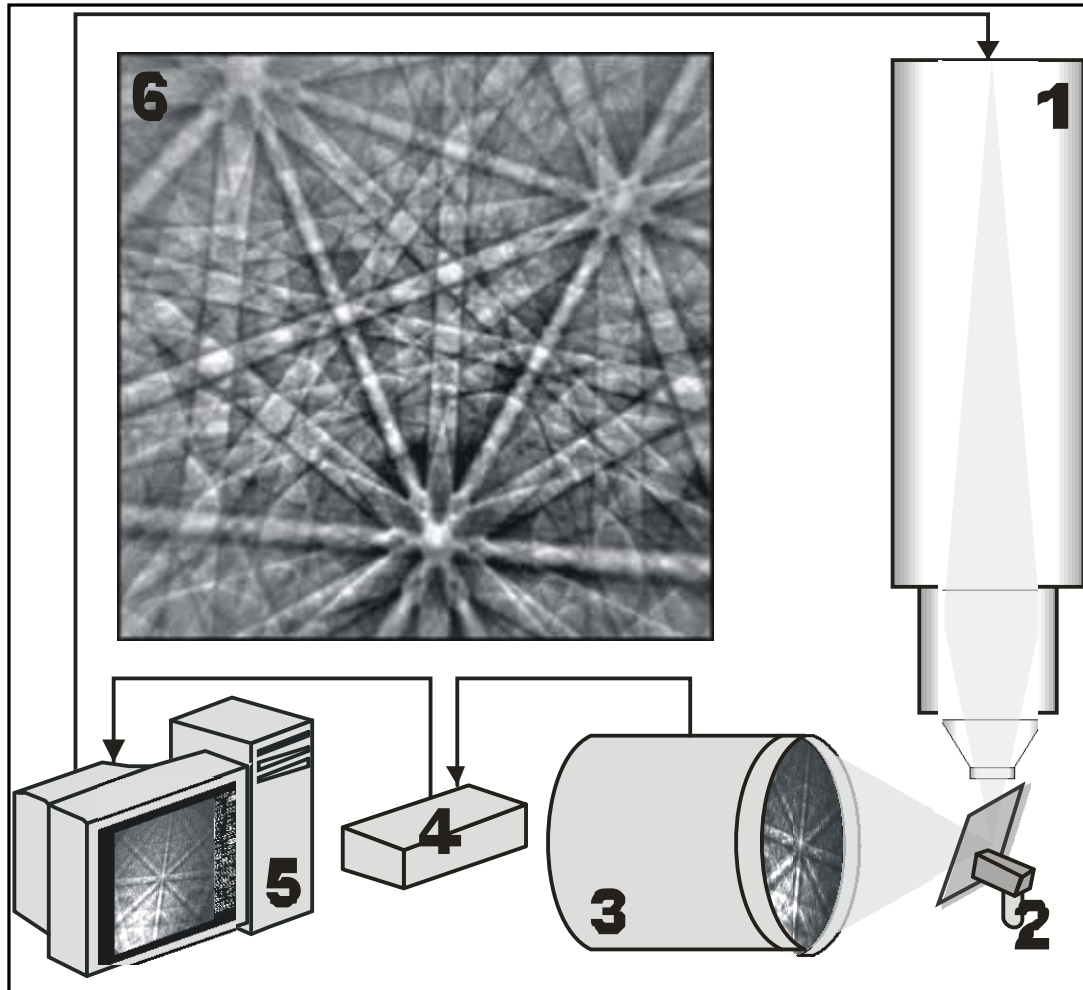


3-3-3 **1-1-1** **4-4-4**

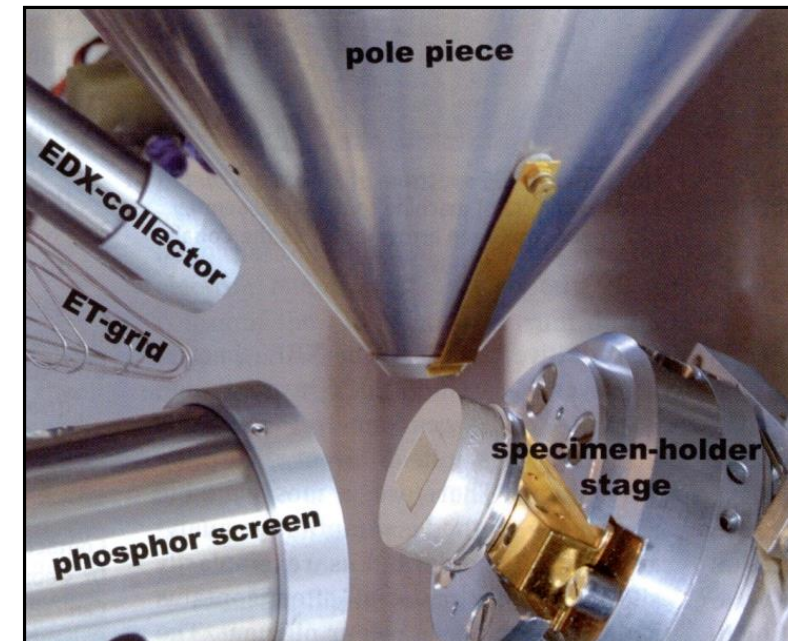
Project WND-POWR.03.02.00-00-1043/16

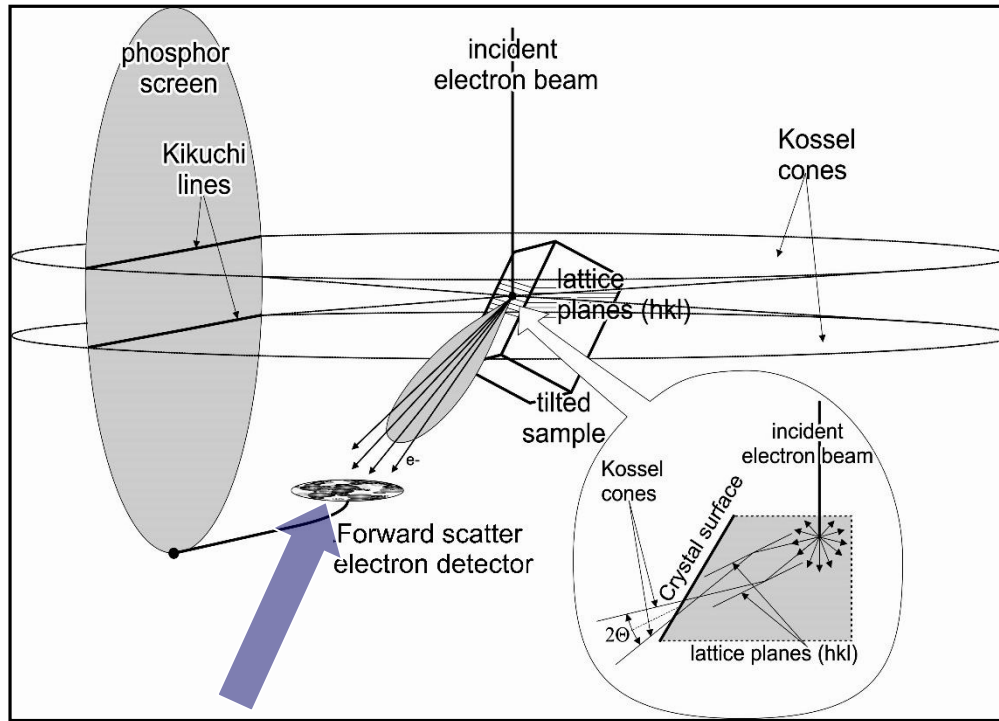
International interdisciplinary PhD Studies in Materials Science with English as the language of instruction

Project co-financed by the European Union within the European Social Funds

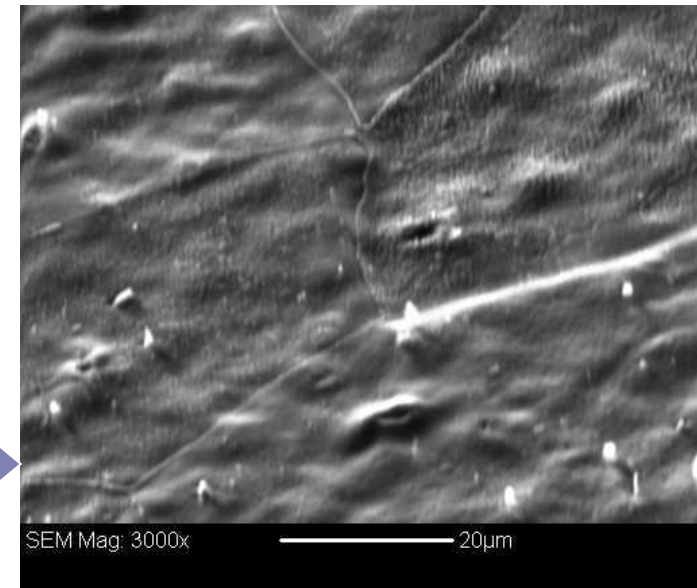


1. SEM
2. A sample tilted at 70° from the horizontal
3. A phosphor screen which is fluoresced by electrons from the sample to form the diffraction pattern. A sensitive charge coupled device (CCD) video camera for viewing the diffraction pattern on the phosphor screen image processor
4. Image processor (at present embedded in the CCD camera)
5. A computer to control EBSD experiments, analyze the diffraction pattern and process and display the results
6. Diffraction pattern





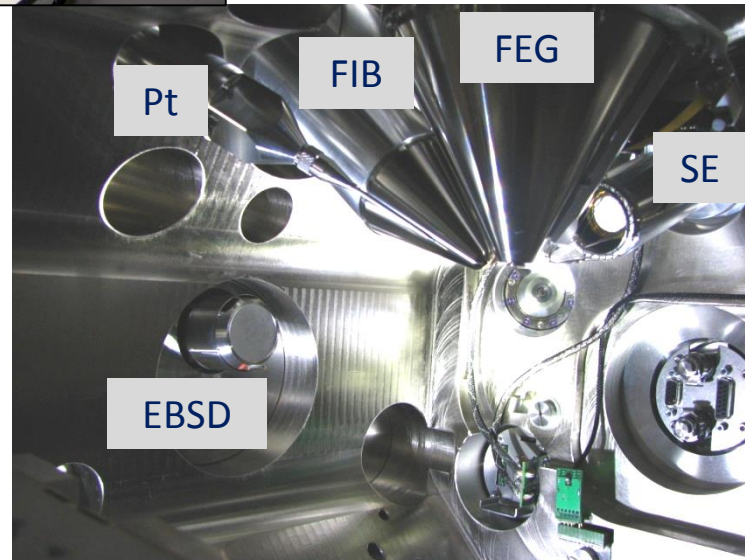
An optional electron solid state detector mounted below the phosphor screen for electrons scattered in the forward direction from the sample





➤ **Post-processing of diffraction data can produce a lot of additional information like lattice strain, size, shape and type of boundaries of grains etc.**

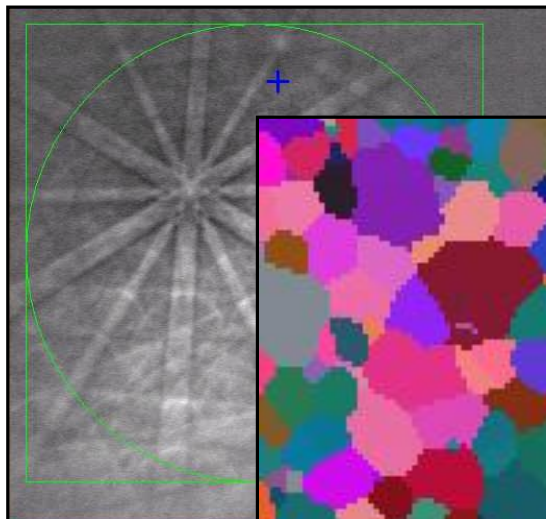
➤ **The results are „comparable” with X-ray diffraction experiments but have advantage of the local assignment!**



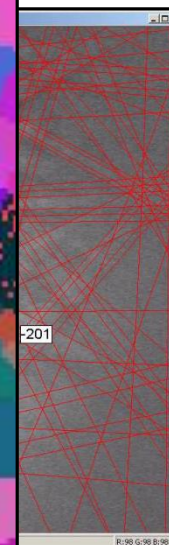
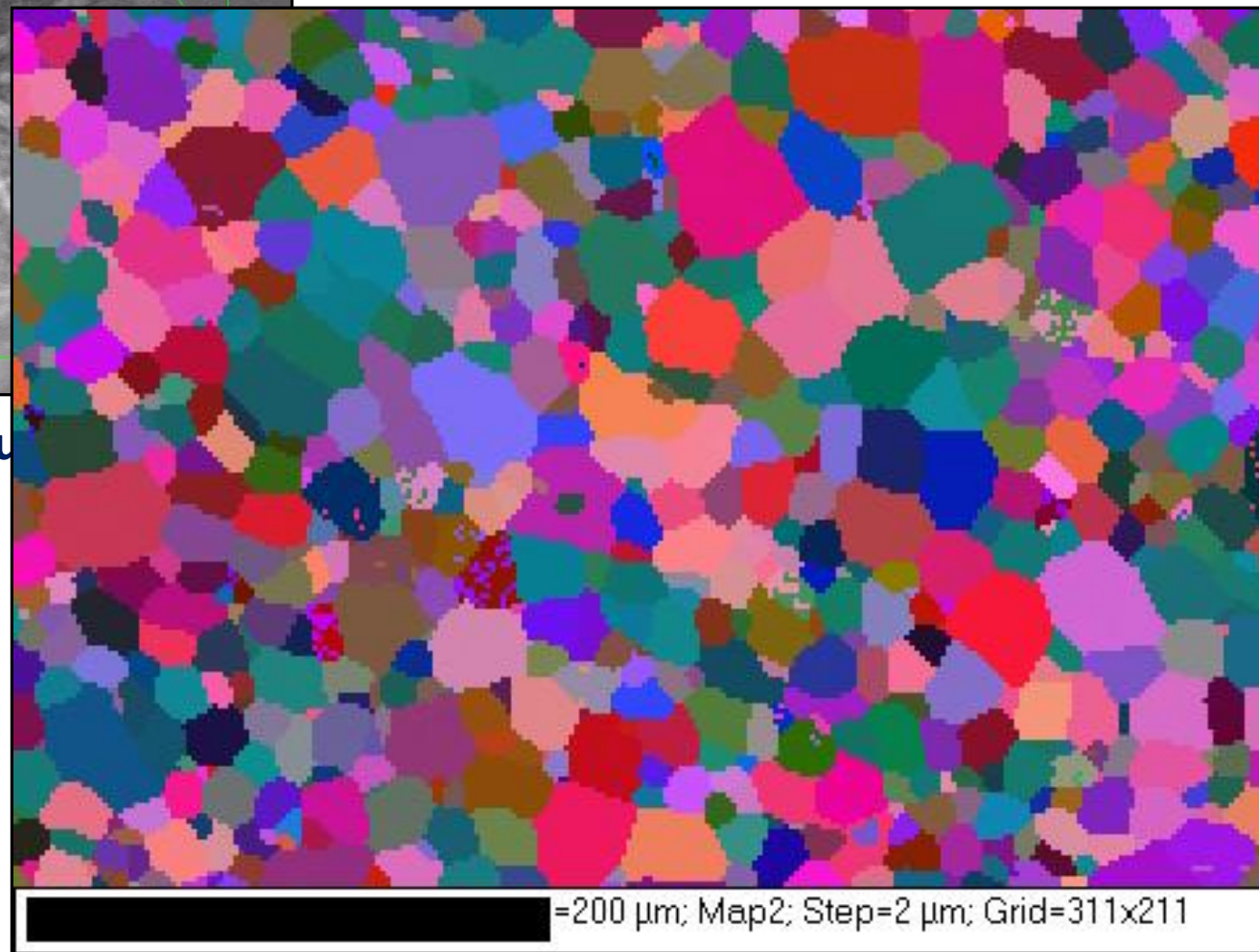
Project WND-POWR.03.02.00-00-1043/16



How to get orientation map?



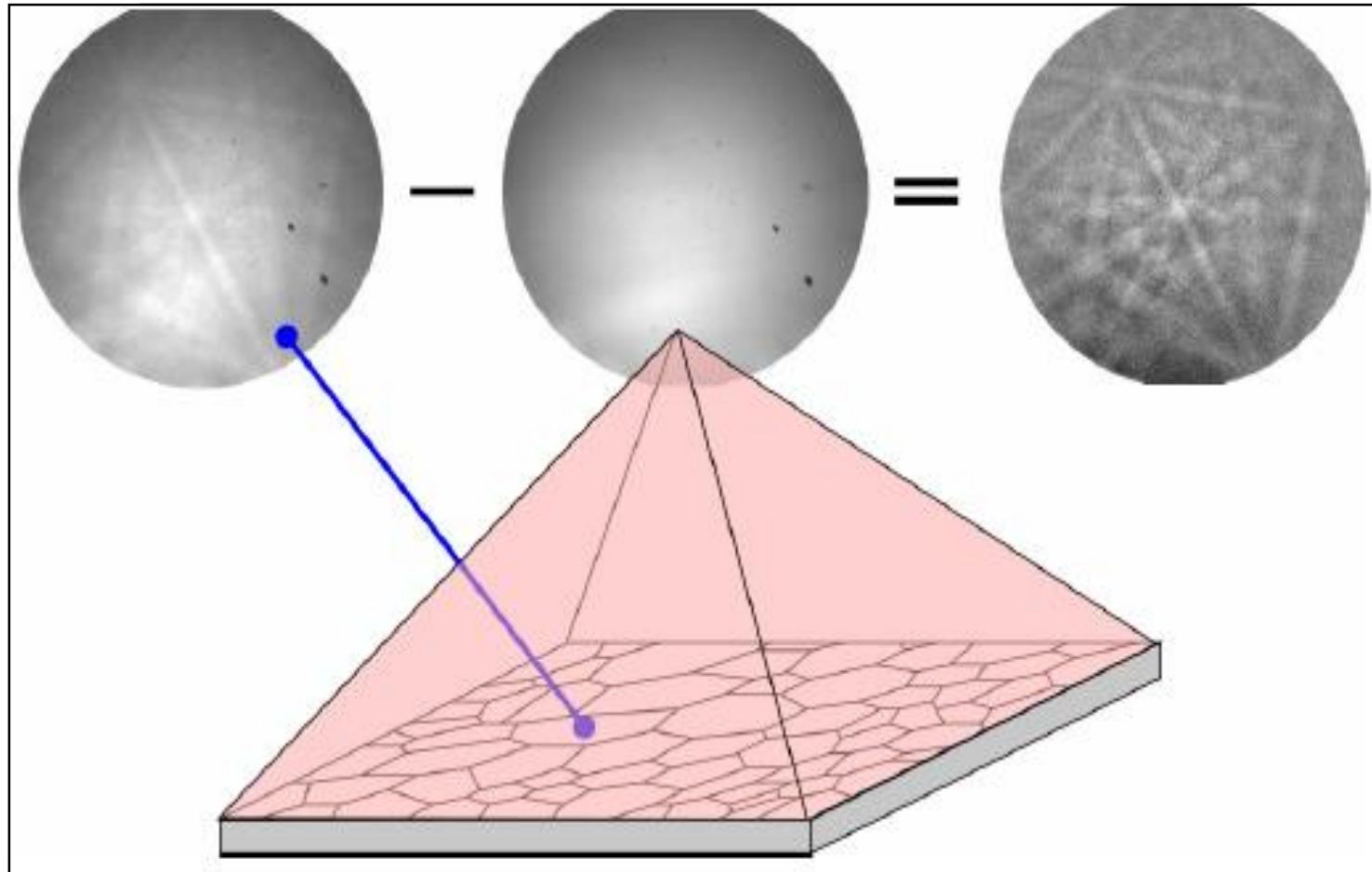
Acqu



tern



Acquisition – Background subtraction



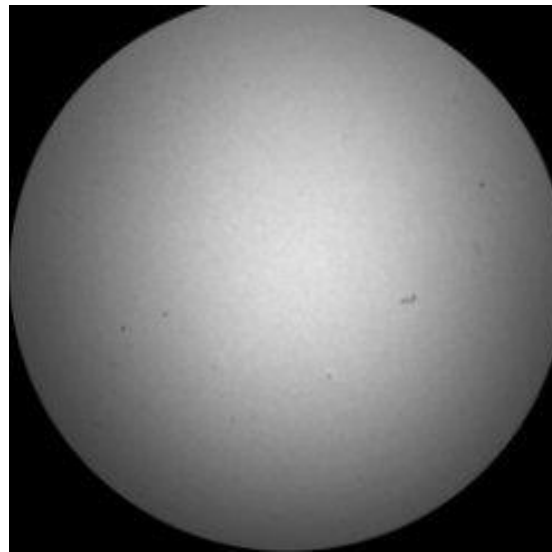
Project WND-POWR.03.02.00-00-1043/16

International interdisciplinary PhD Studies in Materials Science with English as the language of instruction

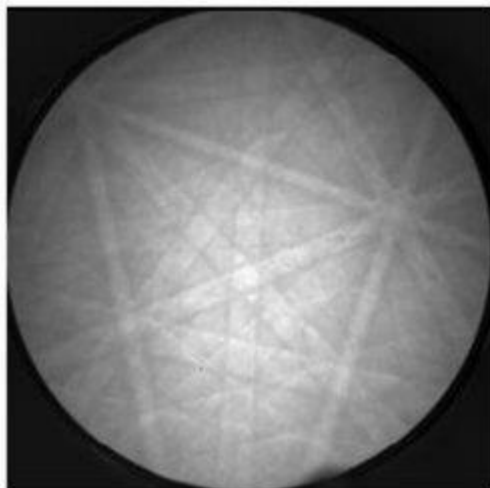
Project co-financed by the European Union within the European Social Funds



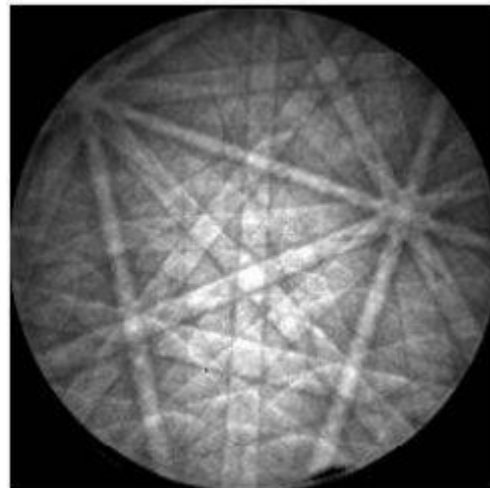
Background



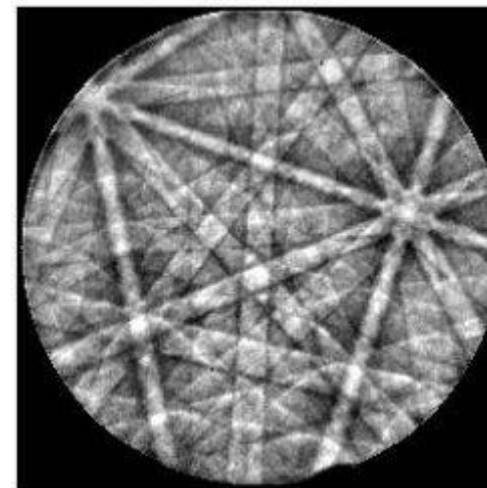
Original pattern



Background subtraction



Background division



Project WND-POWR.03.02.00-00-1043/16

International interdisciplinary PhD Studies in Materials Science with English as the language of instruction

Project co-financed by the European Union within the European Social Funds



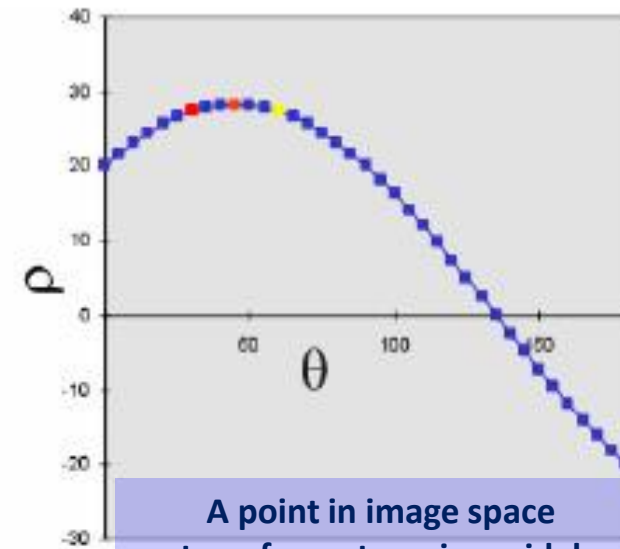
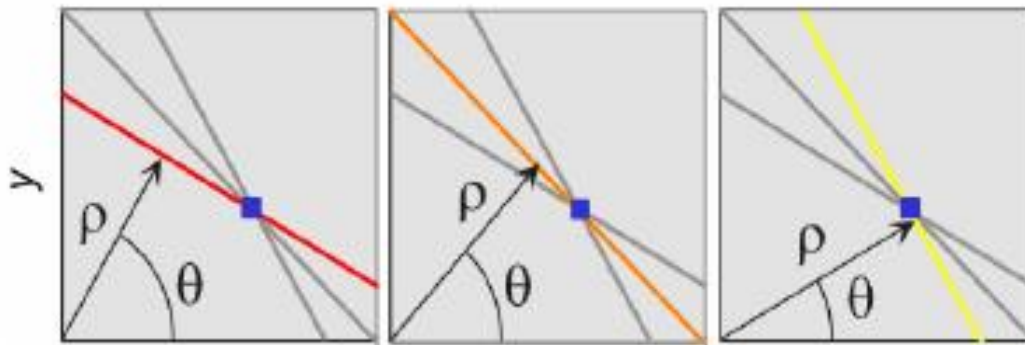
Detection - Hough Transform

P.C.V. Hough „Method and means for recognising complex pattern”

US Patent 3 069 654, 1962

- A given pixel in an image can belong to an infinite number of lines.
- A line can be parameterized by the Hough parameters „ ρ ” and „ θ ”.
- ρ represents the perpendicular distance of the line of the origin,
- θ describes the angle of the line.
- The relationship between the lines passing through a pixel at a coordinate in the image of x and y can be expressed as:

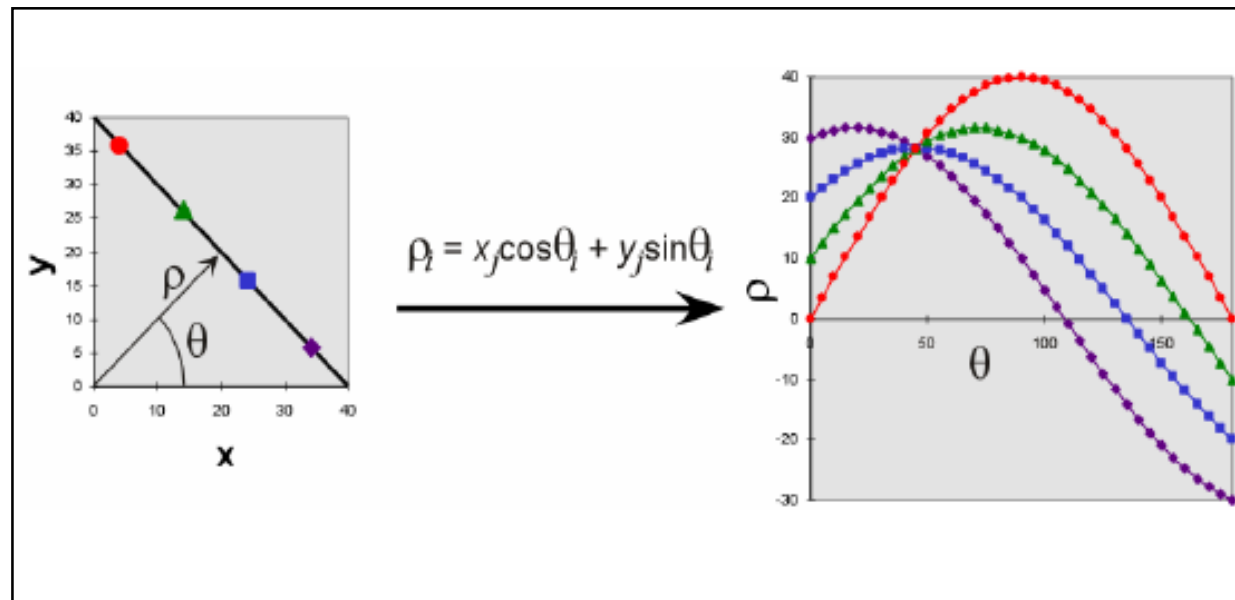
$$\rho_i = x \cos \theta_i + y \sin \theta_i$$



A point in image space
transforms to a sinusoidal
curve in Hough space!



- Consider 4 pixels along a line.
- For each pixel in the line, all possible ρ values are calculated for θ ranging in values from 0 to 180° using the equation: $\rho = x\cos\theta + y\sin\theta$. This produces 4 sinusoidal curves.
- These curves intersect at a point at „ ρ ” and „ θ ” coordinates corresponding to the angle of the line (θ) and its position relative to the origin (ρ).
- Thus, a line in image space transforms to a point in Hough Space.



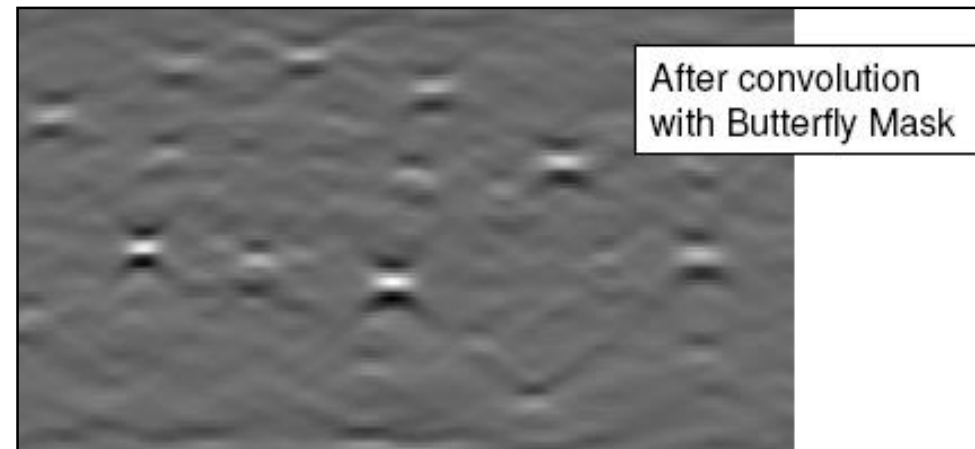
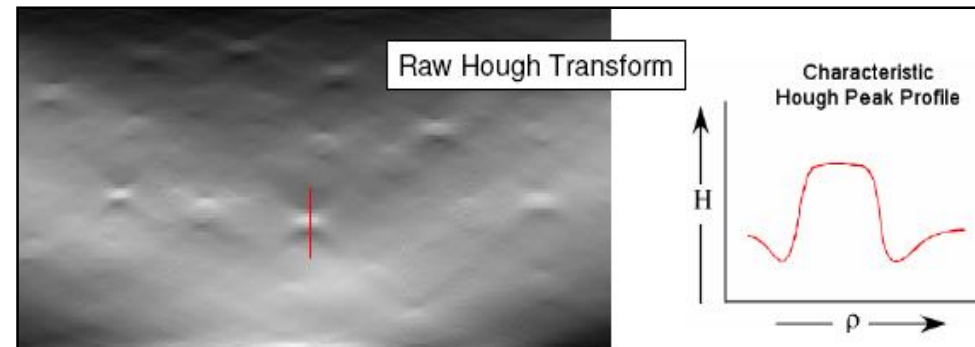
Project WND-POWR.03.02.00-00-1043/16

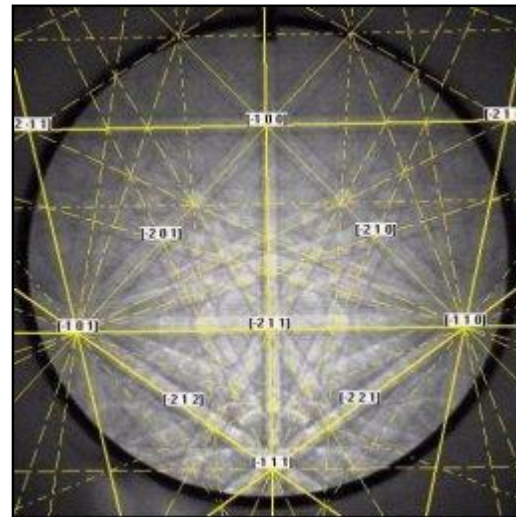
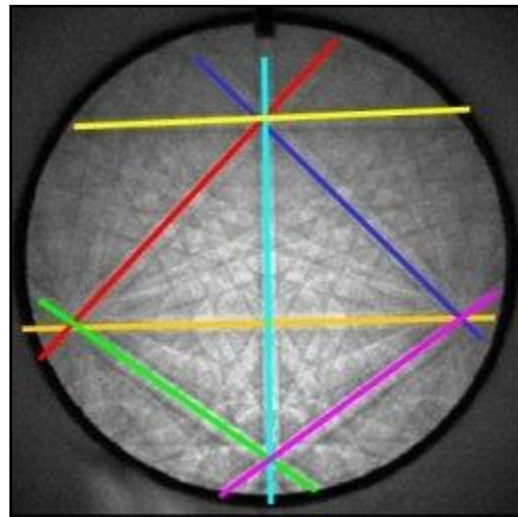
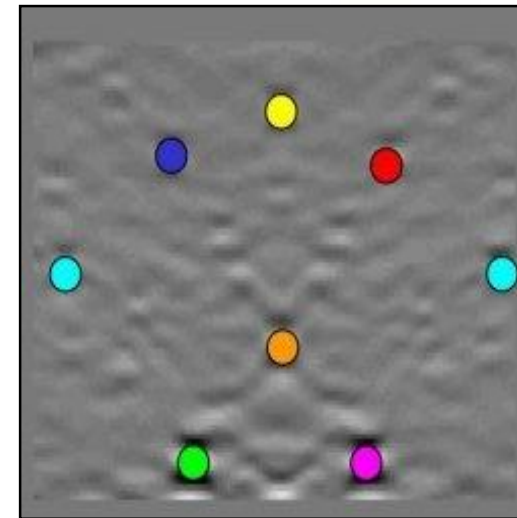
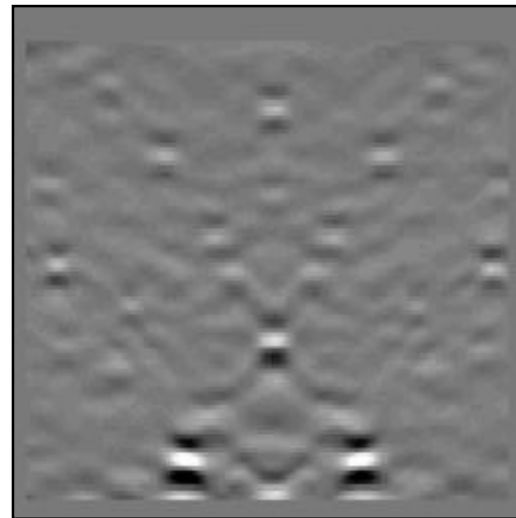
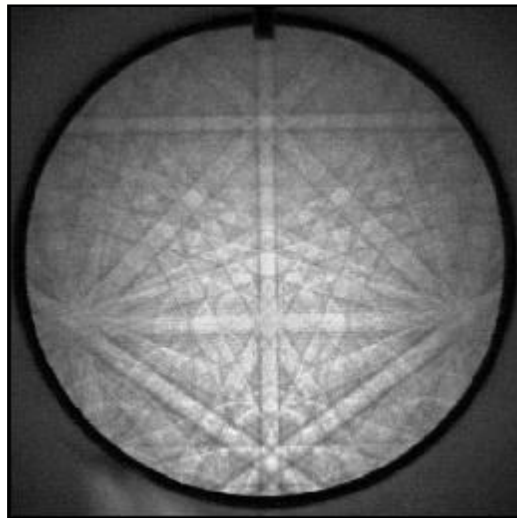
International interdisciplinary PhD Studies in Materials Science with English as the language of instruction

Project co-financed by the European Union within the European Social Funds



Detection - Hough transform





Detection Hough transform



Structure factor

For n number of atoms in unit cell:

$$F_{hkl} = \sum_{j=1}^n f_j(\theta) \exp[-2\pi i(hu_j + kv_j + lw_j)]$$

In some case crystallographic planes do not diffract electrons – diffraction does not occur – *forbidden reflections*

for f.c.c. (Au) – Au atoms on the corners of unit cell and in the middle of unit cell planes.

4 atoms at the following position $[0,0,0]$, $[0,0.5,0.5]$, $[0.5,0,0.5]$, $[0.5,0.5,0]$



Structure factor

$$F_{hkl} = f_1(\theta) \begin{pmatrix} \exp[-2\pi i(1 \cdot 0 + 0 \cdot 0 + 0 \cdot 0)] \\ + \exp[-2\pi i(1 \cdot 0 + 0 \cdot \frac{1}{2} + 0 \cdot \frac{1}{2})] \\ + \exp[-2\pi i(1 \cdot \frac{1}{2} + 0 \cdot 0 + 0 \cdot \frac{1}{2})] \\ + \exp[-2\pi i(1 \cdot \frac{1}{2} + 0 \cdot \frac{1}{2} + 0 \cdot 0)] \end{pmatrix} = \begin{pmatrix} \exp[0] \\ + \exp[0] \\ + \exp[-\pi i] \\ + \exp[-\pi i] \end{pmatrix} = 0$$

For practical reasons „a developed formula” for F_{hkl} calculations is used:

$$F_{hkl} = \sum_{j=1}^n f_j(\Theta) \cos 2\pi(hx_n + ky_n + lz_n) - i \sum_{j=1}^n f_j(\Theta) \sin 2\pi(hx_n + ky_n + lz_n)$$

x, y, z – position of „n” atom

hkl – Miller indices

<http://www.ftj.agh.edu.pl/~Wierzbanowski/Dyfrakcja.pdf>



AI

| Reflectors | No. | d-spacing, Å | Intensity % |
|------------|-----|--------------|-------------|
| {111} | 4 | 2.338 | 100.0 |
| {200} | 3 | 2.025 | 69.4 |
| {202} | 6 | 1.432 | 27.6 |
| {113} | 12 | 1.221 | 18.2 |
| {222} | 4 | 1.169 | 16.2 |
| {400} | 3 | 1.013 | 11.2 |
| {331} | 12 | 0.929 | 9.0 |
| {402} | 12 | 0.906 | 8.4 |
| {422} | 12 | 0.827 | 6.6 |
| etc. | | | |

Mechanisms giving rise to the Kikuchi band intensities and profile shapes are complex. As an approximation, the intensity of a Kikuchi band for the plane (hkl), on which diffraction takes place, is given by:

$$I_{hkl} = \left[\sum_i f_i(\Theta) \cos 2\pi(hx_i + ky_i + lz_i) \right]^2 + \left[\sum_i f_i(\Theta) \sin 2\pi(hx_i + ky_i + lz_i) \right]^2$$

$$I_{hkl} = \sum_i f_i(\Theta) \left[\cos^2 2\pi(hx_i + ky_i + lz_i) + \sin^2 2\pi(hx_i + ky_i + lz_i) \right]$$

where: $f_i(\theta)$ is the atomic scattering factor for electrons and (x_i, y_i, z_i) are the fractional coordinates in the unit cell for atom i (atom positions).

An observed diffraction pattern should be compared with a calculated simulation using above equation to ensure only planes that produce visible Kikuchi bands are used when solving the diffraction pattern. This is especially important when working with materials with more than one atom type.



$$f(\theta) = \frac{m_0 e^2}{2h^2} \left(\frac{\lambda}{\sin\theta} \right)^2 (Z - f_x)$$

where:

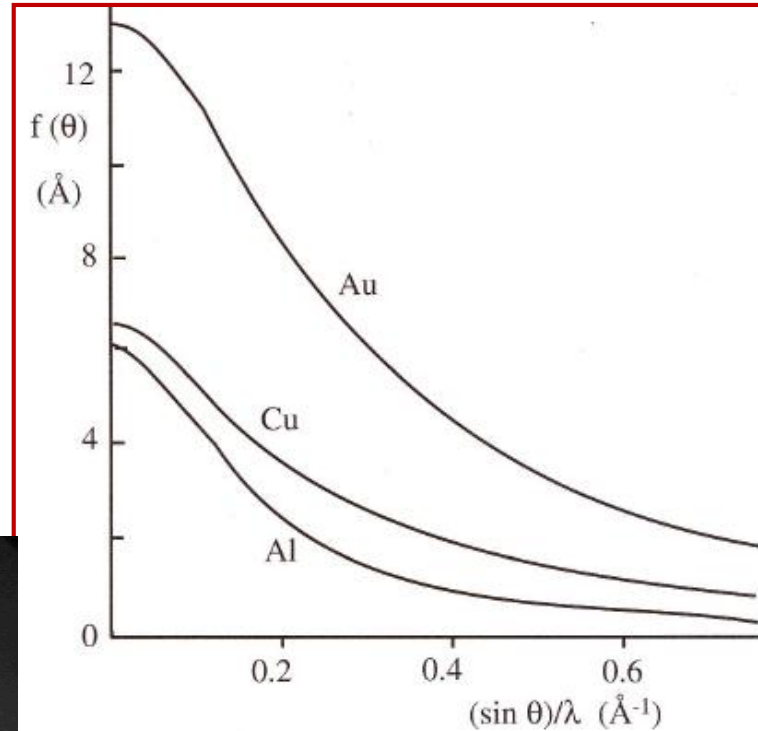
Z – atomic number

f_x – scattering factor for x-rays

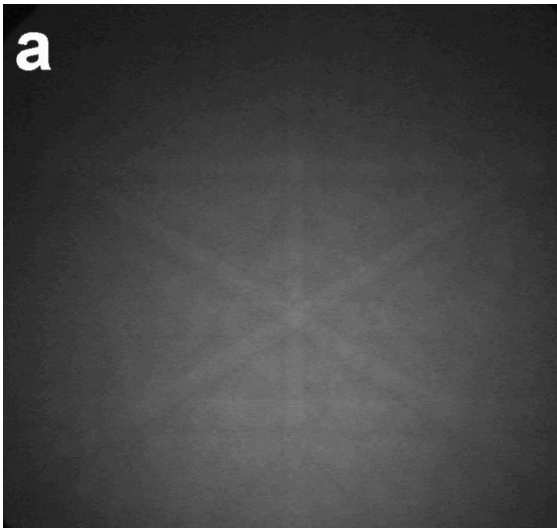
$(\lambda/\sin\theta)$ – Rutherford scattering of electron on atomic core

$(Z-f_x)$ – scattering of electron on inner shell electrons

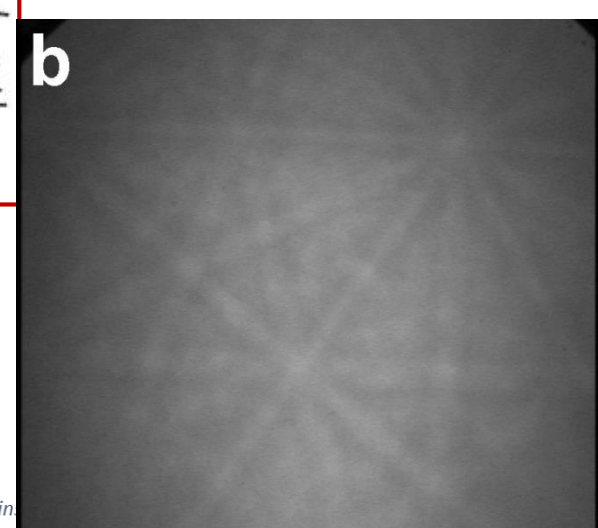
(L.REIMER)

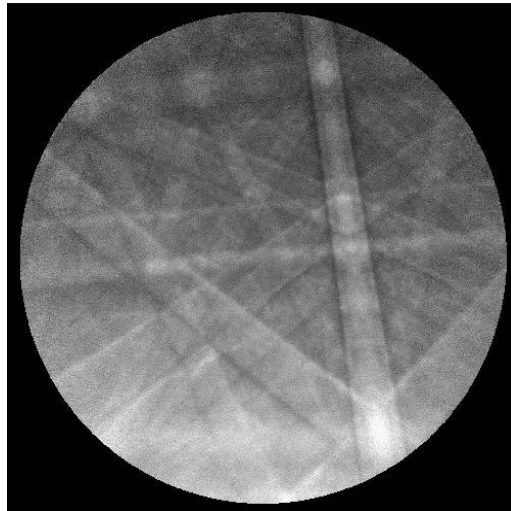


Al

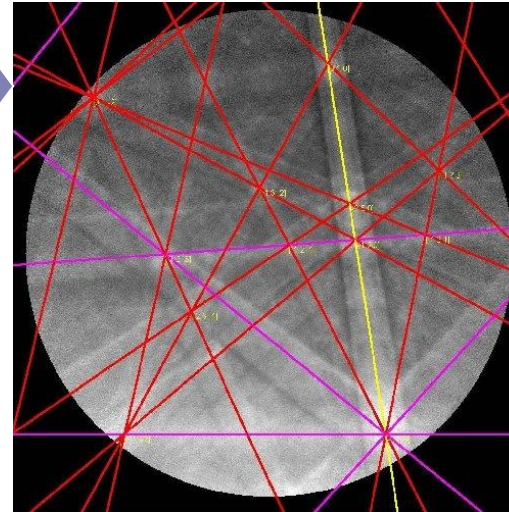


Ta

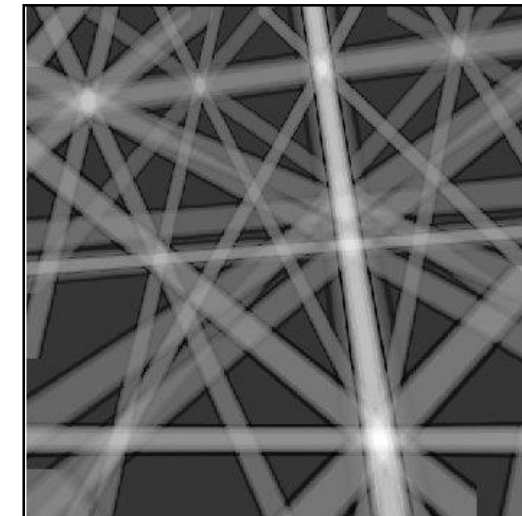
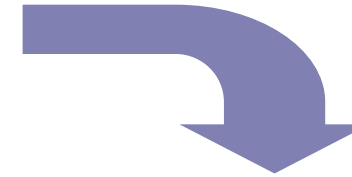




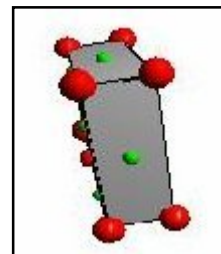
Diffraction pattern from the orthorhombic ceramic mullite ($3\text{Al}_2\text{O}_3 \cdot 2\text{SiO}_2$), 10 kV



Solution overlaid on the diffraction pattern giving the crystal orientation as $\{370\}\langle 7-34 \rangle$



Simulated diffraction pattern showing all Kikuchi bands with intensity greater than 10% of the most intense band.

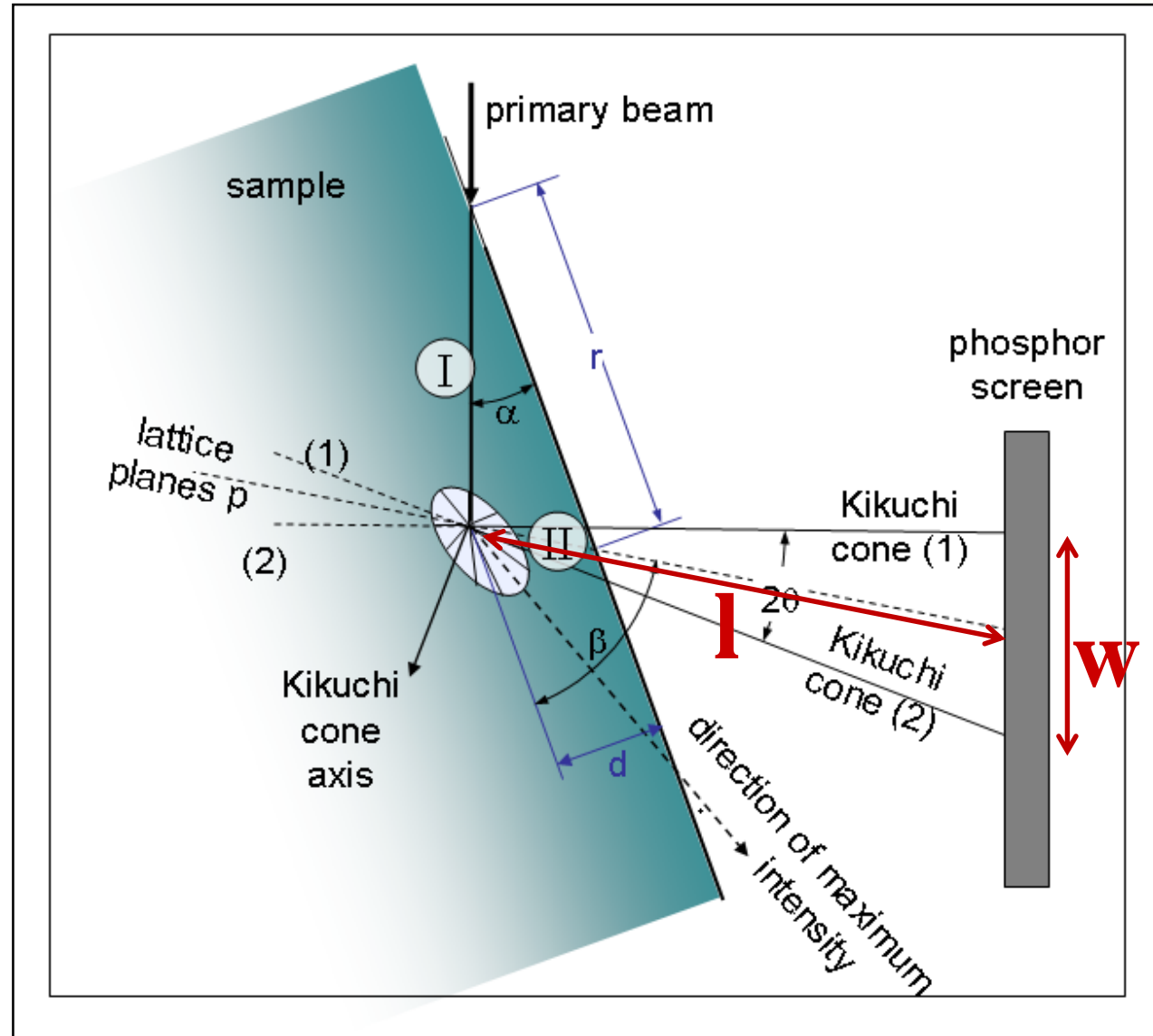


Simulation of crystal orientation

Project WND-POWR.03.02.00-00-1043/16

International interdisciplinary PhD Studies in Materials Science with English as the language of instruction

Project co-financed by the European Union within the European Social Funds



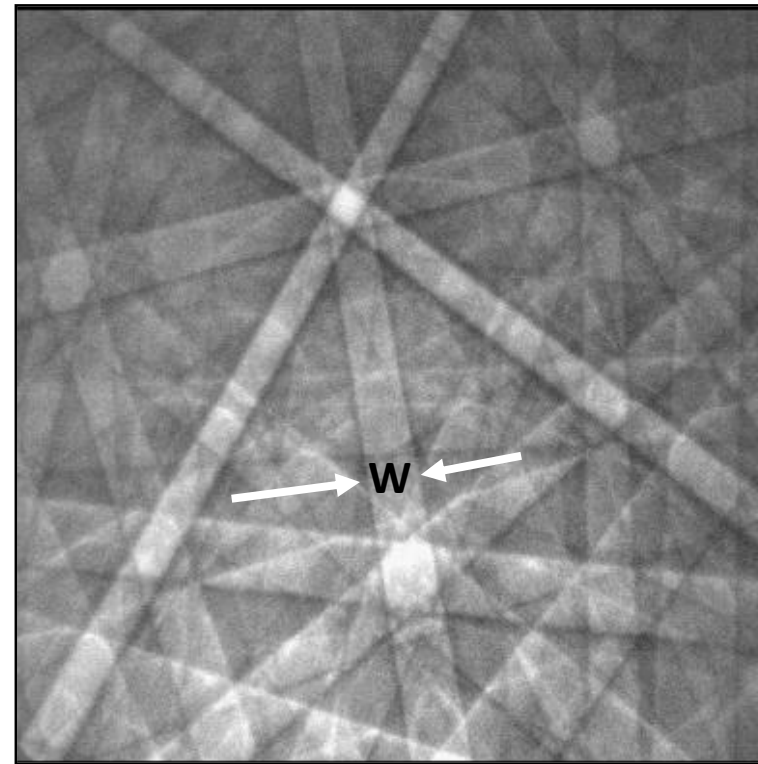
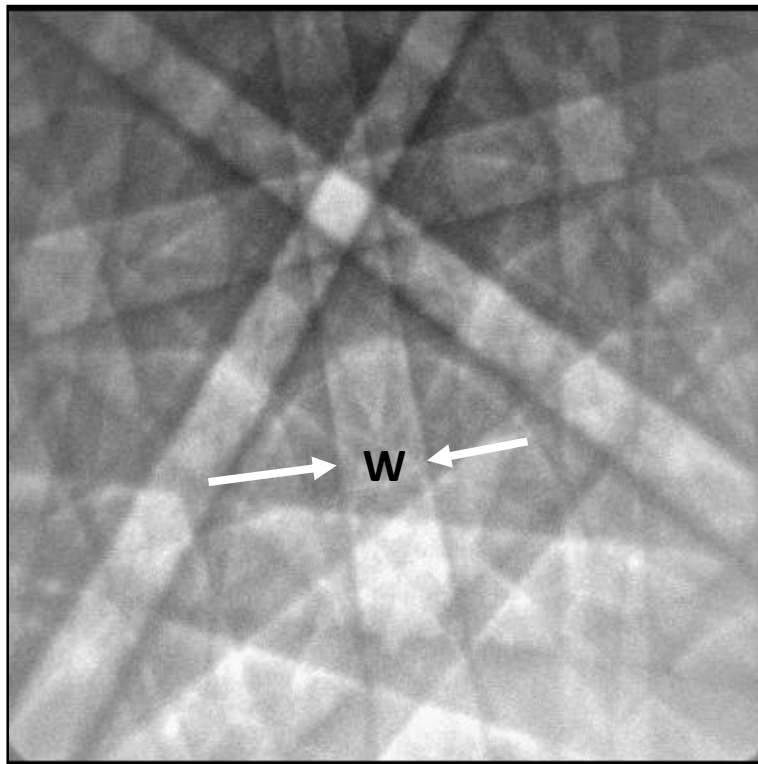


Bragg's Law – Voltage Effect

$$\lambda = 2d_{hkl} \sin \theta$$

$$n\lambda = 2d_{hkl} \sin \theta = 2d_{hkl} \theta$$

$$w = 2l \sin \theta = 2l\theta$$



$$w = \frac{l\lambda}{d}$$

EBSPs from silicon at 10 keV and 30 keV

Project WND-POWR.03.02.00-00-1043/16

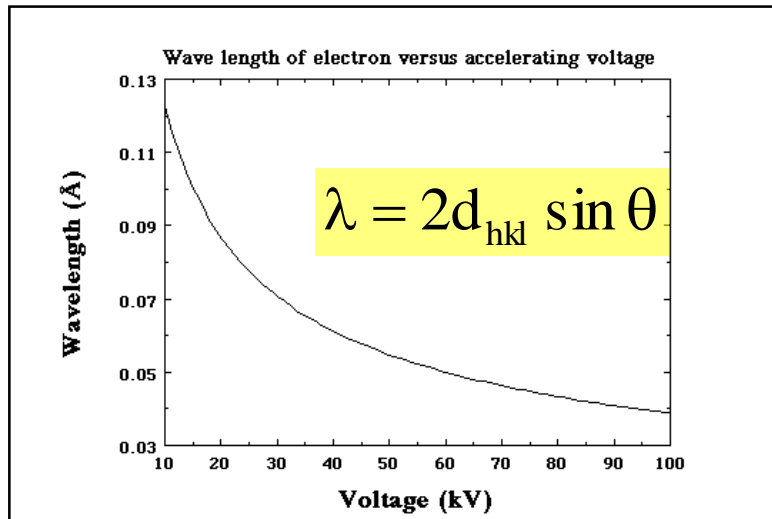
International interdisciplinary PhD Studies in Materials Science with English as the language of instruction

Project co-financed by the European Union within the European Social Funds



$$\lambda = \frac{h}{\sqrt{2m_0eV \left[\frac{1 + eV}{2m_0c^2} \right]}}$$

$$\lambda = \frac{12.2630}{\sqrt{V + 0.97845 \times 10^{-6} V^2}}$$



| V (kV) | λ, nm |
|--------|---------|
| 20 | 0.00859 |
| 30 | 0.00698 |
| 40 | 0.00602 |
| 50 | 0.00536 |
| 60 | 0.00487 |
| 70 | 0.00448 |
| 80 | 0.00418 |
| 90 | 0.00392 |
| 100 | 0.00370 |
| 200 | 0.00251 |
| 300 | 0.00197 |
| 400 | 0.00164 |
| 500 | 0.00142 |
| 600 | 0.00126 |
| 700 | 0.00113 |
| 800 | 0.00103 |
| 900 | 0.00094 |
| 1000 | 0.00087 |
| 2000 | 0.00050 |
| 4000 | 0.00028 |



Summary (1)

- 1. When an electron beam hits a tilted crystalline sample, electron backscatter diffraction patterns are formed on a suitably placed phosphor screen.**
- 2. Diffraction pattern consists of a set of Kikuchi bands which are characteristic for the sample crystal structure and orientation.**
- 3. The center line of each Kikuchi band corresponds to the intersection with the phosphor screen of the diffracting plane responsible for the band.**
- 4. The position of the Kikuchi bands can be found automatically with the Hough transform and used to calculate the orientation of crystal that formed the pattern.**



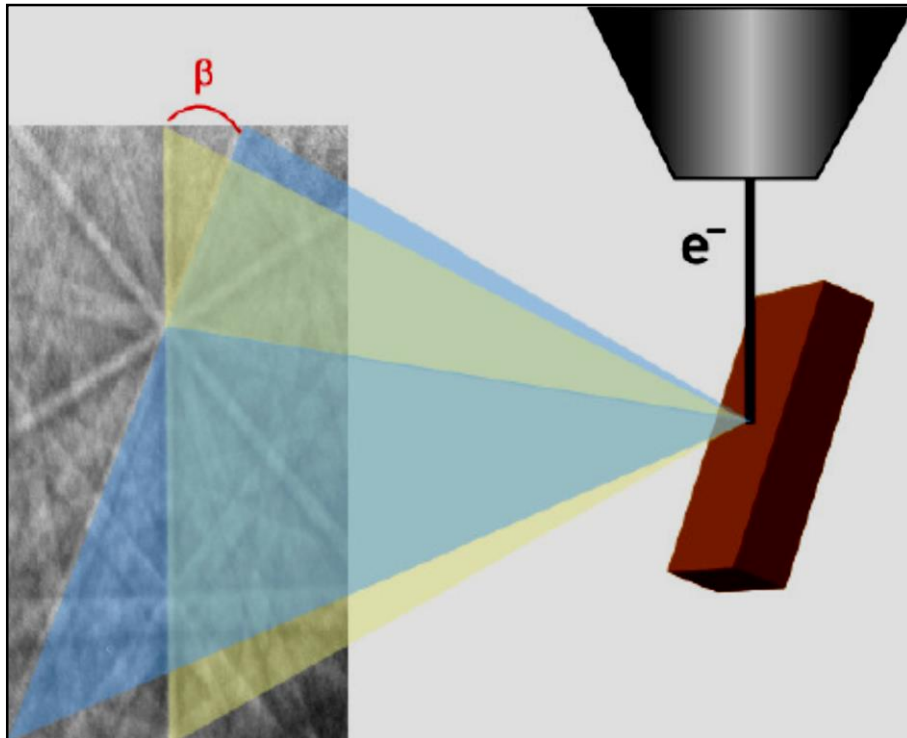
3. EBSD – solving the pattern



If the hkl of two bands in the pattern can be identified then the corresponding orientation can be calculated.

By comparing the angle between two bands with an interplanar angle in Look-up table, the hkl pair associated with the band pair can be identified.

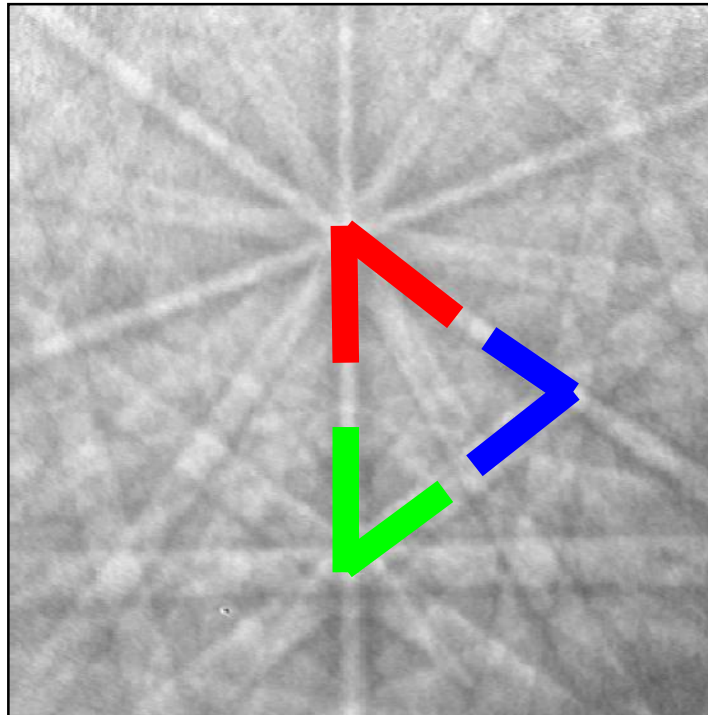
If 3 bands are used then the hkl s associated with all 3 bands can be determined.



| Angle | $(hkl)_1$ | $(hkl)_2$ | Angle | $(hkl)_1$ | $(hkl)_2$ |
|-------|-----------|-------------------|-------|-----------|-------------------|
| 25.2 | 200 | 311 | 64.8 | 220 | $3\bar{1}1$ |
| 29.5 | 111 | 311 | 70.5 | 111 | $11\bar{1}$ |
| 31.5 | 220 | 311 | 72.5 | 200 | 131 |
| 35.1 | 311 | $31\bar{1}$ | 80.0 | 111 | $3\bar{1}\bar{1}$ |
| 35.3 | 111 | 220 | 84.8 | 311 | $1\bar{3}1$ |
| 45.0 | 200 | 220 | 90.0 | 111 | $2\bar{2}0$ |
| 50.5 | 311 | $3\bar{1}\bar{1}$ | 90.0 | 200 | 020 |
| 54.7 | 111 | 200 | 90.0 | 200 | 022 |
| 58.5 | 111 | $31\bar{1}$ | 90.0 | 220 | $11\bar{3}$ |
| 60.0 | 220 | $20\bar{2}$ | 90.0 | 220 | $2\bar{2}0$ |
| 63.0 | 311 | $13\bar{1}$ | | | |



A set of orientations is obtained from triplet of bands by comparing the interplanar angles against a Look-up table

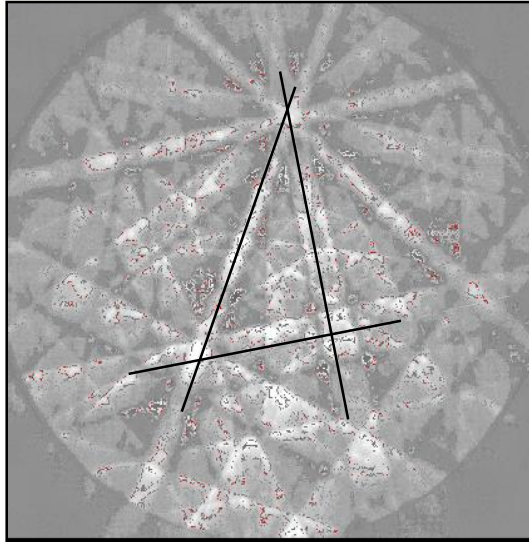


| Angle (hkl)1 (hkl)2 |
|---------------------|
| 25.2 200 311 |
| 29.5 111 311 |
| 31.5 220 311 |
| 35.1 311 311 |
| 35.3 111 220 |
| 45.0 200 220 |
| 50.5 311 311 |
| 54.7 111 200 |
| 58.5 111 311 |
| 60.0 220 202 |
| 63.0 311 131 |
| 64.8 220 311 |
| 70.5 111 111 |
| 72.5 200 131 |
| 80.0 111 311 |
| 84.8 311 131 |
| 90.0 111 220 |
| 90.0 200 020 |
| 90.0 200 022 |
| 90.0 220 113 |
| 90.0 220 220 |

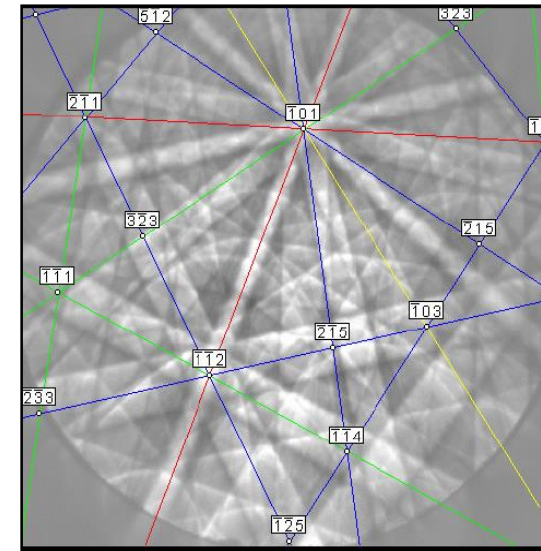
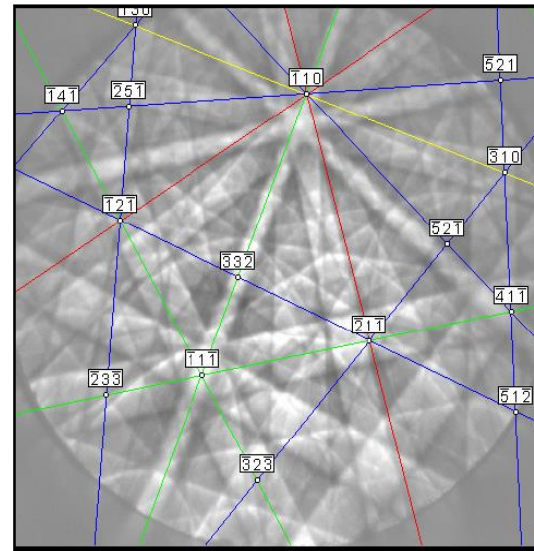
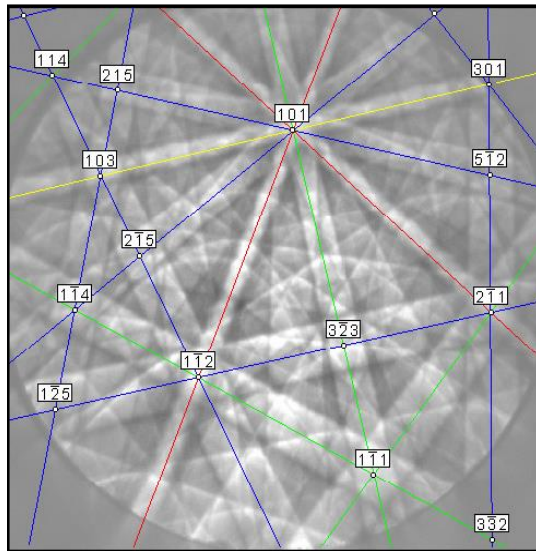


Building an interplanar Look-up table

| | |
|--|--|
| 1) Identify the hkl of the high contrast bands (bands likely to be detected by the Hough transform). | 200 111 220 311 |
| 2) Determine all of the symmetrically equivalent hkl 's. | 200, 020, 002 111, 11 $\bar{1}$, 1 $\bar{1}$ 1, $\bar{1}$ 11 220, 2 $\bar{2}$ 0, 202, 20 $\bar{2}$, 022, 02 $\bar{2}$ 311, $\bar{3}$ 11, 3 $\bar{1}$ 1, 31 $\bar{1}$, 131, $\bar{1}$ 31, 1 $\bar{3}$ 1, 13 $\bar{1}$, 113, $\bar{1}$ 13, 1 $\bar{1}$ 3, 11 $\bar{3}$ |
| 3) Form all possible pairs. | 200, 020 200, 002 200, 111 200, 11 $\bar{1}$... 020, 002 020, 111 020, 11 $\bar{1}$ 020, 1 $\bar{1}$ 1 ... 002, 111 002, 11 $\bar{1}$ 002, 1 $\bar{1}$ 1 002, $\bar{1}$ 11 ... ⋮ |
| 4) Calculate the angles between the plane pairs. | 200∠020 = 90° 200∠002 = 90° 200∠111 = 54.7° 200∠11 $\bar{1}$ = 54.7° ... 020∠002 = 90° 020∠111 = 54.7° 020∠11 $\bar{1}$ = 54.7° 020∠1 $\bar{1}$ 1 = 54.7° ... 002∠111 = 90° 002∠11 $\bar{1}$ = 90° 002∠1 $\bar{1}$ 1 = 90° 002∠ $\bar{1}$ 11 = 90° ... ⋮ |
| 5) Throw out duplicates and sort. | 200∠311 = 25.2° 111∠220 = 35.3° 111∠ $\bar{3}$ 11 = 58.5° 111∠11 $\bar{1}$ = 70.5° 111∠311 = 29.5° 200∠220 = 45.0° 220∠202 = 60° 200∠131 = 72.5° 220∠311 = 31.5° 311∠ $\bar{3}$ 11 = 50.5° 311∠13 $\bar{1}$ = 63.0° 111∠ $\bar{3}$ 11 = 80° 311∠ $\bar{3}$ 11 = 35.1° 200∠111 = 54.7° 220∠3 $\bar{1}$ 1 = 64.8° ⋮ |



For a set of three bands, compare the interplanar angles against the Look-up table and determine all possible indexing solution



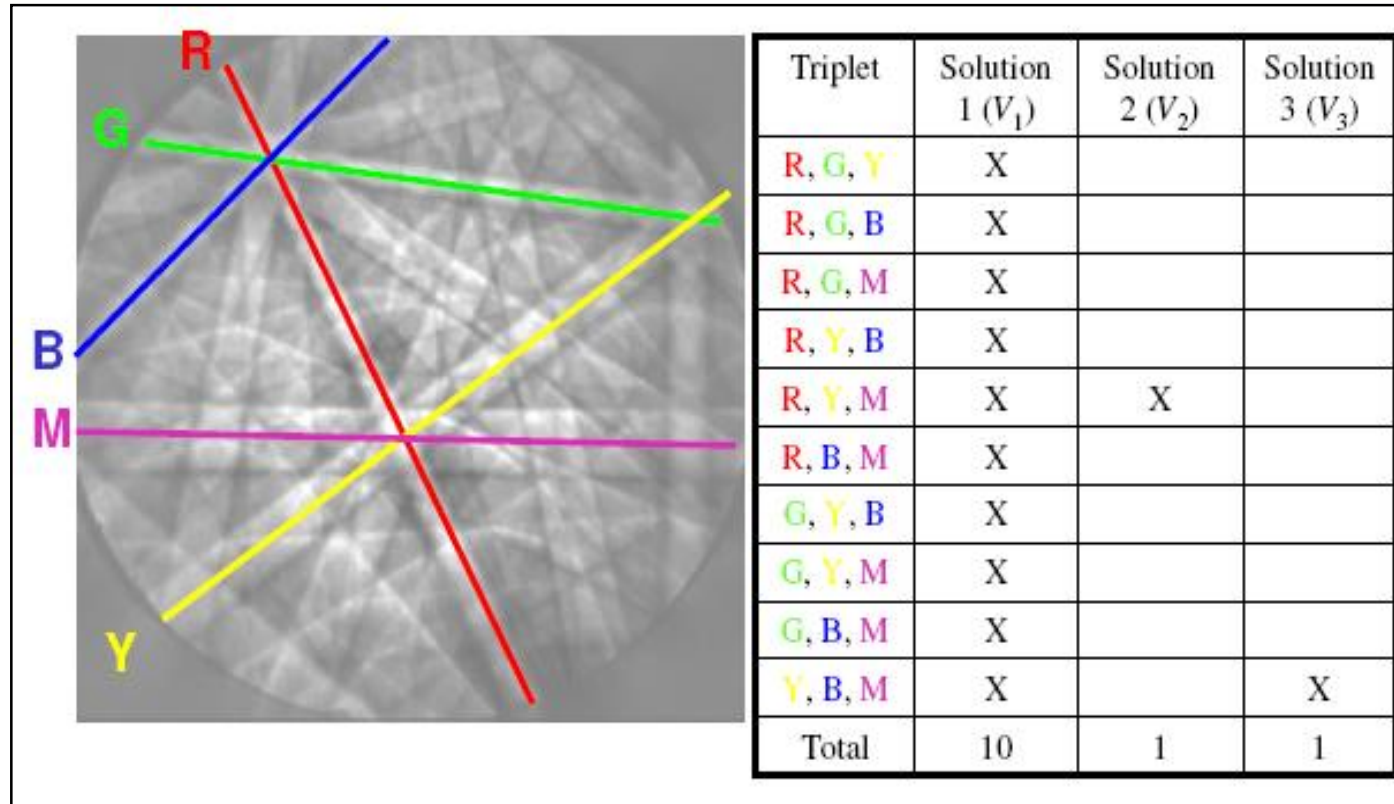


$$\# triplets = \frac{n!}{(n-3)! \cdot 3!}$$

For a given number of bands, n , used for pattern indexing, the number of band triplets is determined by this formula.

Typically 7 to 9 detected bands are used for automatic indexing.

| n | # triplets |
|-----|------------|
| 3 | 1 |
| 4 | 4 |
| 5 | 10 |
| 6 | 20 |
| 7 | 35 |
| 8 | 56 |
| 9 | 84 |



For this set of 5 detected bands, 10 triplet combinations are possible.

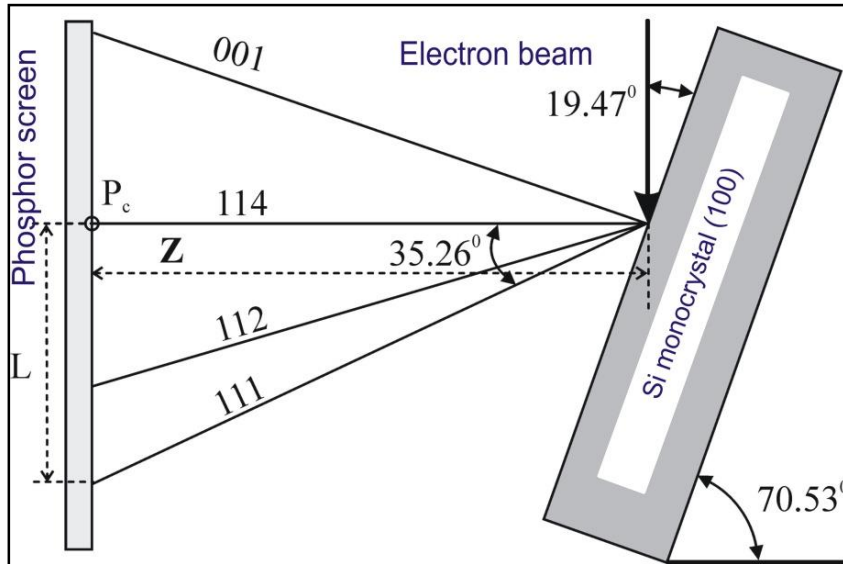
For each of these 10 triples solution V_1 matched.

Solutions V_2 and V_3 each matched one triplet only.

Confidence Index (CI - TSL) – information whether the matching is good or bad

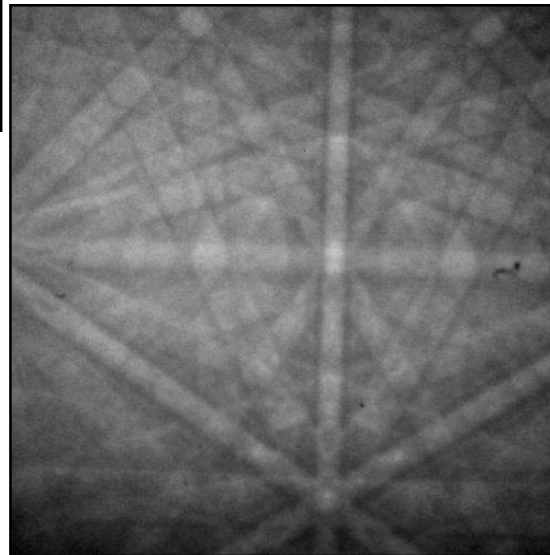


Pattern Centre – why do we tilt up to 70°?

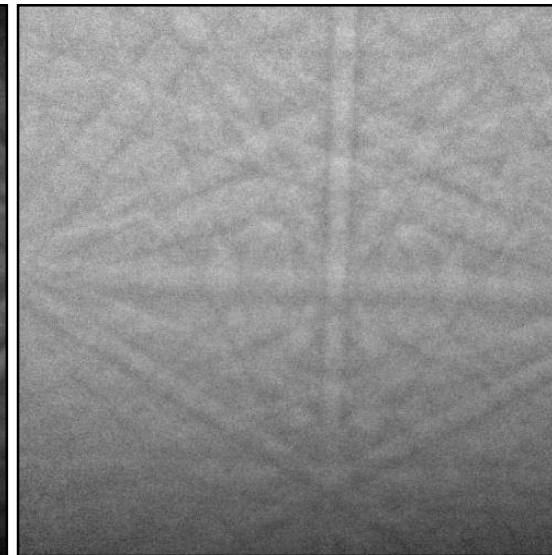


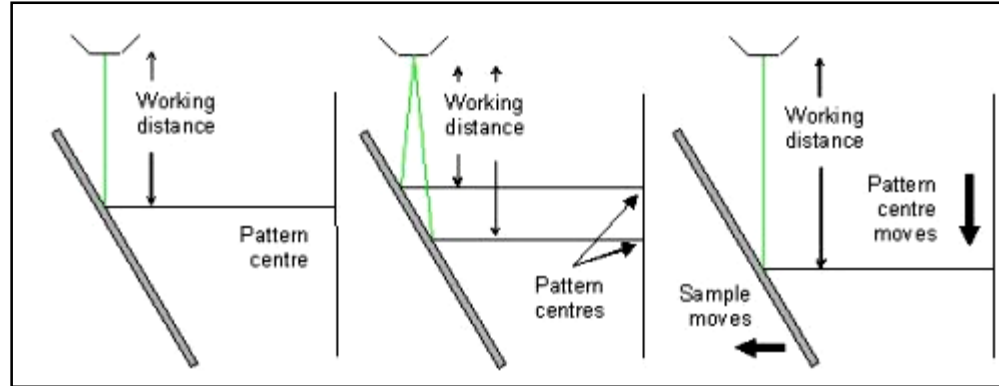
The pattern centre (PC) is the point on the screen closest to the generation point of the diffraction pattern on the sample

Tilt 70°

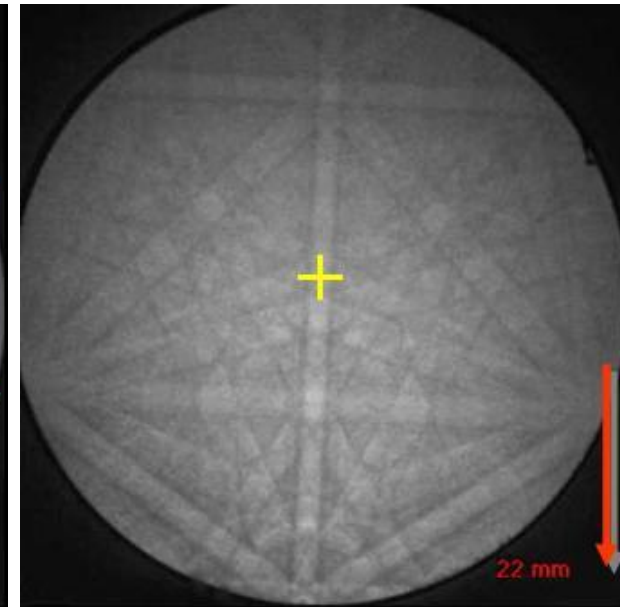
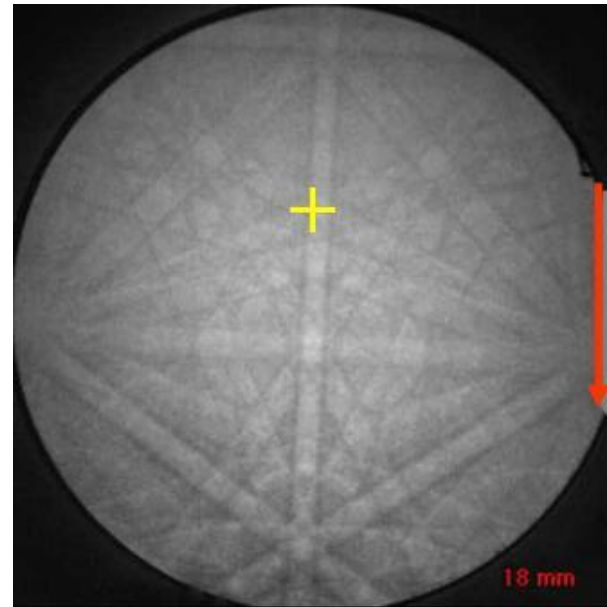
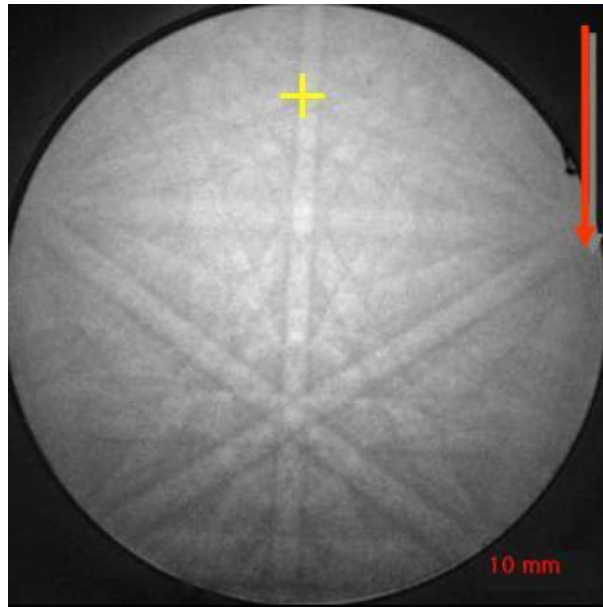


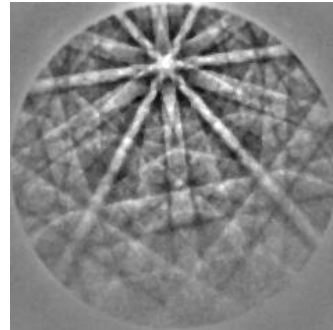
Tilt 50°



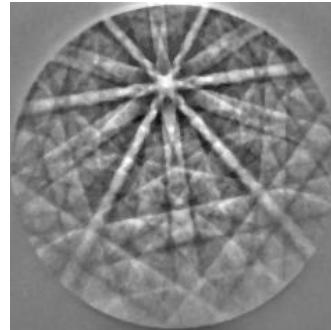


As the working distance changes the pattern centre changes as well

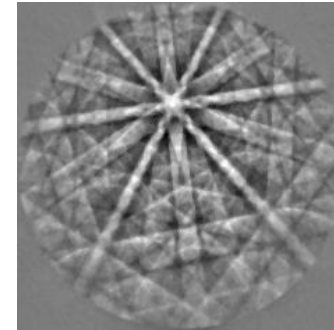




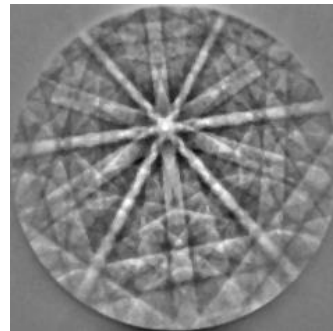
WD 7 mm



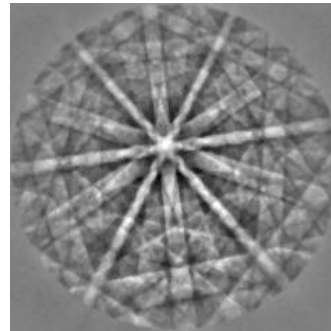
WD 9 mm



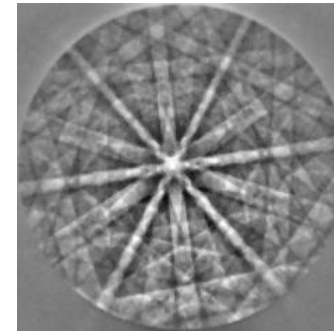
WD 11 mm



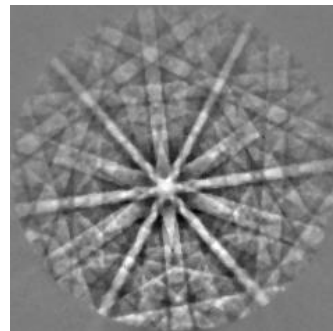
WD 13 mm



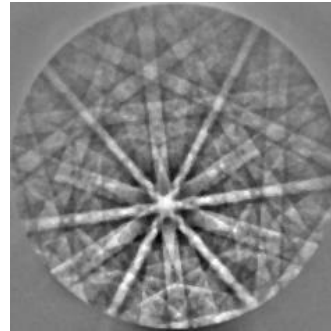
WD 15 mm



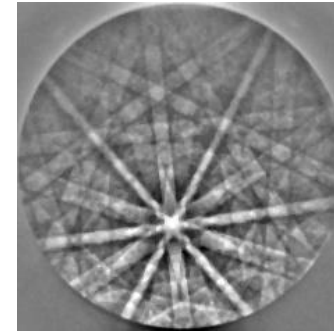
WD 17 mm



WD 19 mm



WD 21 mm

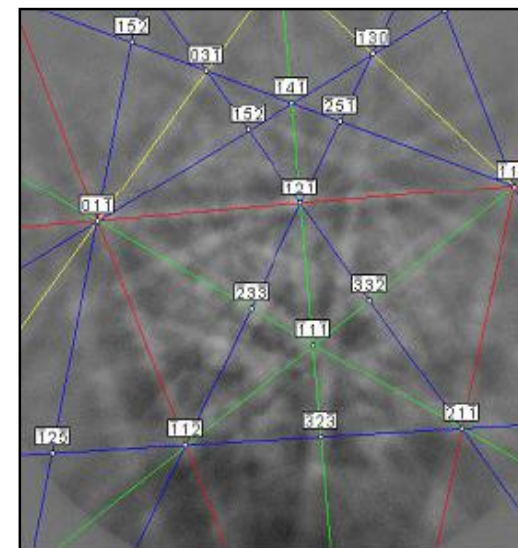
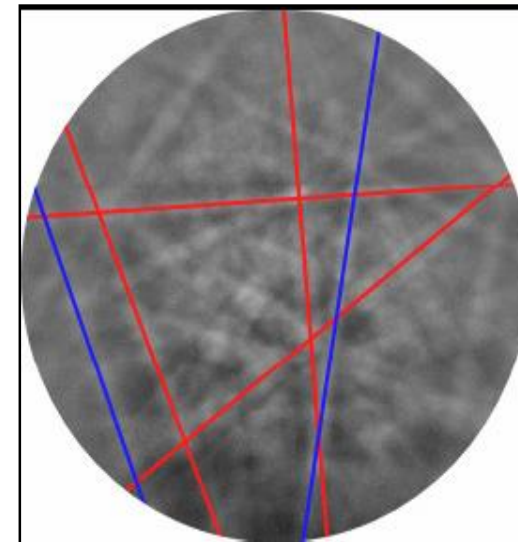
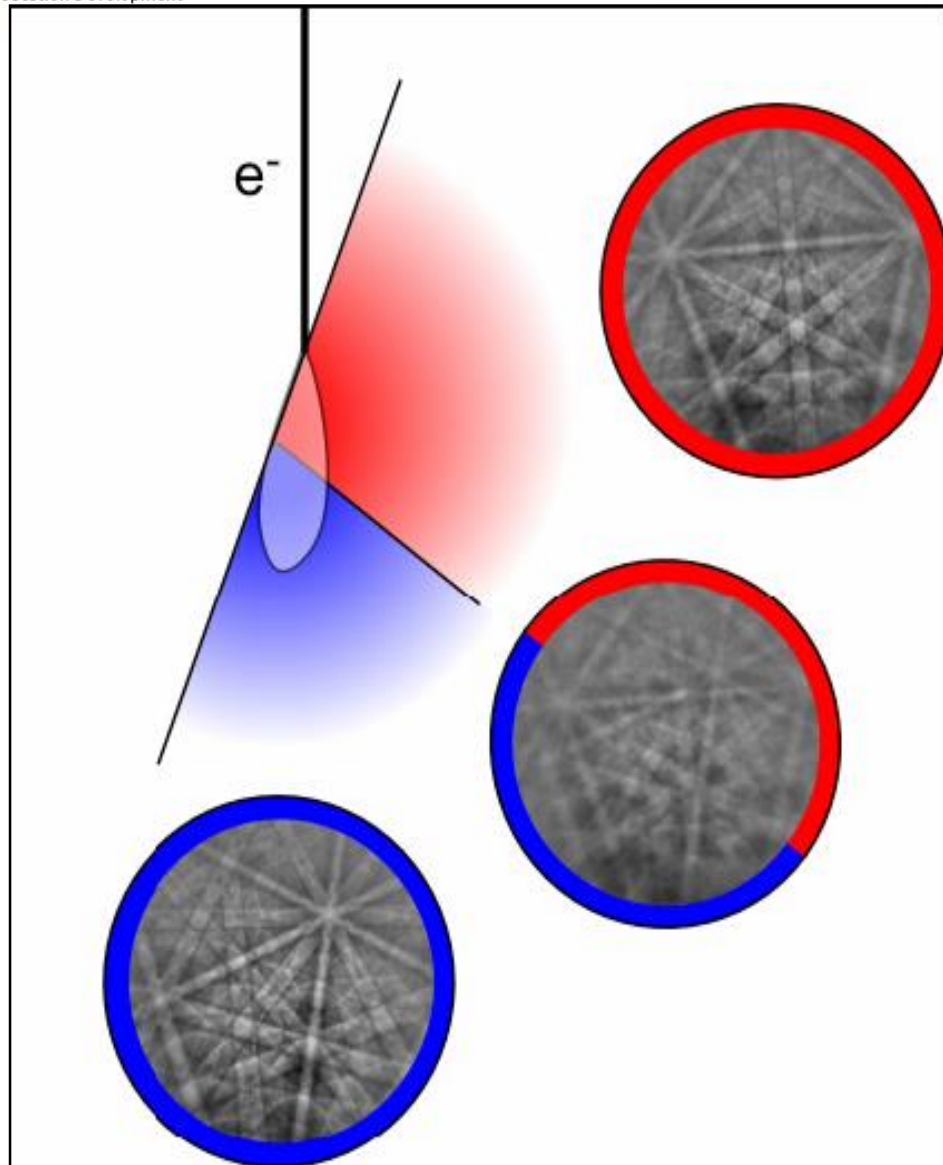


WD 23 mm

Project WND-POWR.03.02.00-00-1043/16

International interdisciplinary PhD Studies in Materials Science with English as the language of instruction

Project co-financed by the European Union within the European Social Funds



Project WND-POWR.03.02.00-00-1043/16

International interdisciplinary PhD Studies in Materials Science with English as the language of instruction

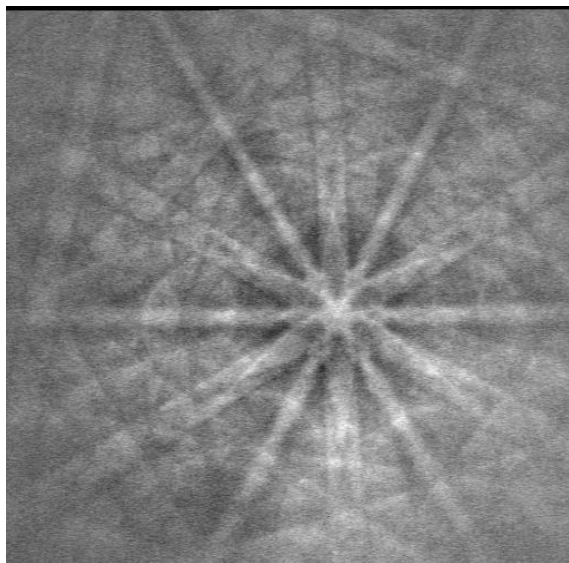
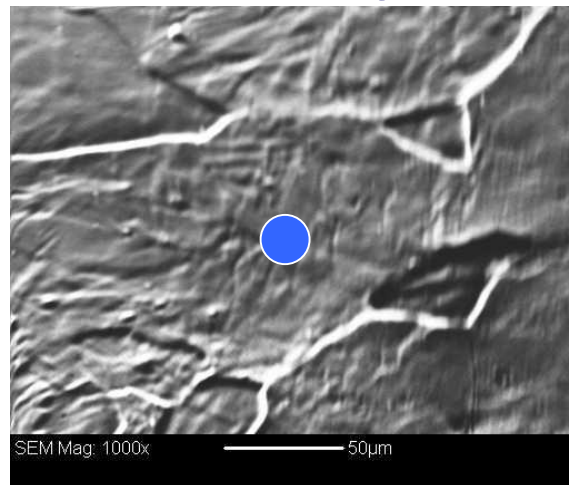
Project co-financed by the European Union within the European Social Funds



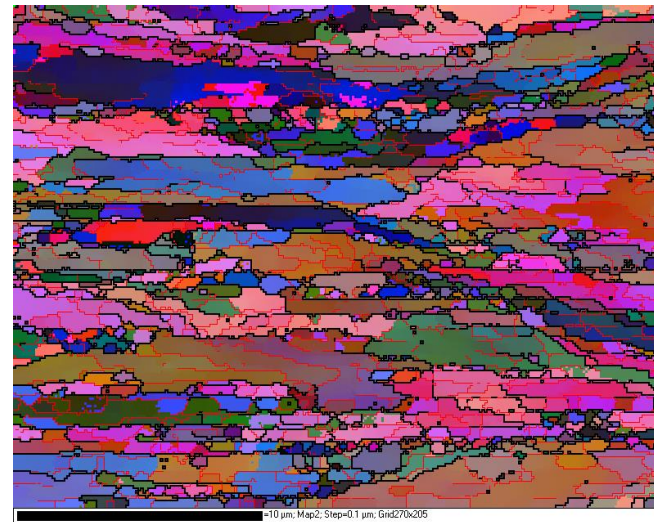
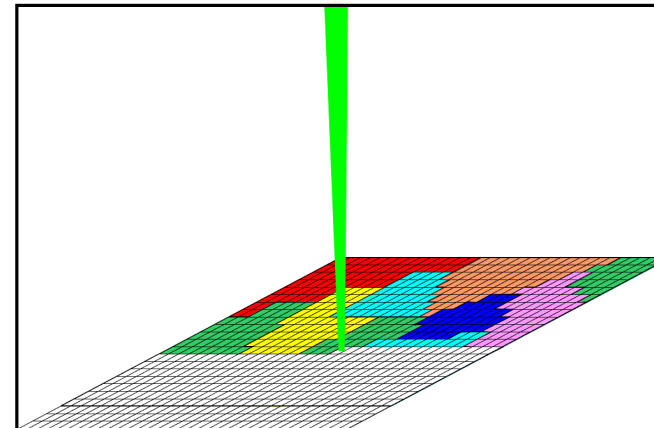
4. Information available from EBSD



Point analysis

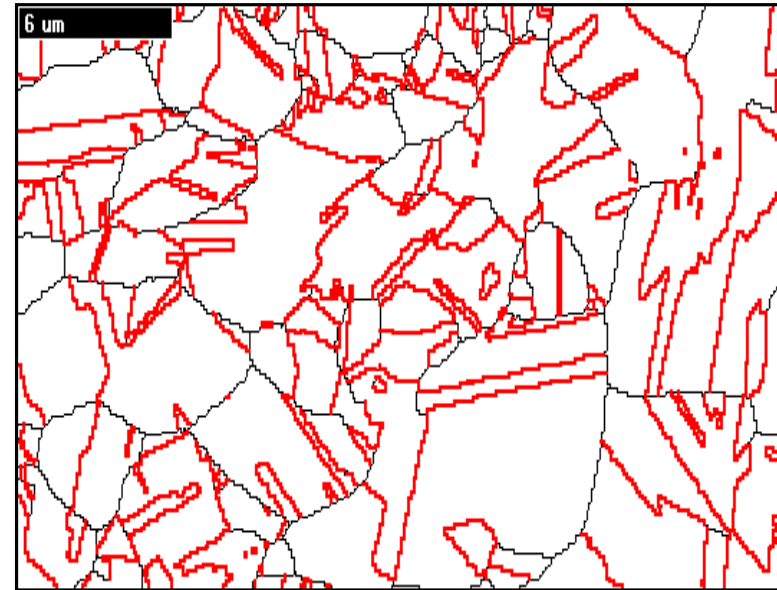


Scan analysis





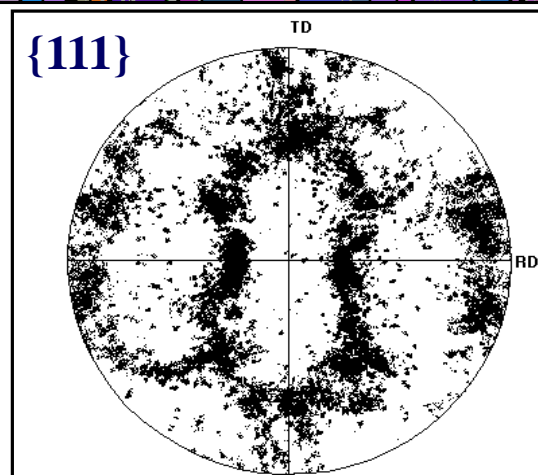
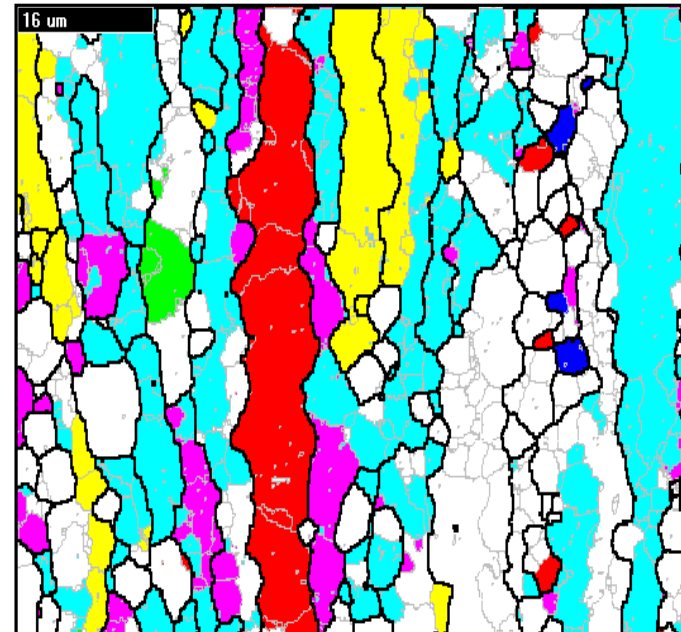
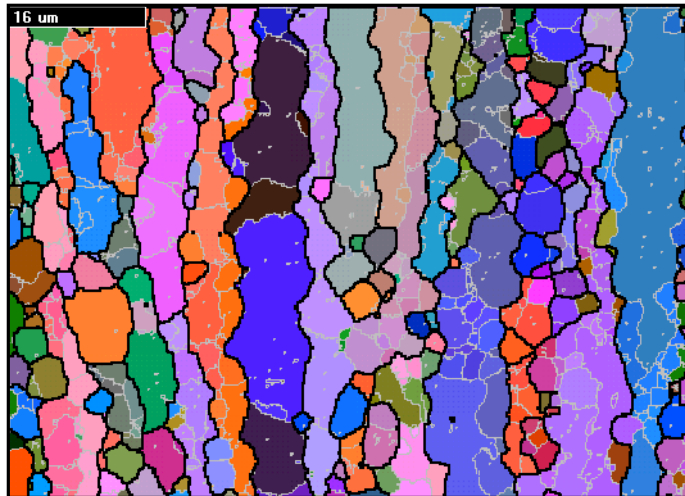
**Grain boundaries in brass
All Euler angles map**



**Coincidence Site Lattice (CSL)
boundaries in brass $\Sigma 3$ (twins) –
67% red lines**



The „preferred orientation”, i.e. the non-random orientation of single crystal lattices within a materials usually obtained by its processing



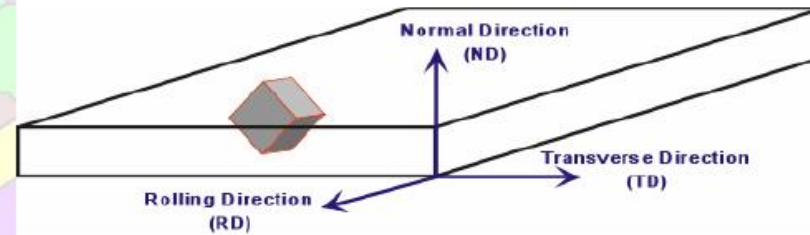
-  Brass {011}<112>
 -  Copper {112}<111>
 -  Cube {001}<100>
 -  Goss {011}<100>
 -  P {011}<122>
 -  S {123}<634>
- Hot rolled AA5182 alloy**

Texture Analysis

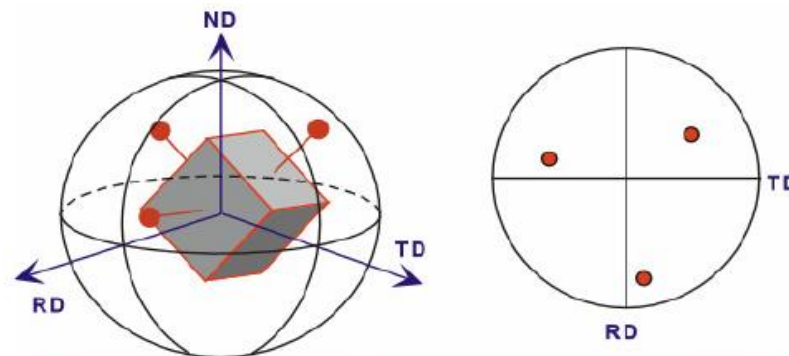


Pole Figures

Consider a cubic crystal in a rolled sheet sample with "laboratory" or "sample" axes as shown below.



The Pole Figure plots the orientation of a given plane normal (pole) with respect to the sample reference frame. The example below is a (001) pole figure. Note the three points shown in the pole figure are for three symmetrically equivalent planes in the crystal.



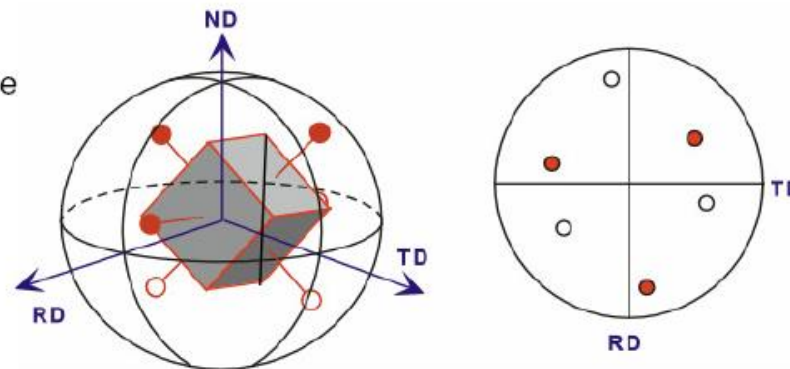


Pole Figures: Negative Hemisphere



Positive hemisphere

Negative Hemisphere



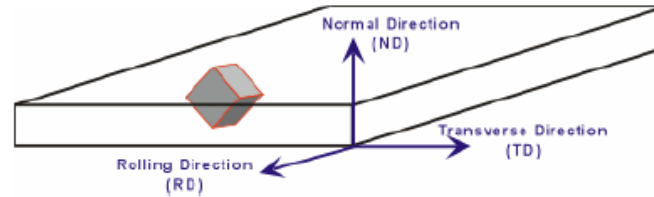
Open circles can be used to distinguish points in the negative hemisphere from points in the positive hemisphere in the same pole figure.



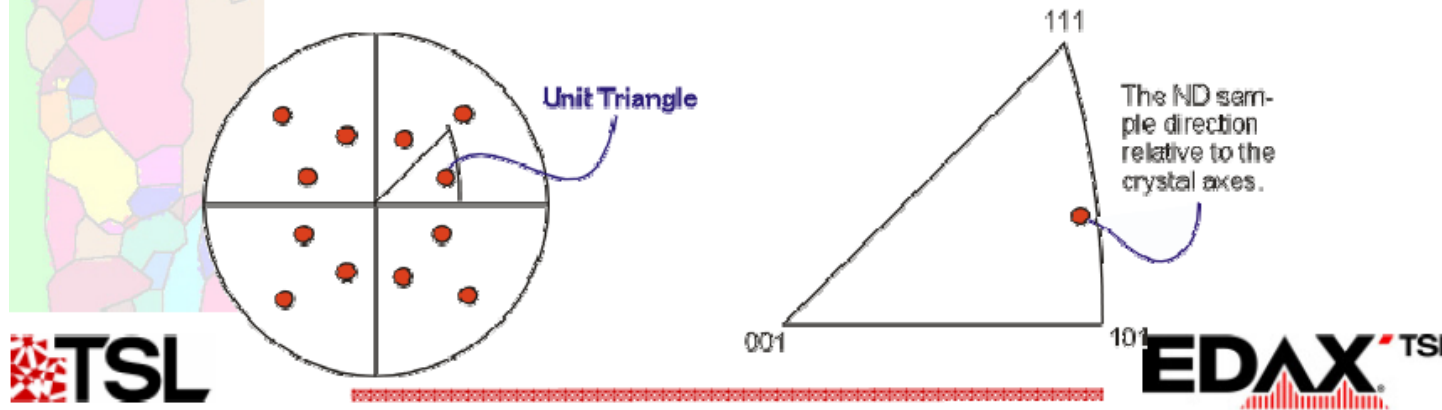


Inverse Pole Figures

Consider a cubic crystal in a rolled sheet sample with "laboratory" or "sample" axes as shown below.

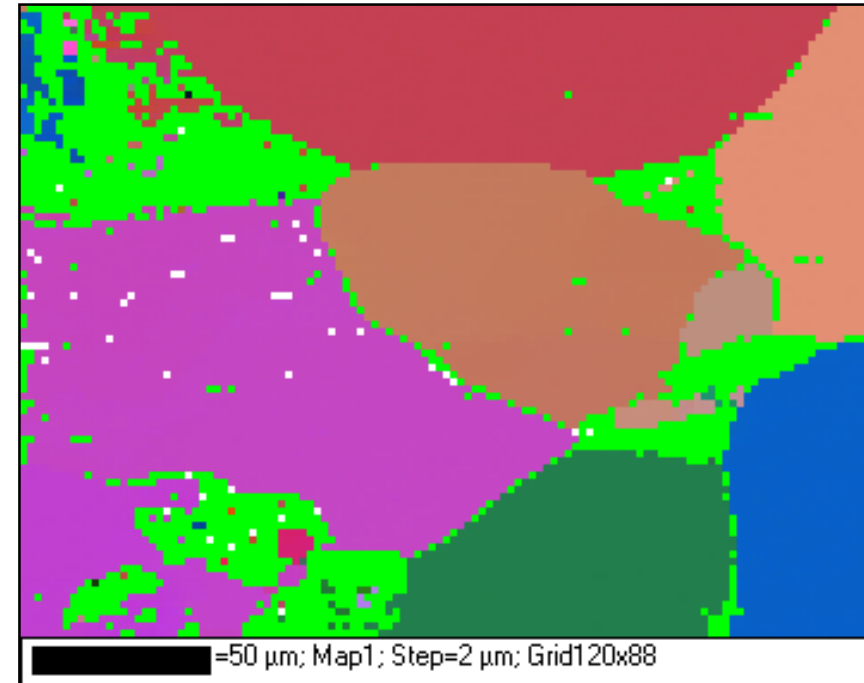
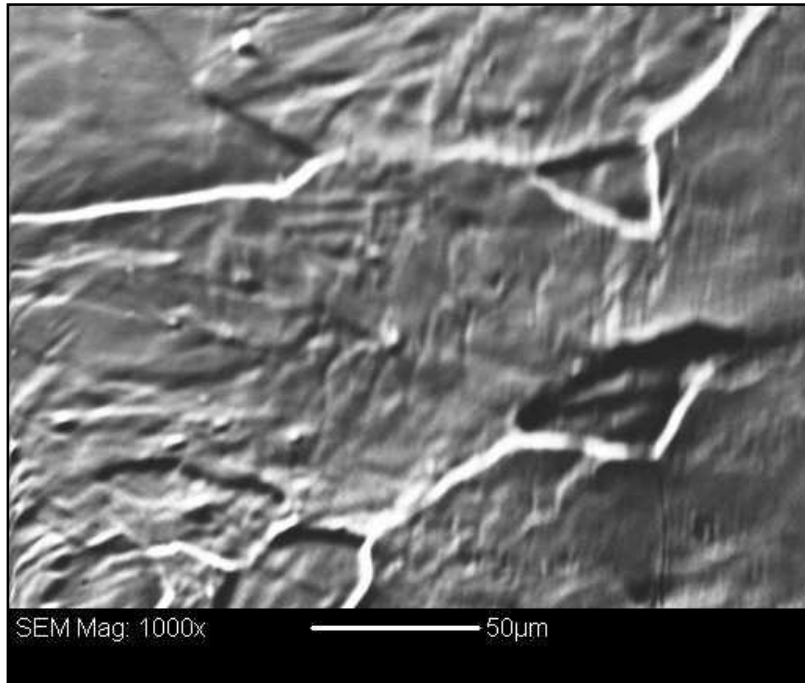


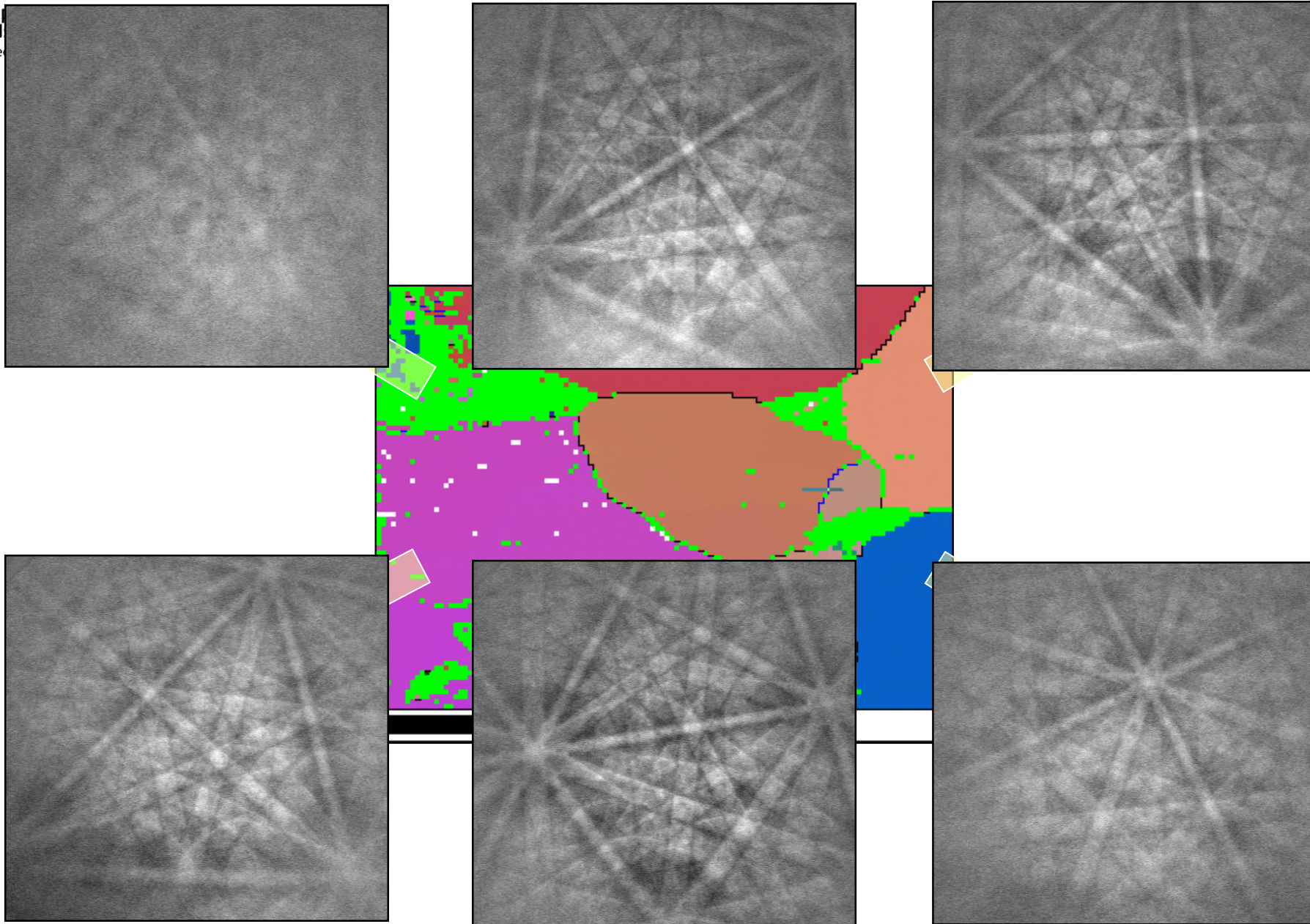
There are two ways of looking at inverse pole figures: 1) Which crystal axis is aligned with a specified sample axis. 2) The orientation of the specified sample axis with respect to the crystal axes. The example below is a normal direction inverse pole figure. In the full inverse pole figure all symmetrically equivalent points are shown.





Fe0.05wt%C 725°C 554h





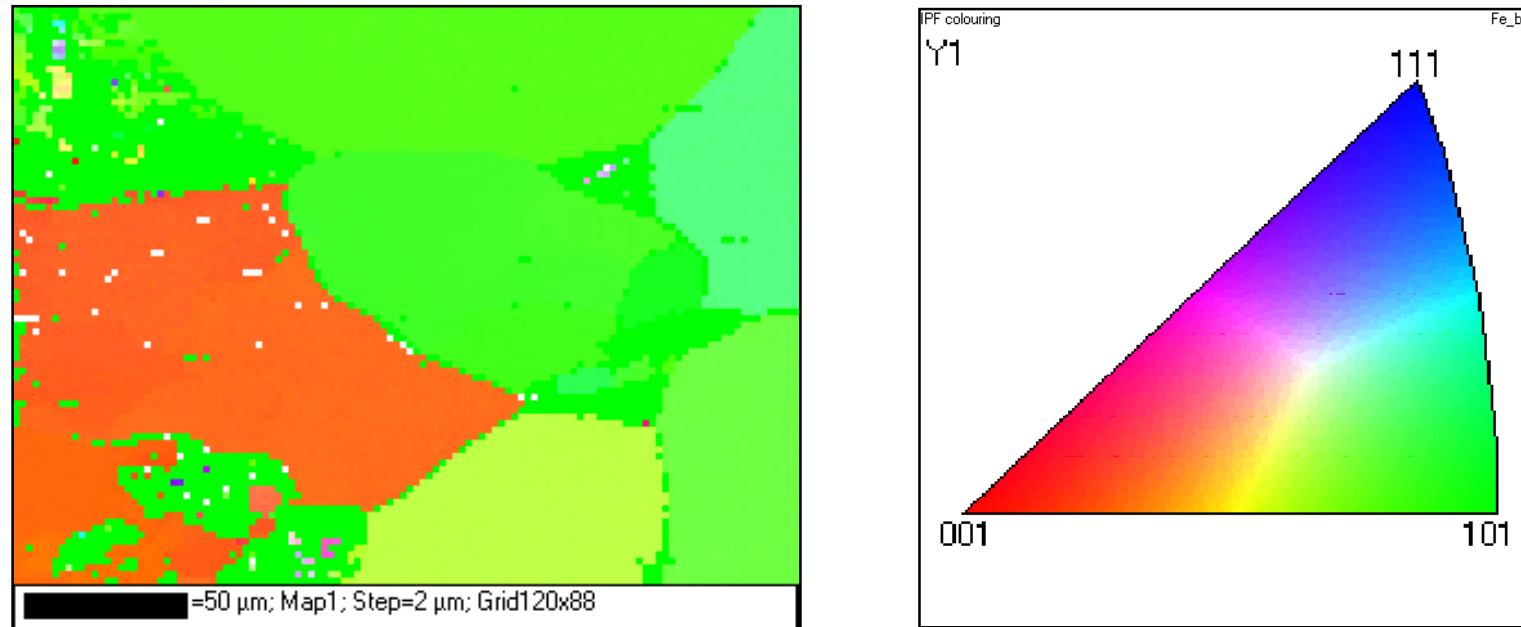
Project WIND-POWRK.05.02.00-00-1043/10

International interdisciplinary PhD Studies in Materials Science with English as the language of instruction

Project co-financed by the European Union within the European Social Funds



Fe0.05wt%C 725°C 554h

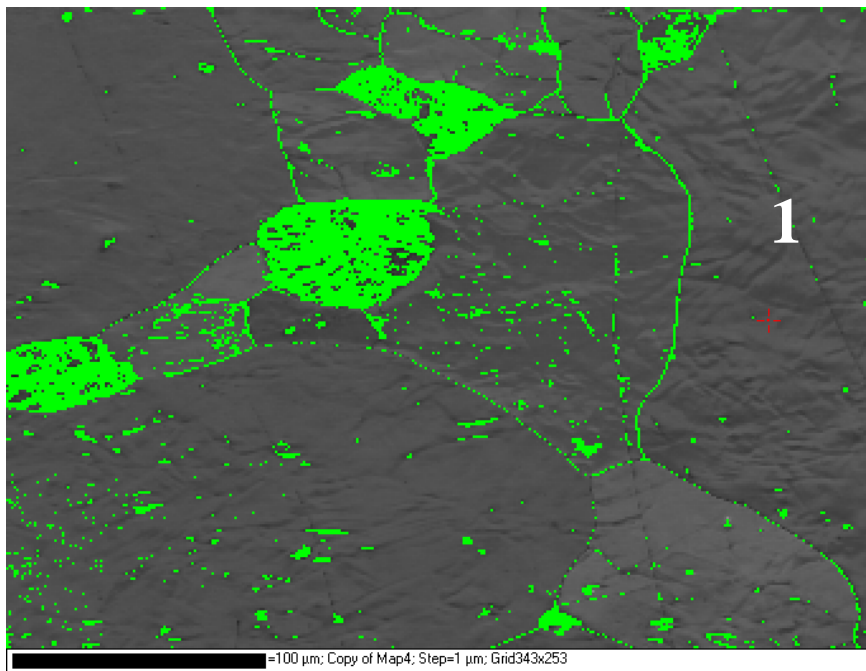


OIM Inverse Pole Figure Map

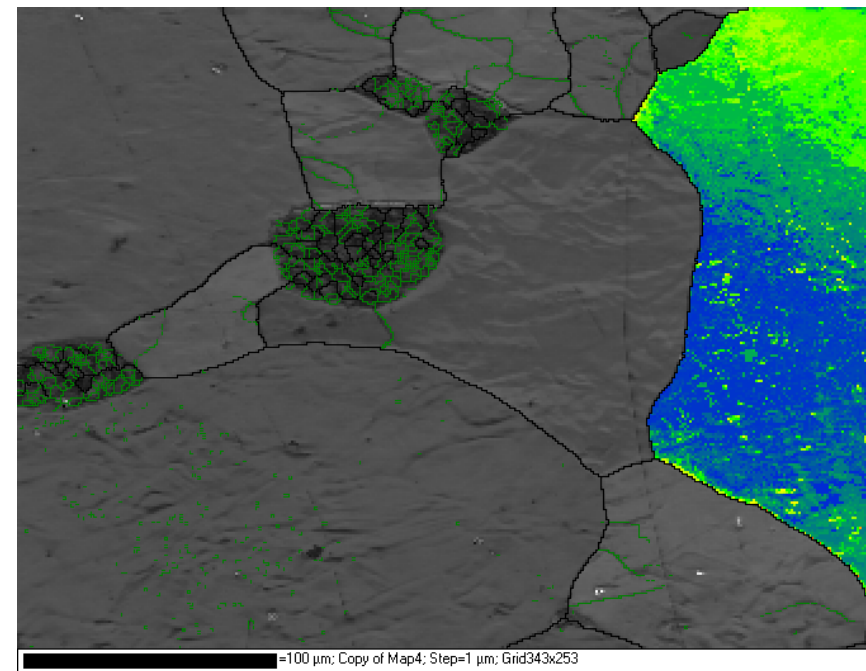
Color coding indicates crystal direction parallel to a reference direction (here // to transverse direction)



Fe0.05wt%C 725°C 554h



BC map (*Band Contrast*)



TC map (*Texture Component Map*)

Ideal orientation grain 1:

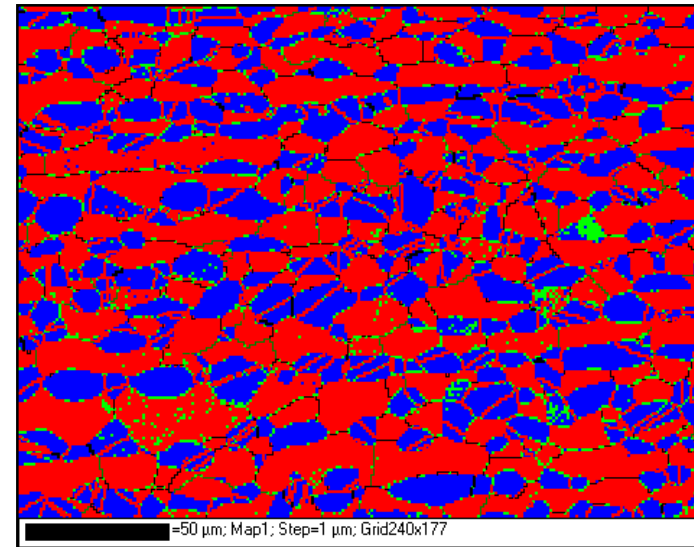
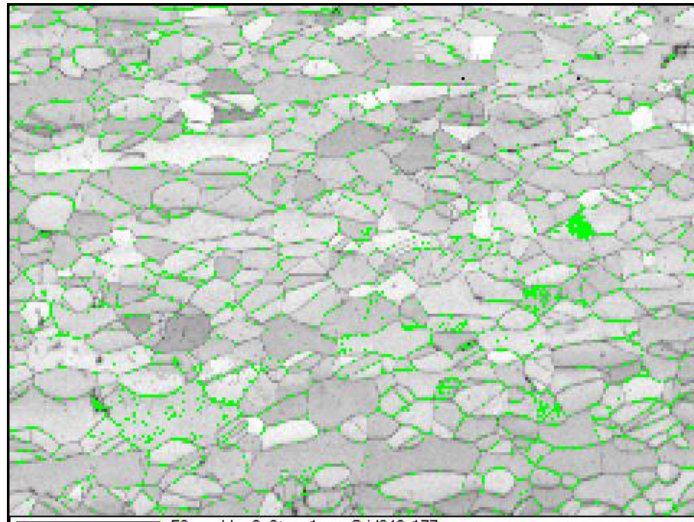
$$\phi_1=130,6^\circ, \Phi=40,1^\circ, \phi_2=67,0^\circ,$$

deviation from ideal orientation 1°

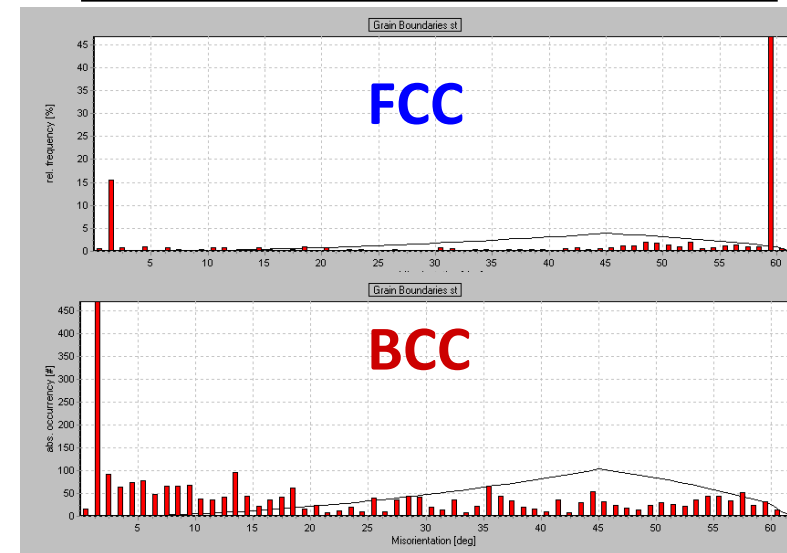
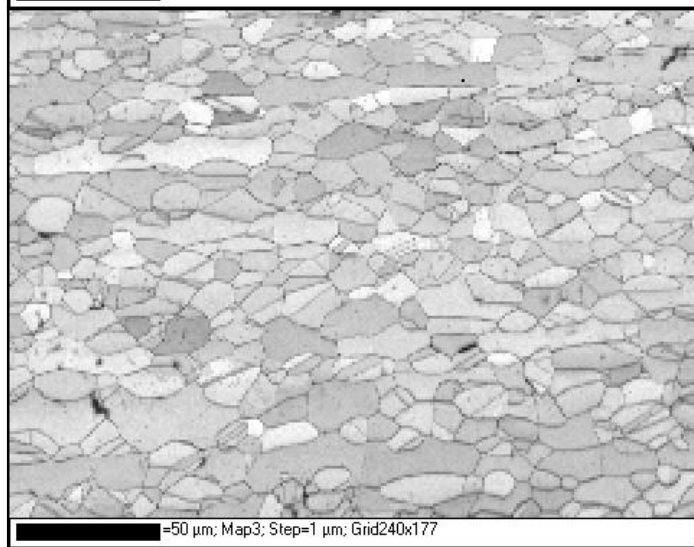


DUPLEX Steel

BC map (*Band Contrast + Noise*)



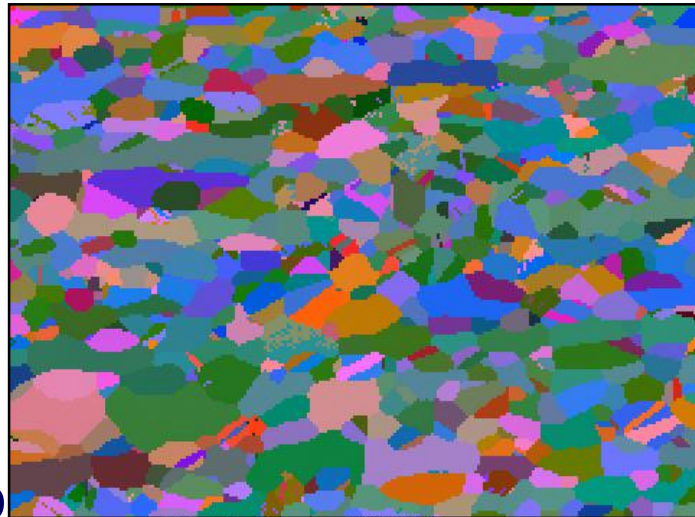
BC map after
noise reduction



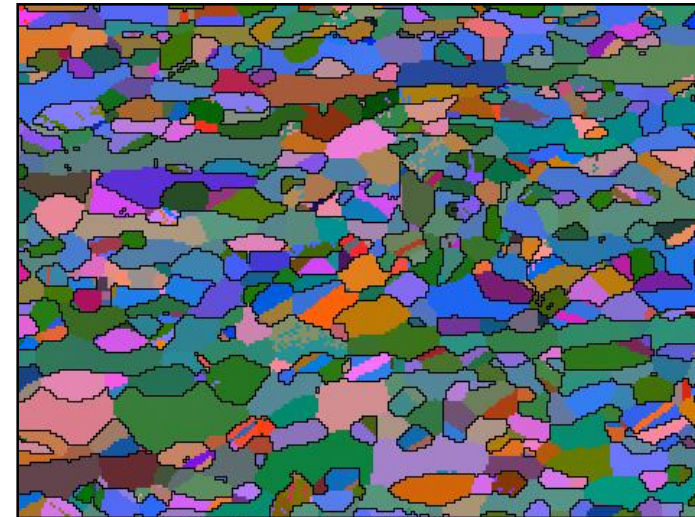
Phase map +
boundaries
distribution



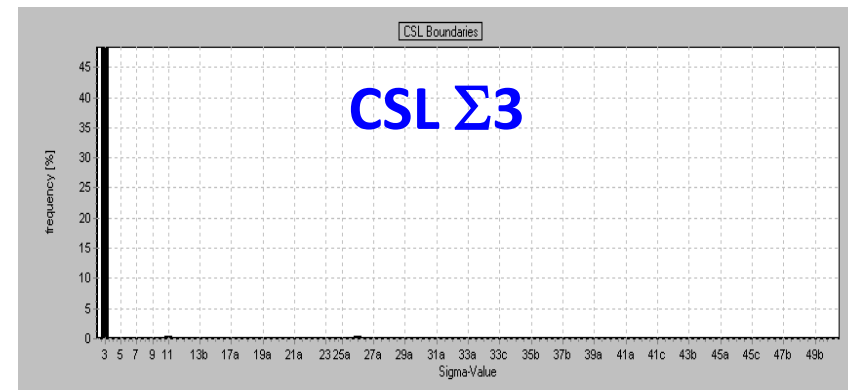
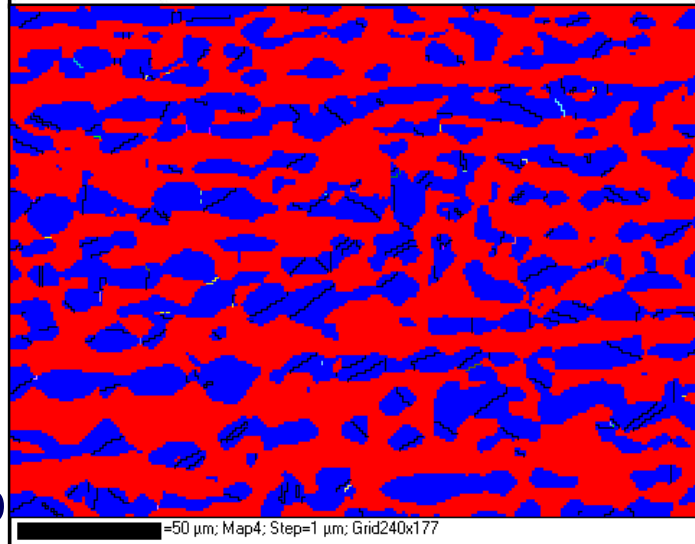
Orientation map



Orientation map + grain boundaries



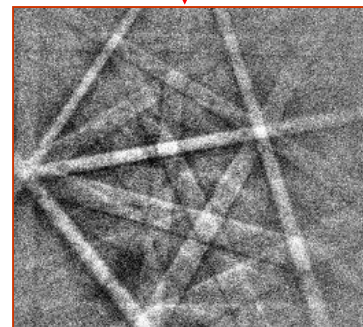
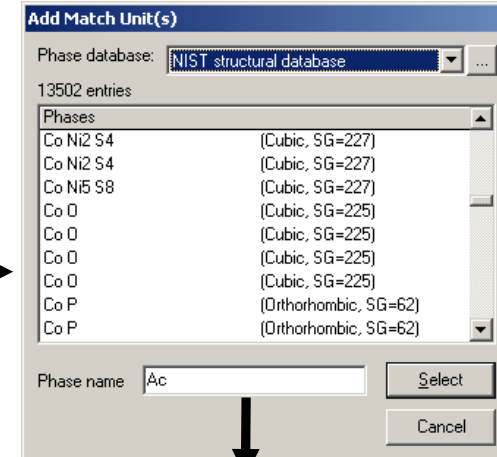
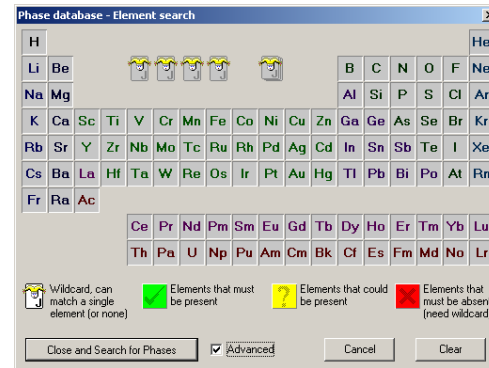
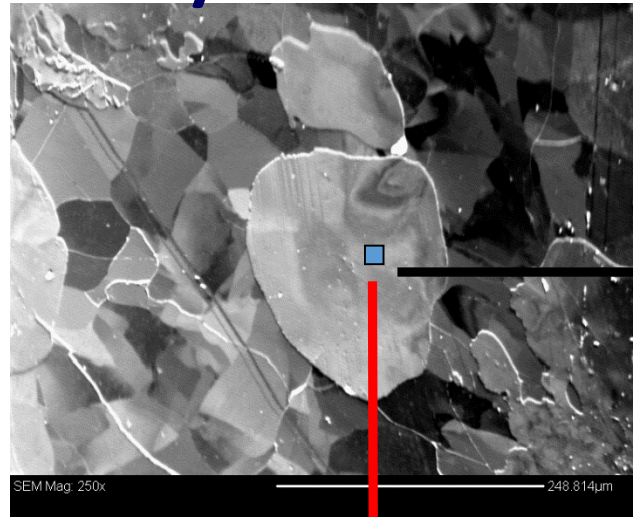
Phase map



CSL boundary – the description of a grain boundary by a specific coincidence of the crystal lattices across the boundary. The most common CSL boundaries (e.g. $\Sigma 3$, $\Sigma 9$, and $\Sigma 27$) are twin boundaries



EBSD/OIM – a techniques which requires standards



| Solutions: | | |
|------------------------------------|--------|-------|
| Phase | MAD | Bands |
| Aluminium | 0.0521 | 6 |
| Al As ₂ Cs ₃ | 1.9693 | 6 |
| Al As ₂ Cs ₃ | 1.9697 | 6 |
| Al As ₂ Cs ₃ | 1.9829 | 6 |

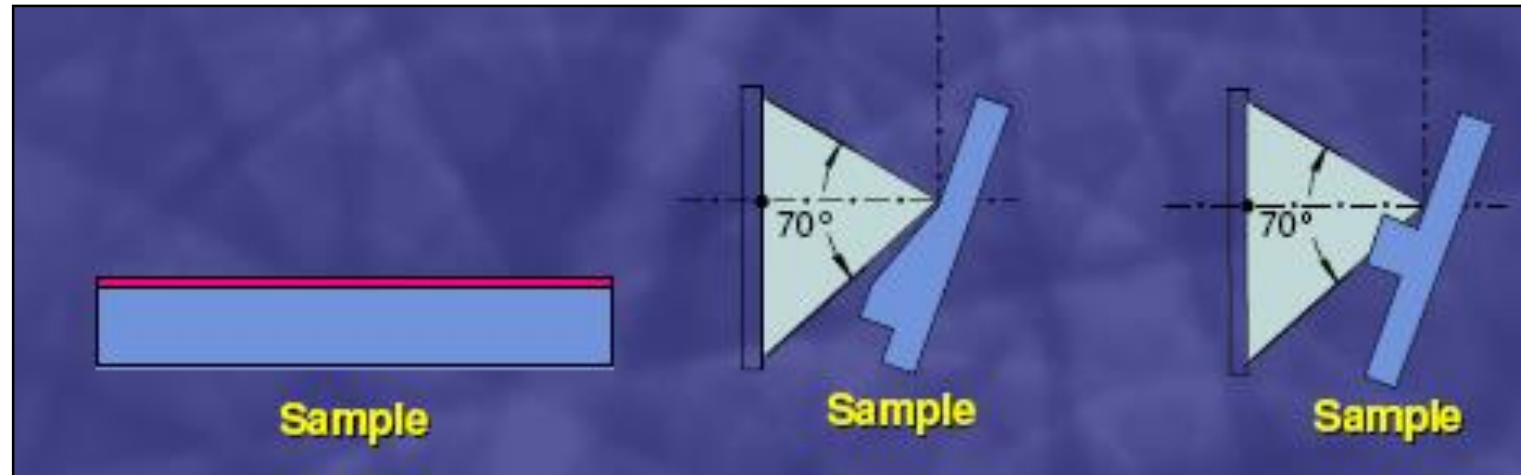
Project WND-POWR.03.02.00-00-1043/16

International interdisciplinary PhD Studies in Materials Science with English as the language of instruction

Project co-financed by the European Union within the European Social Funds



Sample preparation



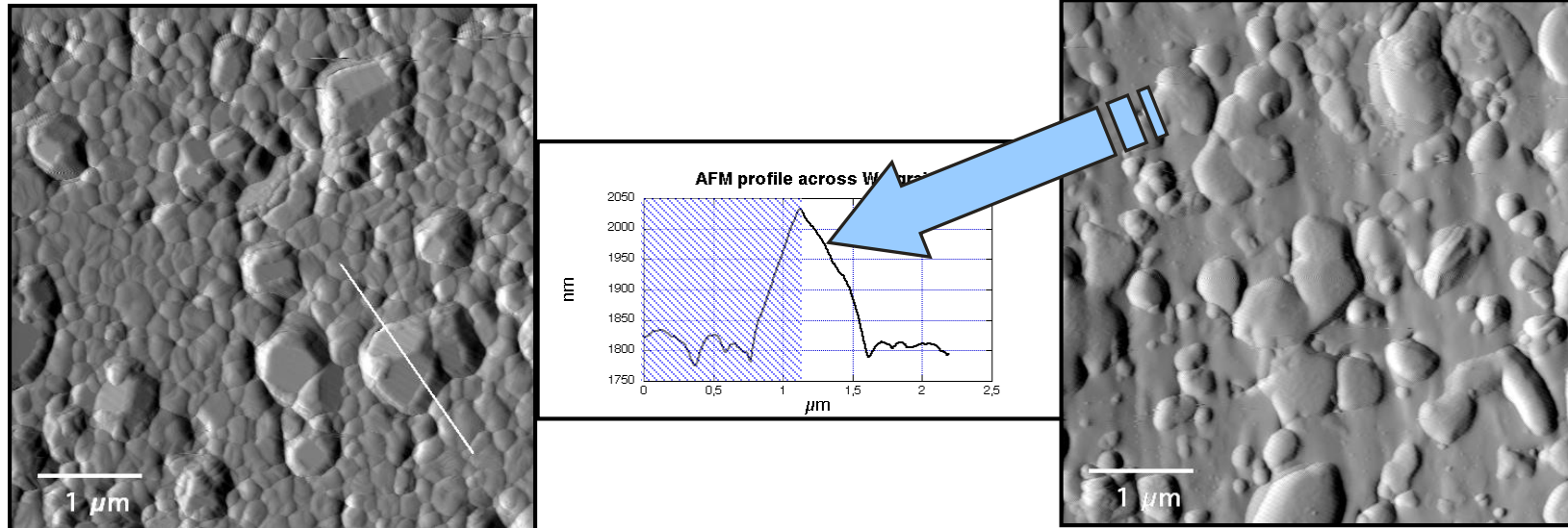
Specimen requirements for EBSD analysis:

Information depth is ~50 nm therefore:

- **Crystal structure should be continuous up the specimen surface**
- **No deformation layer, no oxidation layer, no coating**
- **Smooth surface layer only required to avoid shadowing**

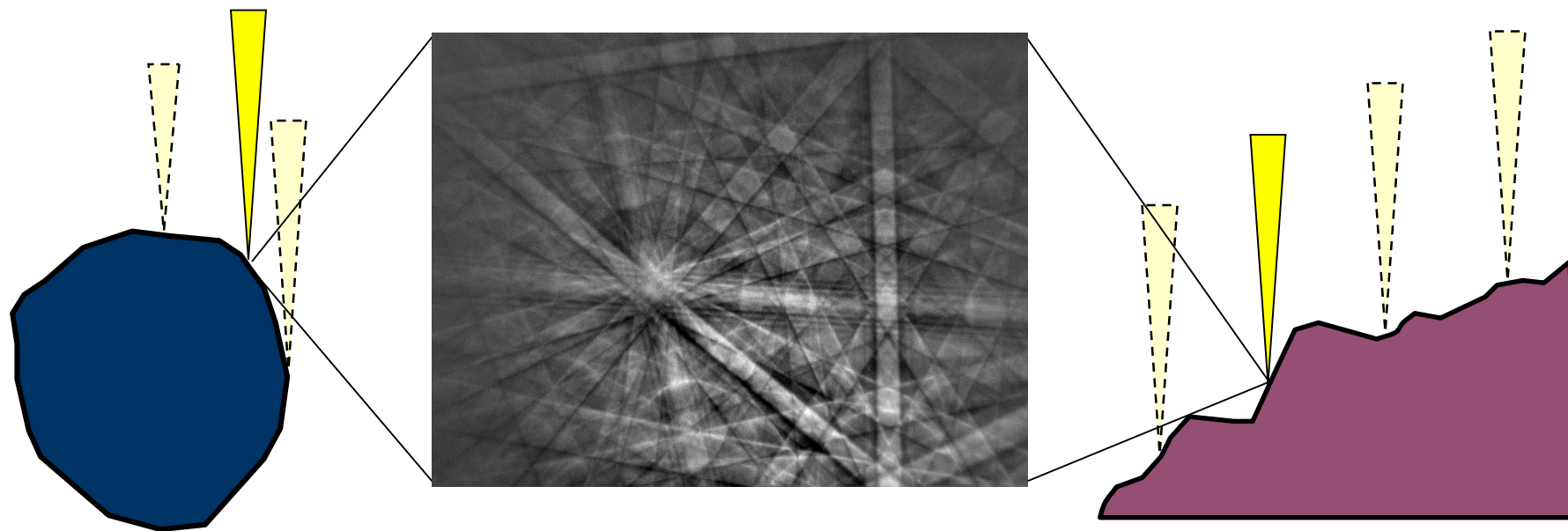


Y-TZP (0,2 – 0,3 μm) /WC composite



Thermal etching

**Mechanical
polishing by use of
colloidal silica**





5. A few examples

Project WND-POWR.03.02.00-00-1043/16

International interdisciplinary PhD Studies in Materials Science with English as the language of instruction

Project co-financed by the European Union within the European Social Funds



Phase map from emery rock sample

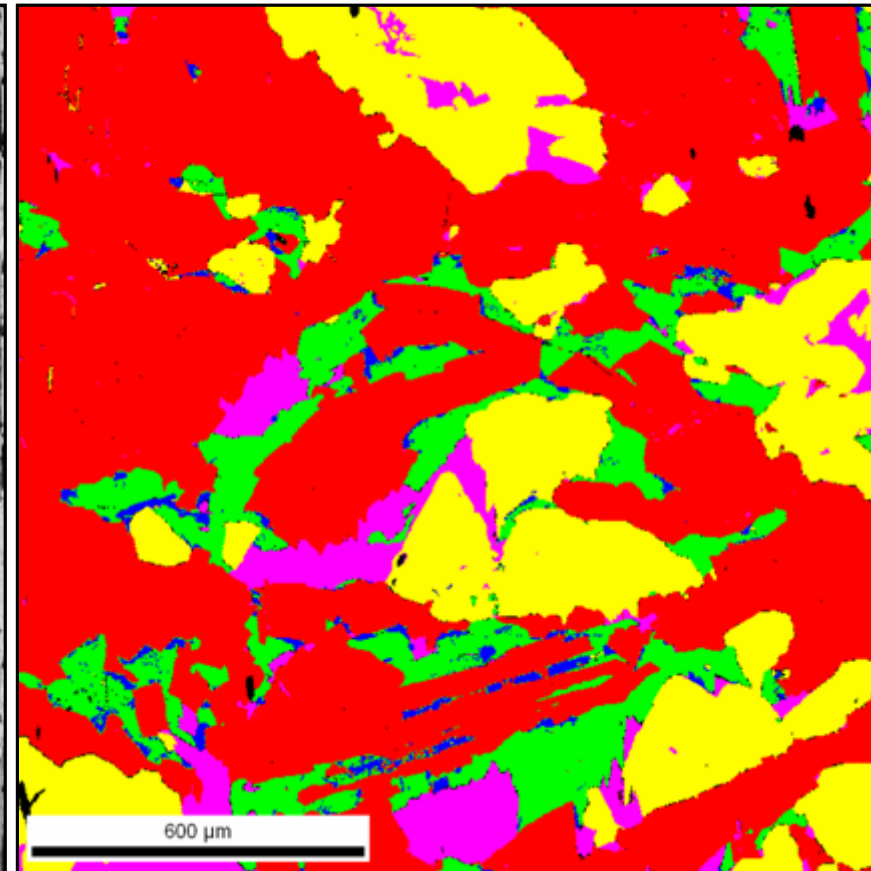
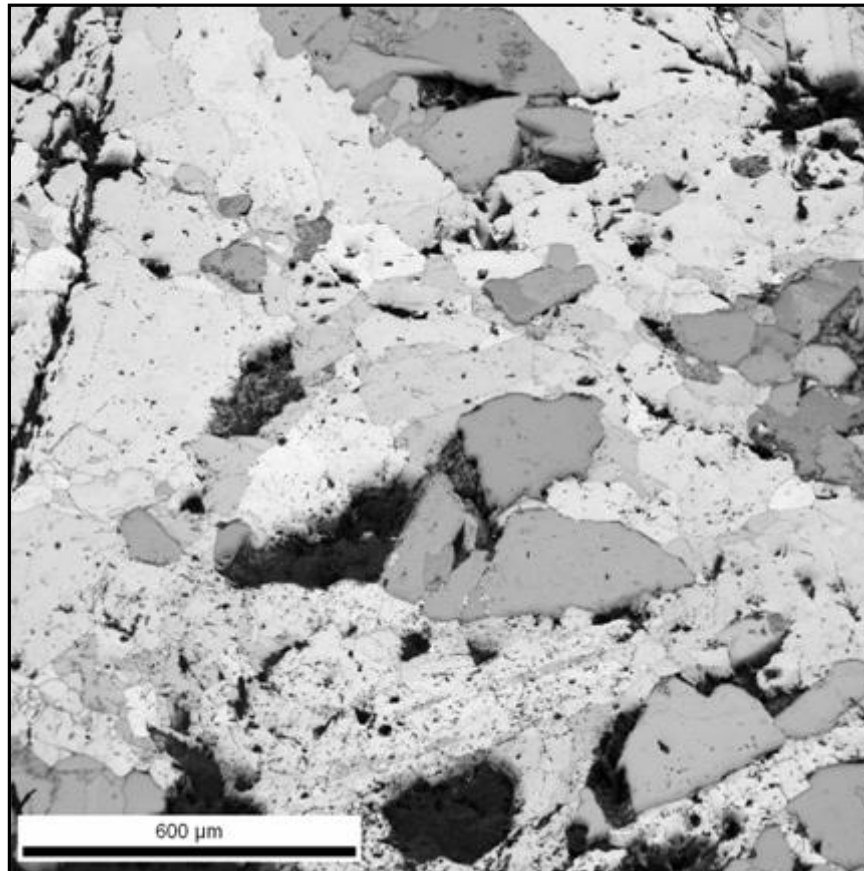


Image quality based on Band Contrast
(left) and Phase Map (right)

| Phase | |
|---|--|
|  | Fe ₃ O ₄ |
|  | FeTiO ₃ |
|  | Al ₂ O ₃ |
|  | TiO ₂ |
|  | Magnesium Iron Aluminum Silicate Hydroxide |

Courtesy of EDAX

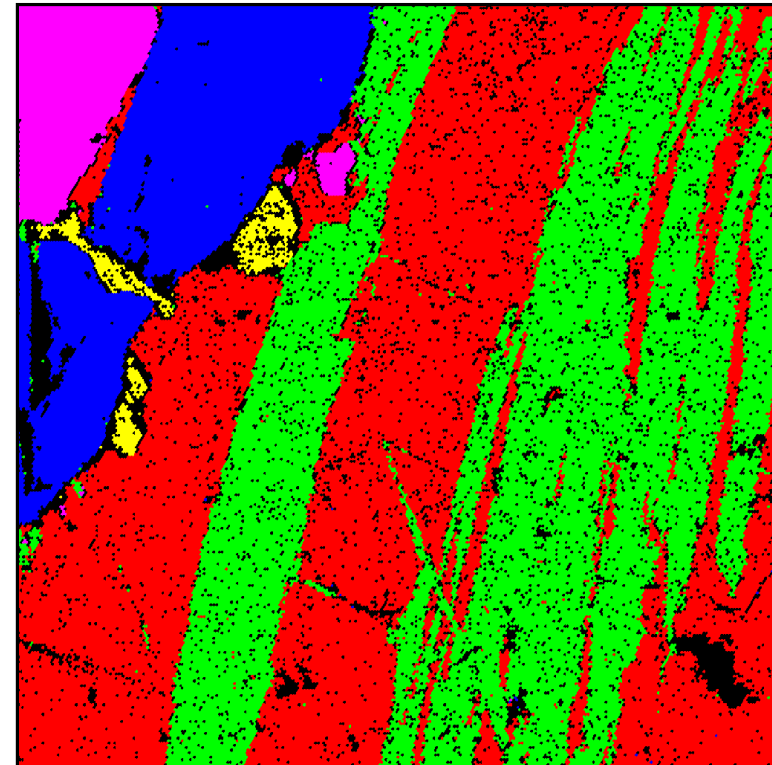
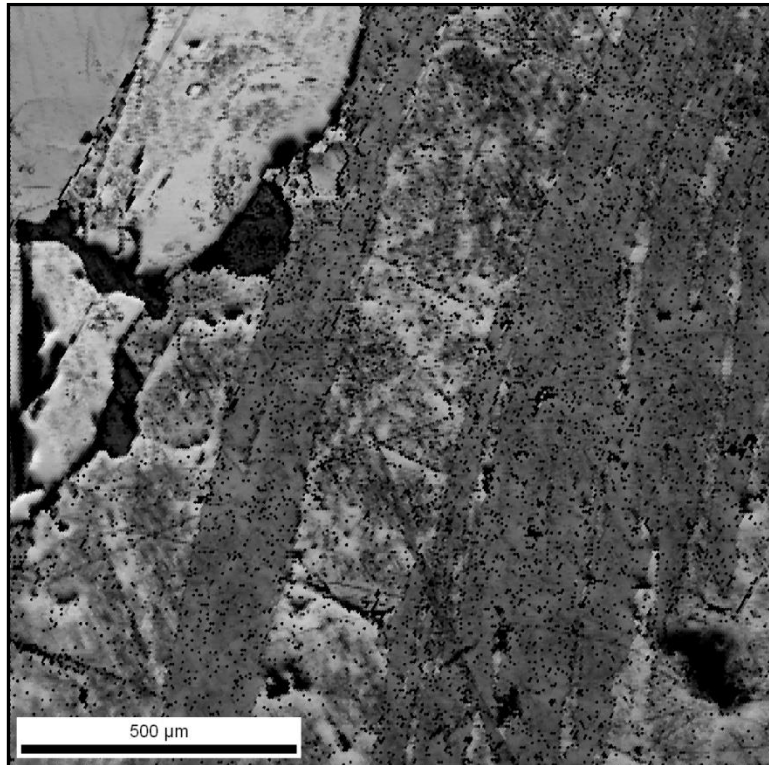


Image quality based on Band Contrast (left) and Phase Map (right)

| Phase | Total Fraction | Partition Fraction |
|--------------|----------------|--------------------|
| Chalcopyrite | 0.395 | 0.445 |
| Cubanite | 0.330 | 0.372 |
| Amphibole | 0.010 | 0.011 |
| Iron Oxide | 0.115 | 0.130 |
| Iron Sulfide | 0.039 | 0.044 |

Courtesy of EDAX



EBSD mapping can be used to identify coesite-quartz inclusions within garnet and provide unique data about the deformation of the surrounding garnet

Sample preparation: Final polish with colloidal silica, uncoated

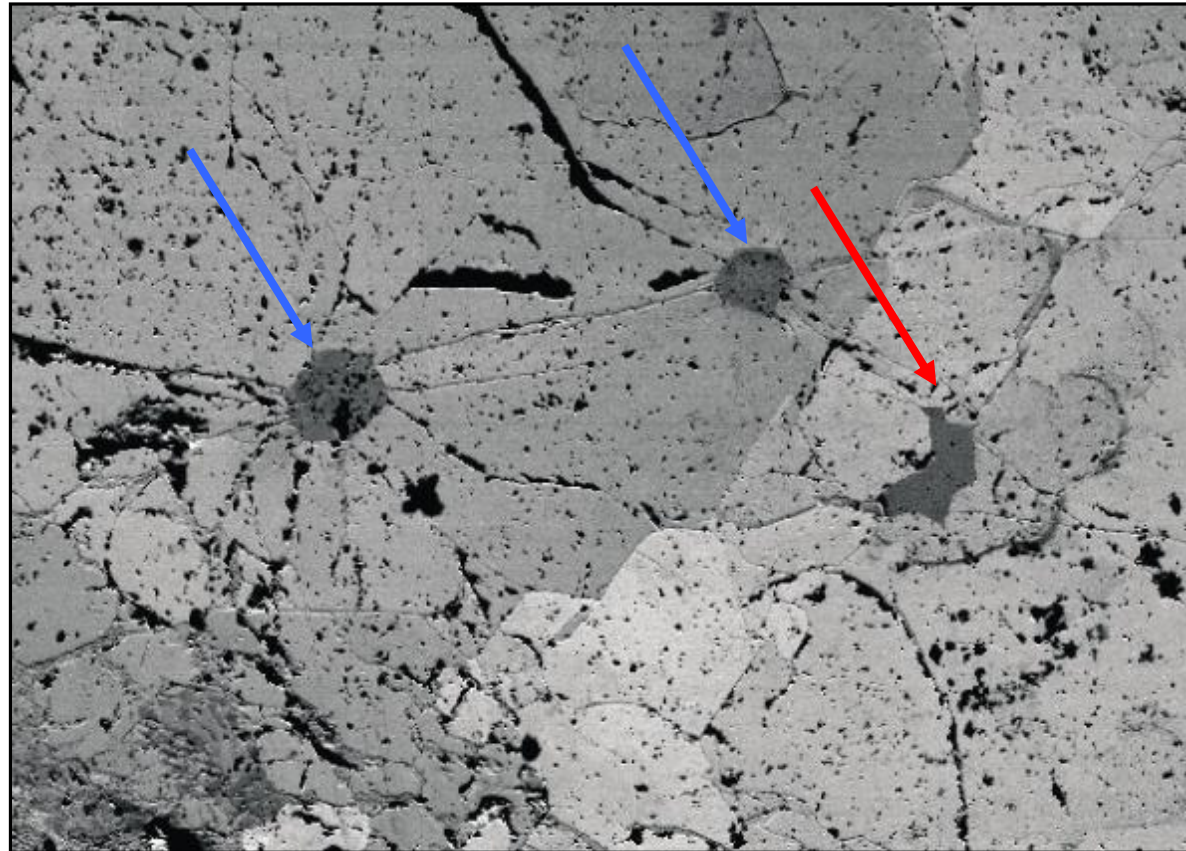
SEM type: FEG SEM

EBSD System: HKL CHANNEL5

Accelerating voltage: 20 kV

Probe Current: 12 nA

HKL Technology EBSD Application Catalogue 2005



Forward scattered electron image

General microstructure of the analyzed area.

Three prominent inclusions in dark grey, two of which shows the coesite-quartz transformation (radial fractures visible as dark lines).

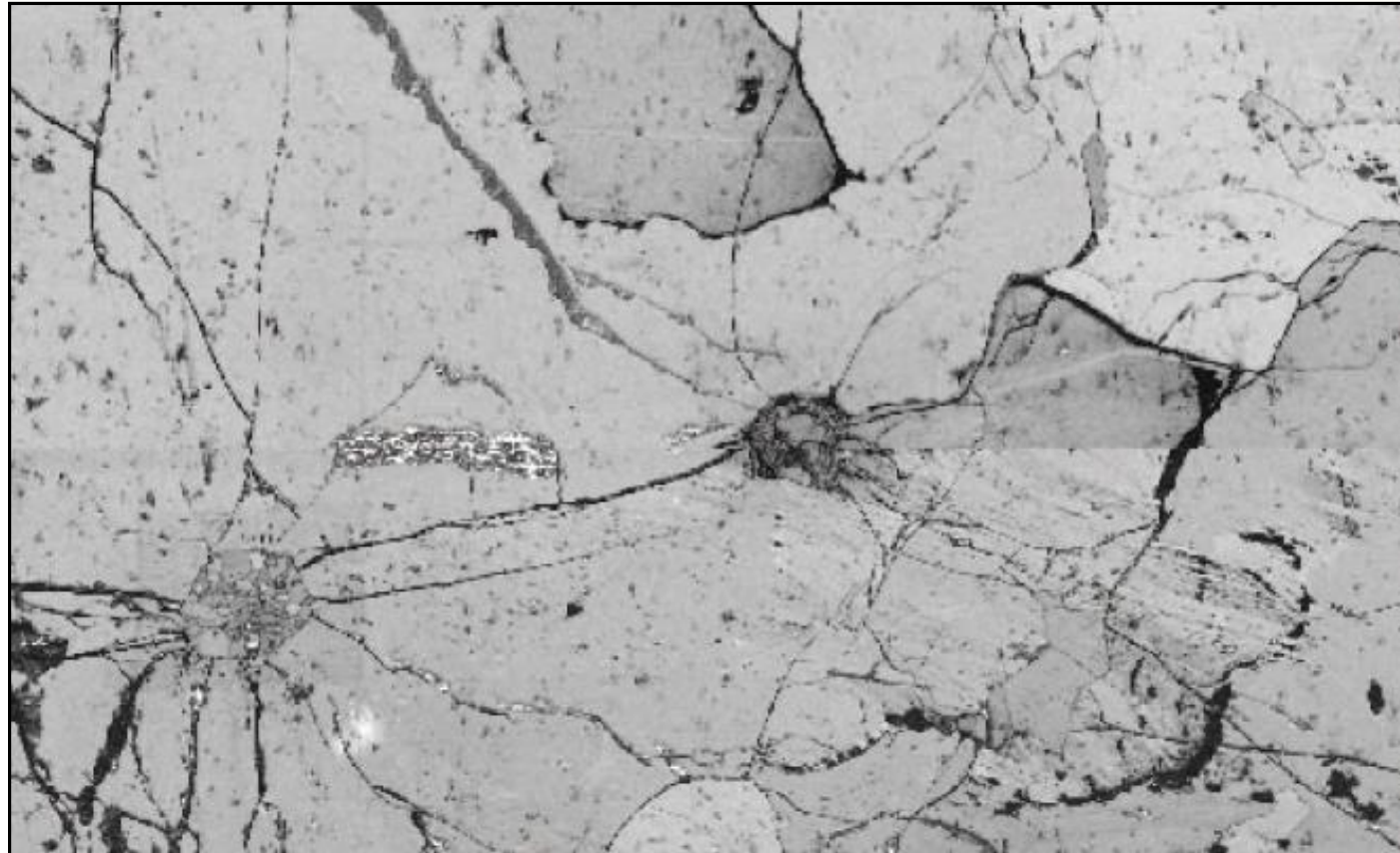
Grey scale variations in the surrounding garnet represent differences in crystal orientations („channeling contrast”)

Field of view = 1.2 mm

Project WND-POWR.03.02.00-00-1043/16

International interdisciplinary PhD Studies in Materials Science with English as the language of instruction

Project co-financed by the European Union within the European Social Funds



**EBSD quality
map**

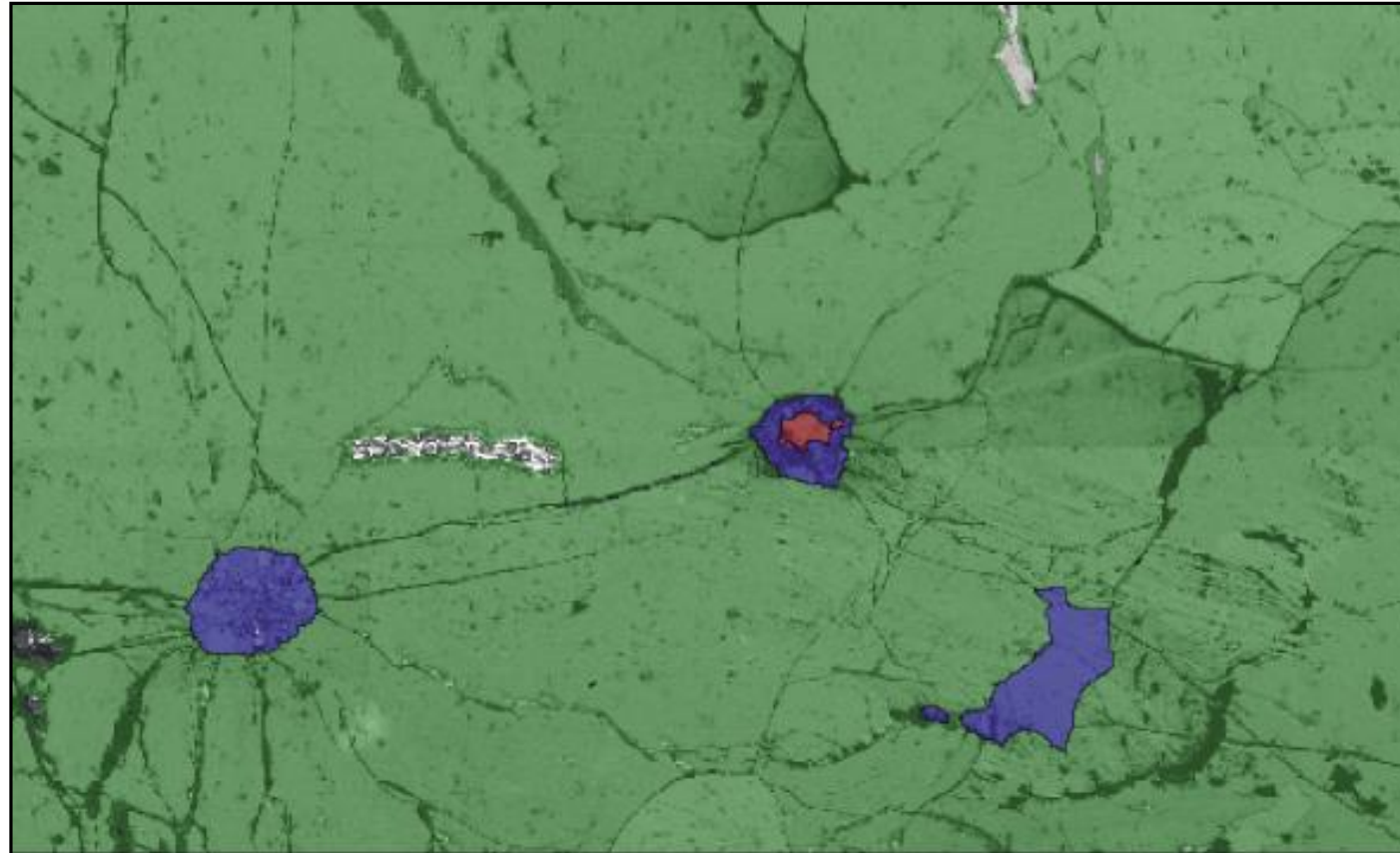
General microstructure of the analyzed area

Two of the inclusions (in the center and lower left part of the image) are prominent with radiating fractures, visible as black lines (poor EBSD quality)

Horizontal join of the 2 maps is visible across the center of the image.

Scale bar = 400 μ m

Project WND-POWR.03.02.00-00-1043/16



Phase map

Distribution of three phases across the area

Garnet is marked in green, quartz in blue and coesite in red.

The central inclusion has a core of coesite surrounded by a rim of quartz.

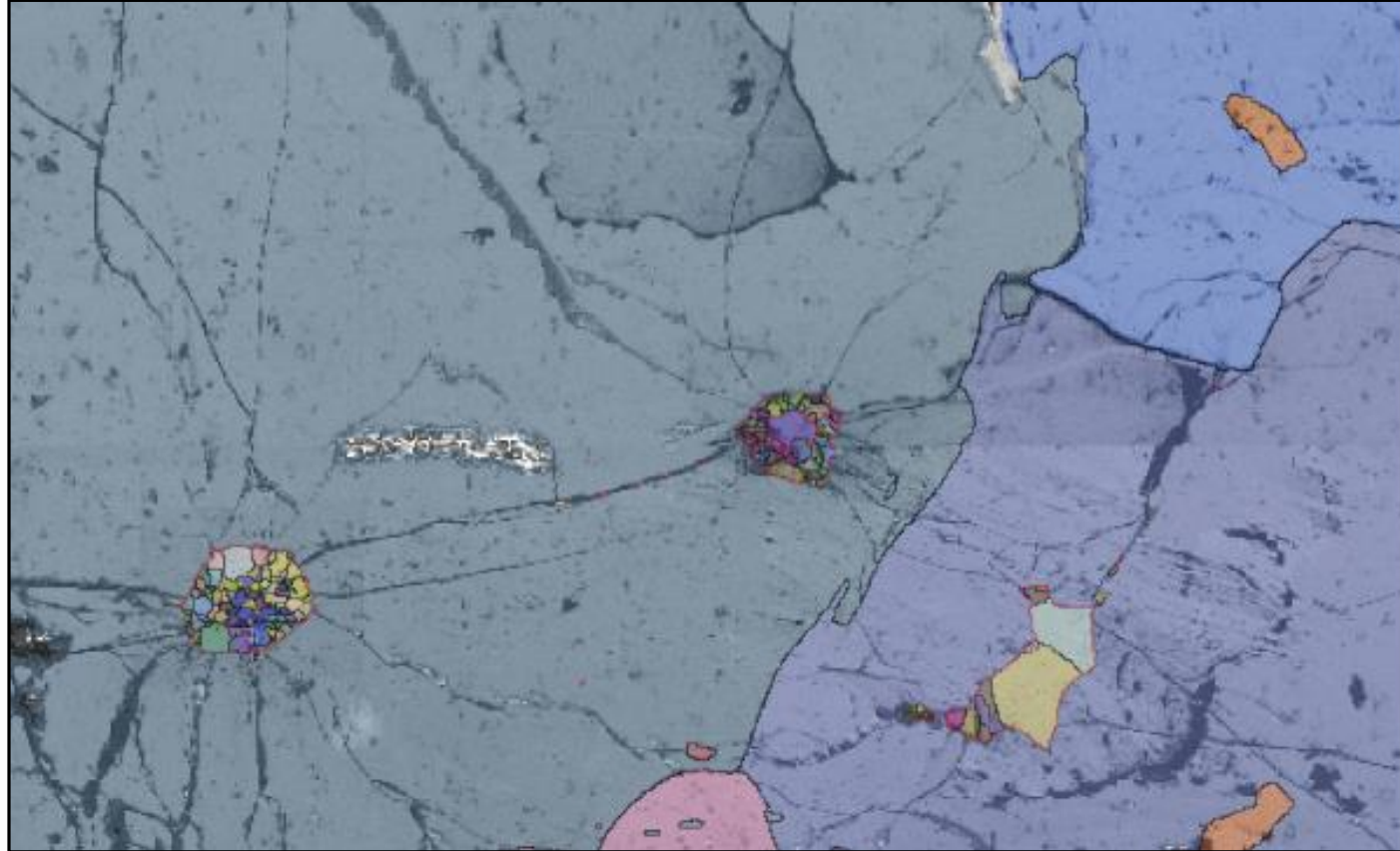
The lower-left inclusion has completely reverted to quartz.

Radiating from the prominent inclusions are fractures, visible as black lines (poor EBSD quality)

Project WND-POWR.03.02.00-00-1043/16

International interdisciplinary PhD Studies in Materials Science with English as the language of instruction

Project co-financed by the European Union within the European Social Funds



Orientation map

**Crystallographic orientations of all three minerals
Colors corresponding to the Euler angles.**

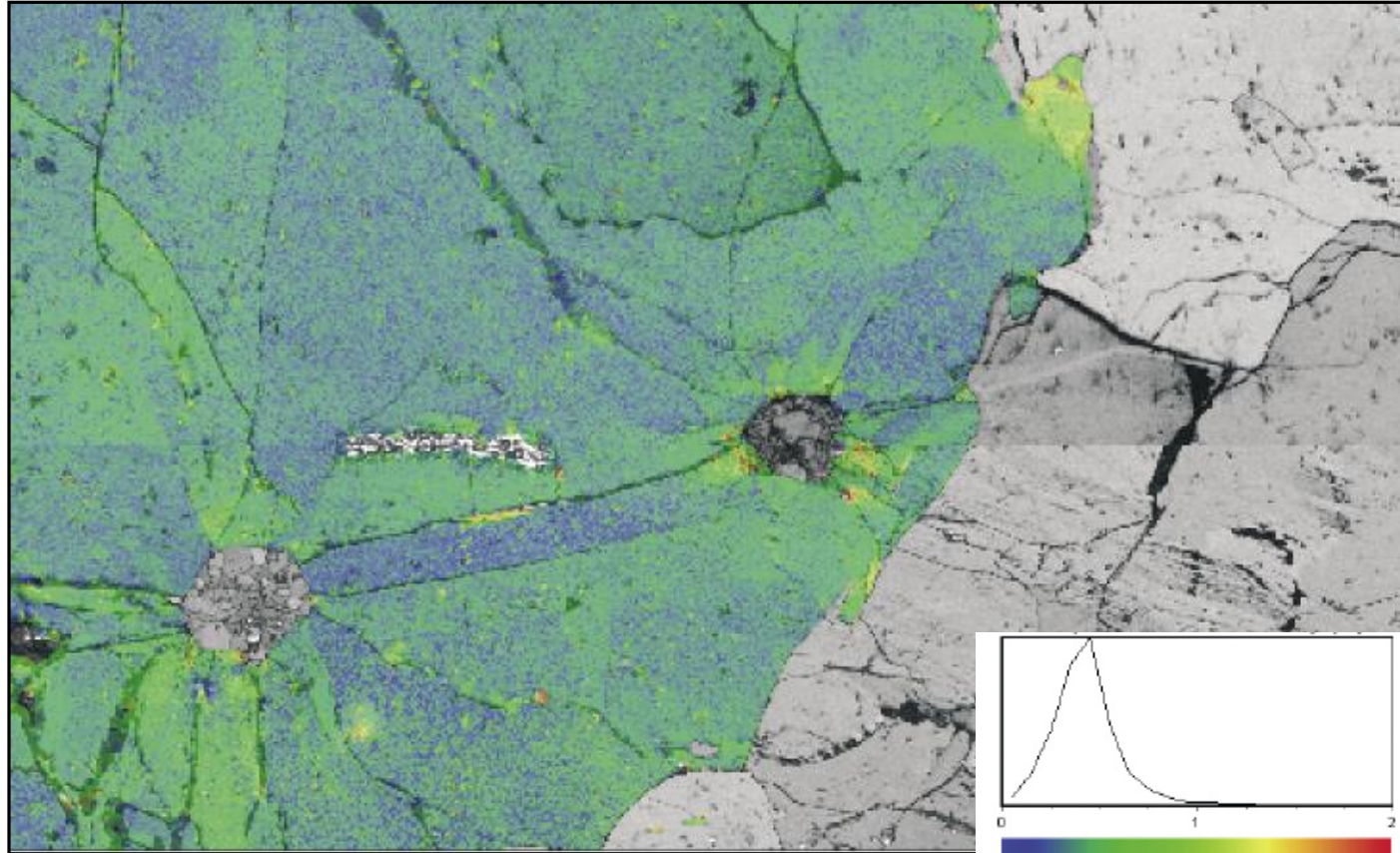
Grain boundaries are marked in black, phase boundaries are marked in red

The whole area is comprised of only a few garnet grains. The quartz in the inclusions is polycrystalline with grain boundaries radiating from the center. The coesite in the central inclusion is a single crystal

Project WND-POWR.03.02.00-00-1043/16

International interdisciplinary PhD Studies in Materials Science with English as the language of instruction

Project co-financed by the European Union within the European Social Funds



Deformation map

Deformation of the garnet around the coesite/quartz inclusions

The attempted change from coesite to quartz has tried to expand the inclusion, thereby causing radial cracks and deformation in the garnet.

This means that the garnet crystal has acted as a protective pressure vessel, so that pieces of coesite have been preserved.

Small scale of deformation in the large garnet grain (less than 2°)

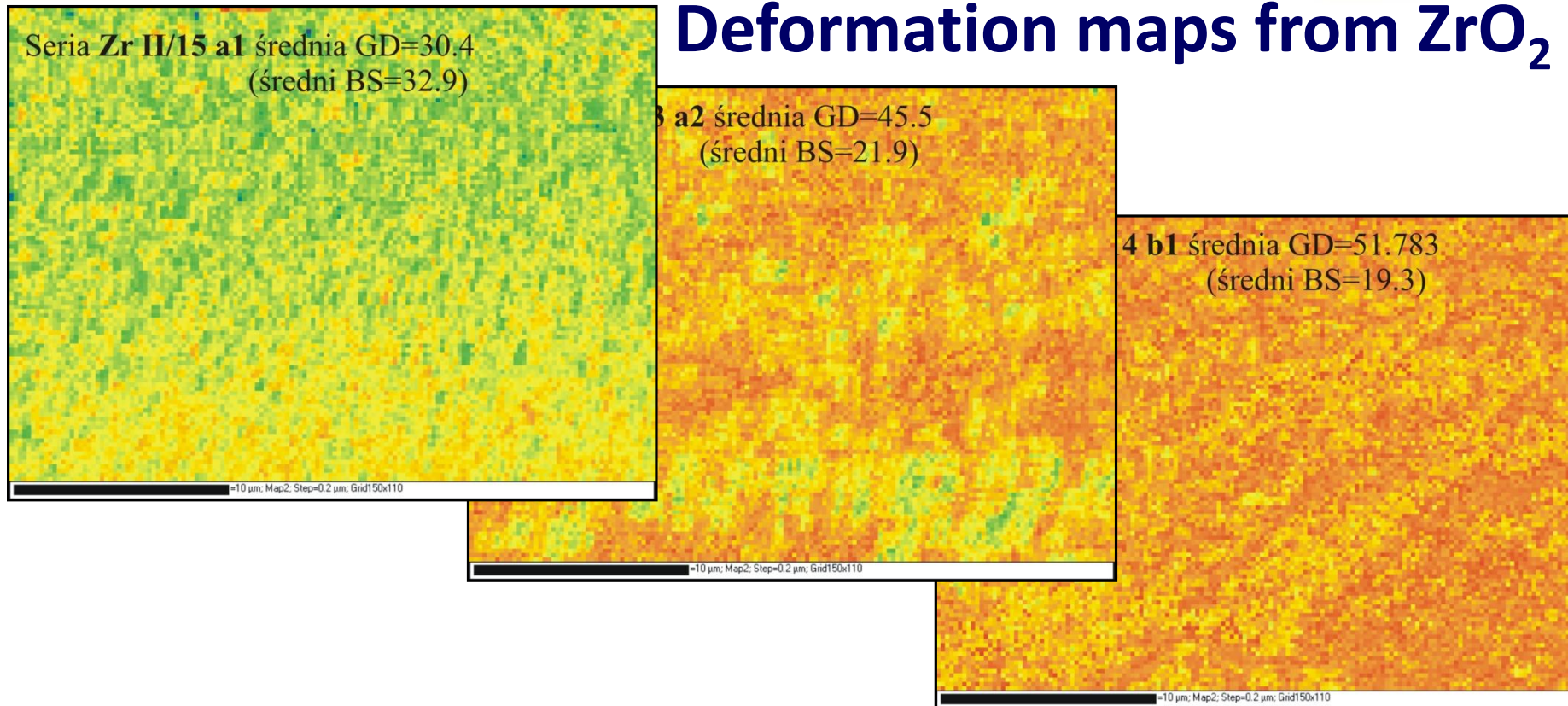
Project WND-POWR.03.02.00-00-1043/16

International interdisciplinary PhD Studies in Materials Science with English as the language of instruction

Project co-financed by the European Union within the European Social Funds



Deformation maps from ZrO_2



Development of deformation in the zirconia polycrystals exposed to „shot peening”

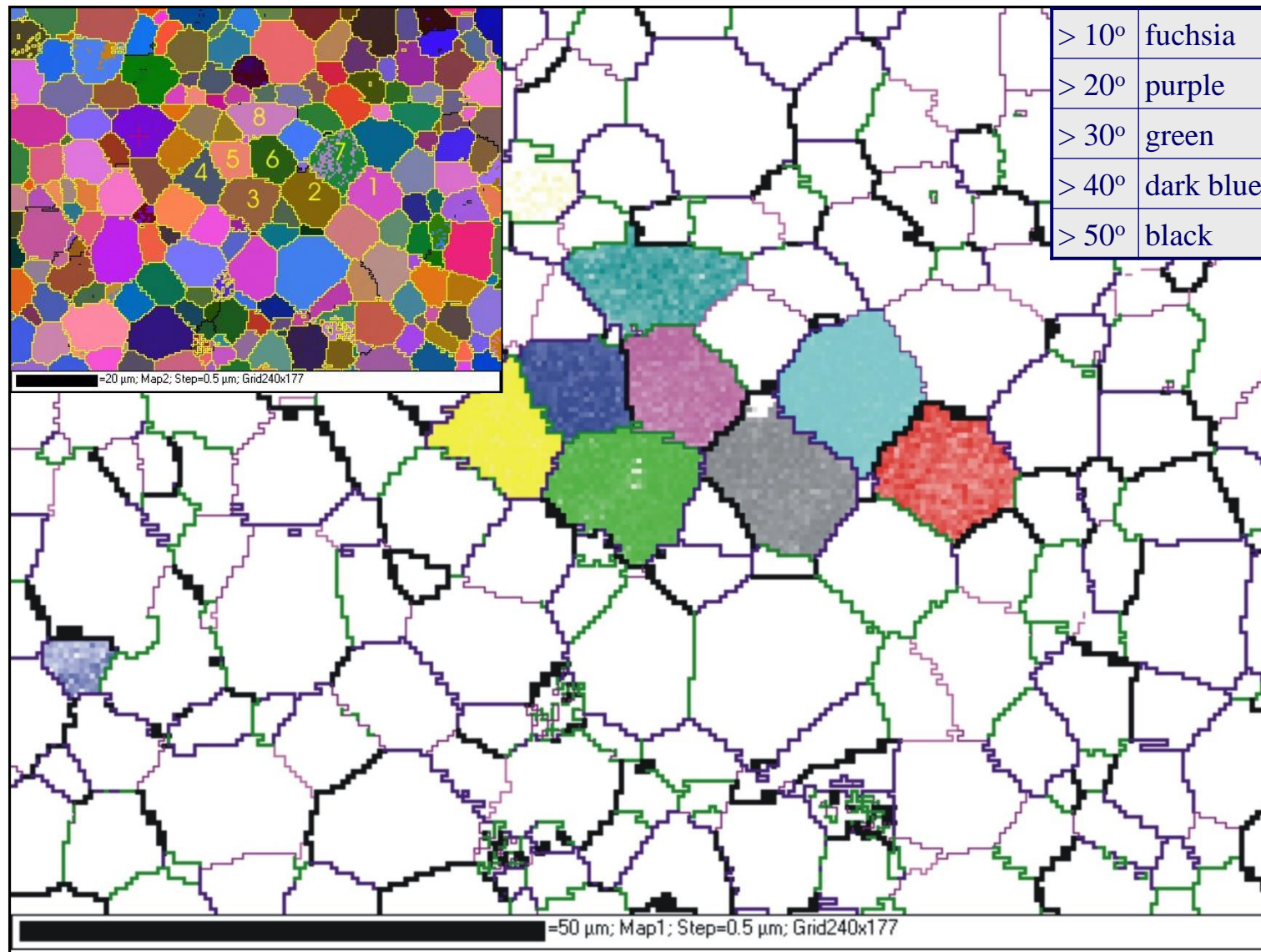
Deformation maps exhibit the increase of dislocation density.

Shot peening is a process used to produce a compressive residual stress layer and modify mechanical properties of surface layers in metals and ceramics by impacting a surface with shot (round metallic, glass or ceramic particles) with force sufficient to create plastic deformation.

Project WND-POWR.03.02.00-00-1043/16

International interdisciplinary PhD Studies in Materials Science with English as the language of instruction

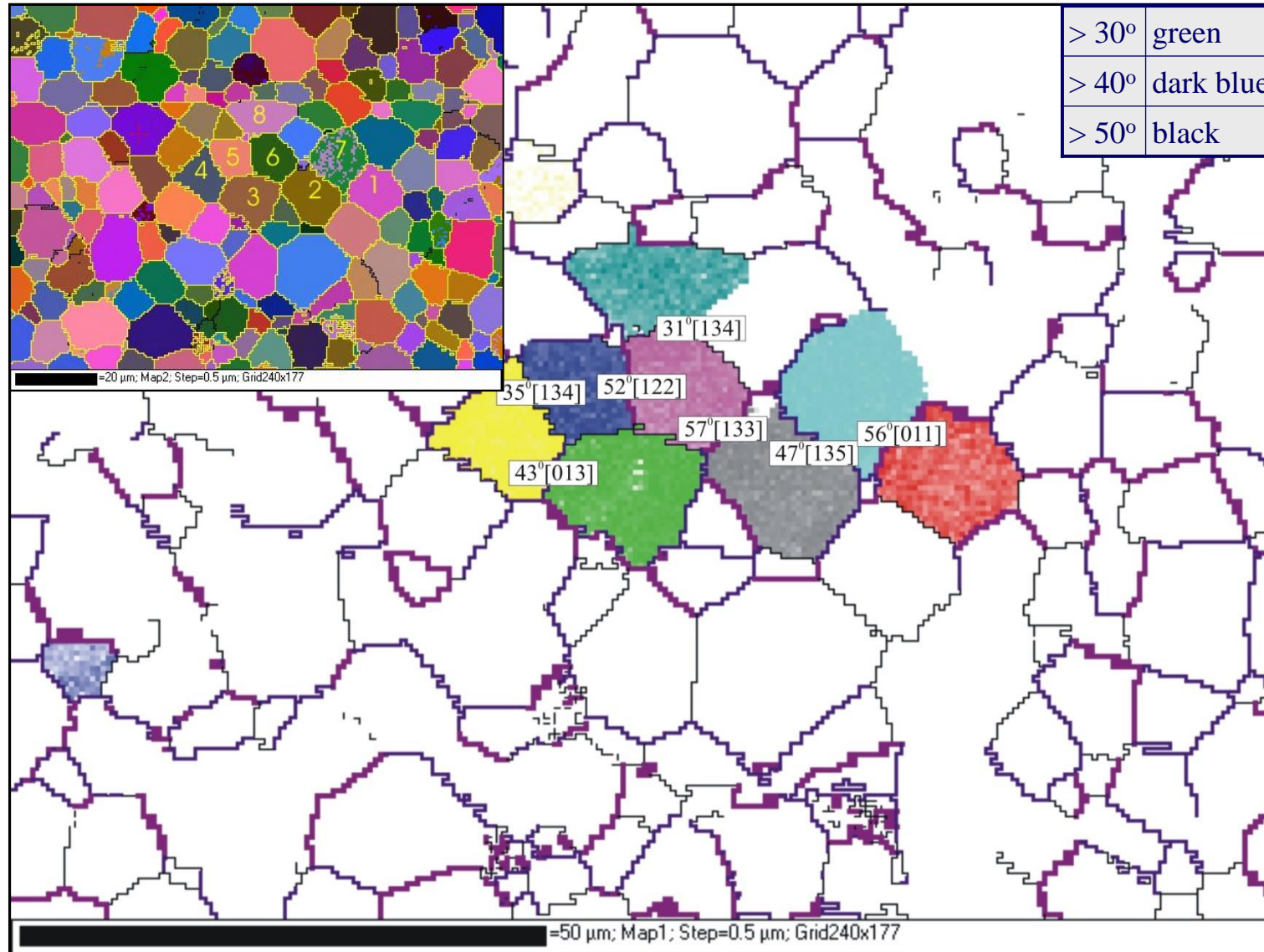
Project co-financed by the European Union within the European Social Funds



Project WND-POWR.03.02.00-00-1043/16

International interdisciplinary PhD Studies in Materials Science with English as the language of instruction

Project co-financed by the European Union within the European Social Funds



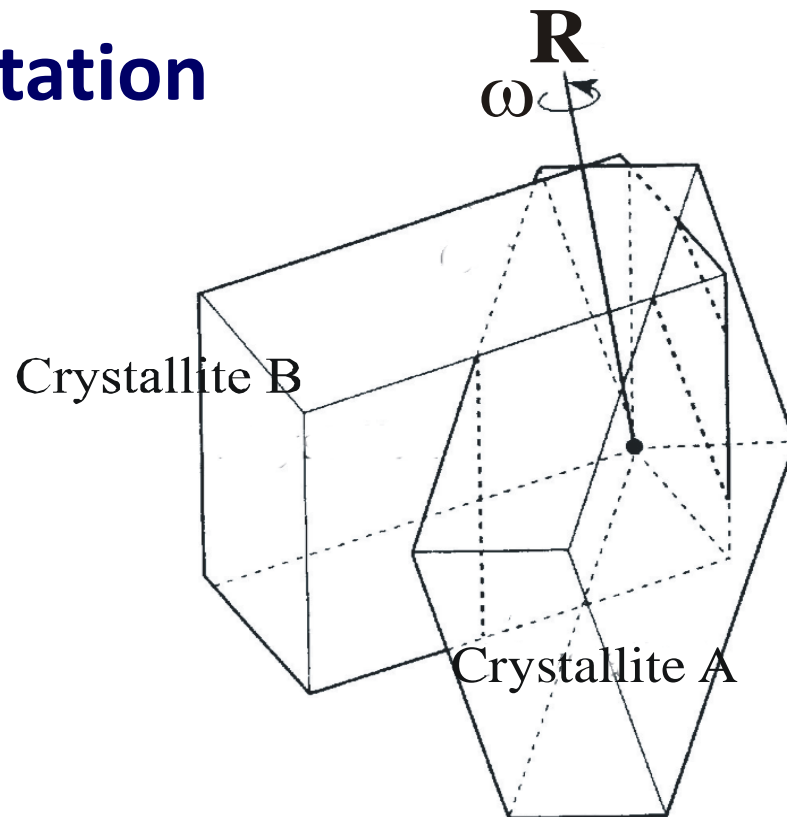
Project WND-POWR.03.02.00-00-1043/16

International interdisciplinary PhD Studies in Materials Science with English as the language of instruction

Project co-financed by the European Union within the European Social Funds



Misorientation



Misorientation between two crystals A and B is defined as rotation transforming the crystallite B reference system into the crystallite A reference system.

$$K_A = \Gamma_{AB} \cdot K_B$$

$$\Gamma_{AB}^e = S_i \cdot \Gamma_{AB} \cdot P_j$$

$(i = 1, \dots, M, j = 1, \dots, N)$

where: S_i and P_j are symmetry elements of the first and second crystal

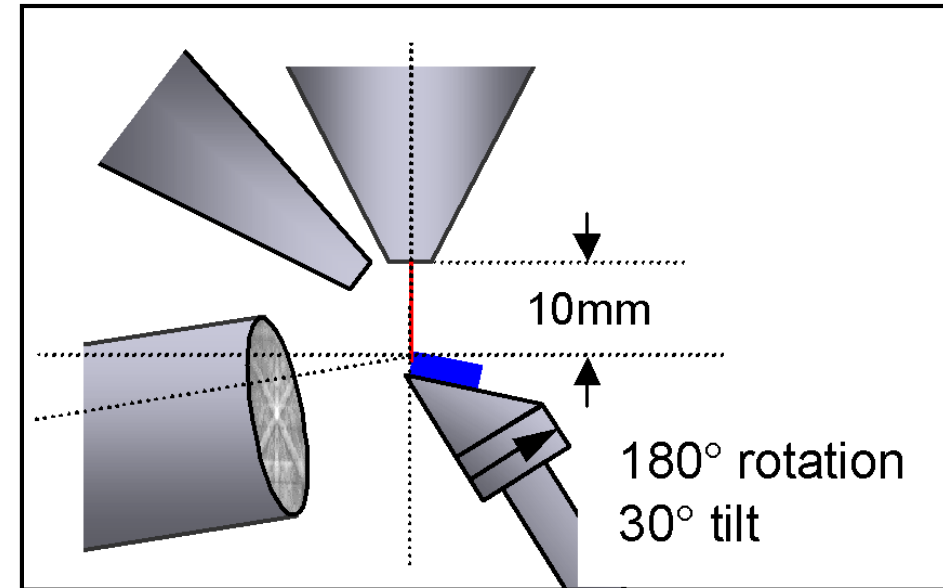
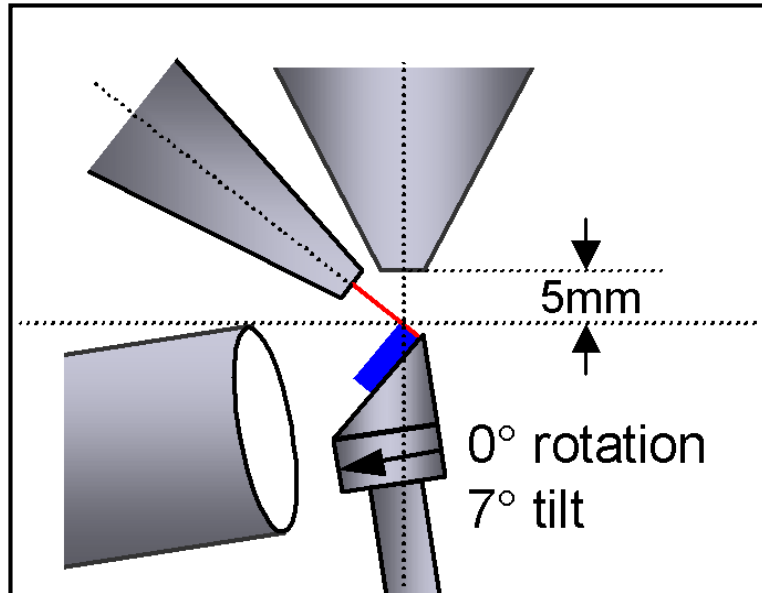
Misorientation can be described mathematically in several ways:

- axis/angle pair
- rotation matrix,
- Euler angles,
- quaternions,
- Rodrigues vectors

K. Sztwiertnia, M. Faryna, G. Sawina, Journal of Journal of Microscopy, Vol. 224, 2006, 4

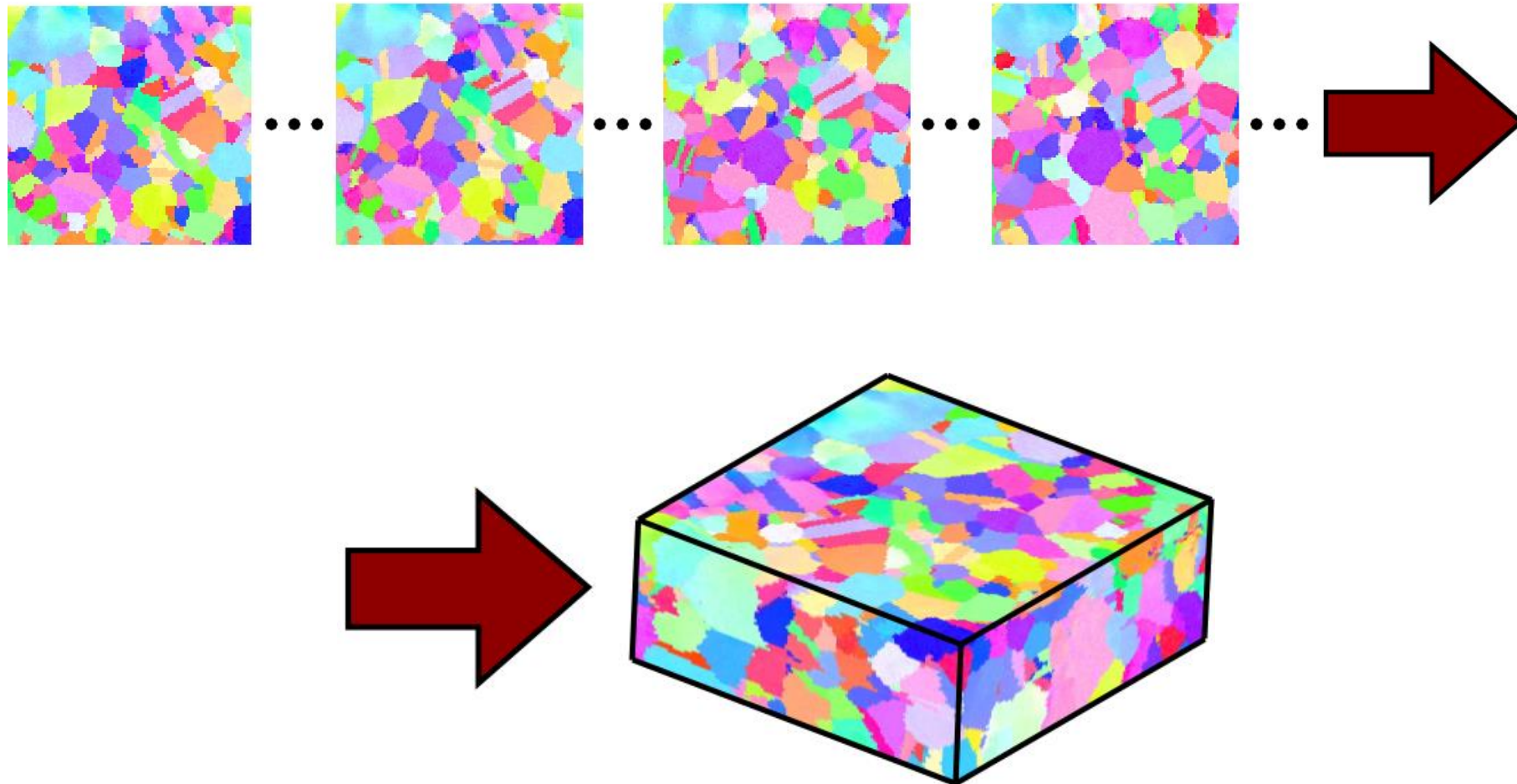


Serial Sectioning in a Dual Beam FIB-SEM





Serial Sectioning – Volume View



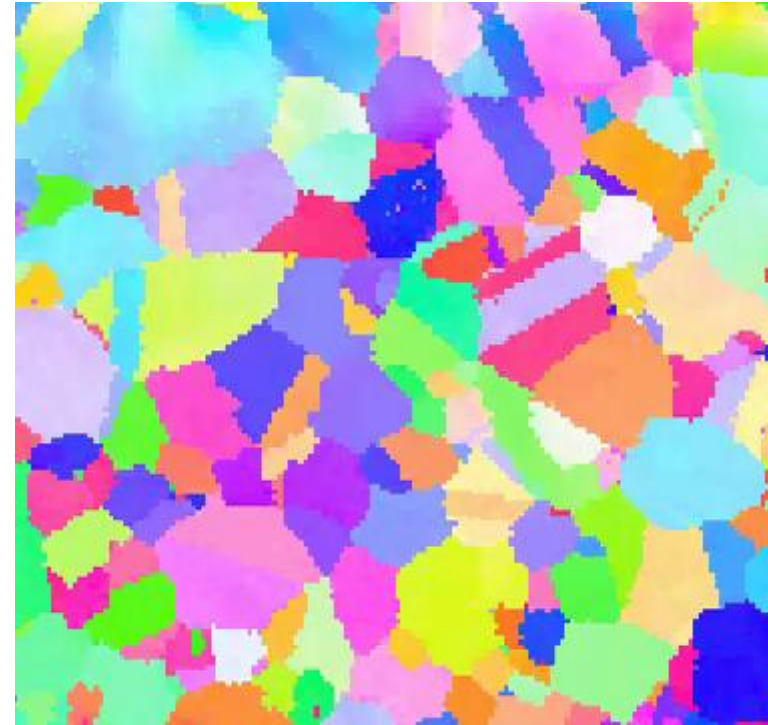
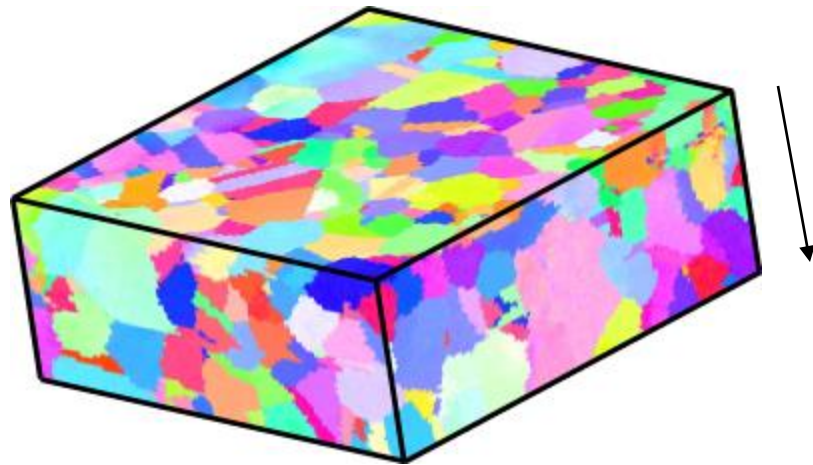
Project WND-POWR.03.02.00-00-1043/16

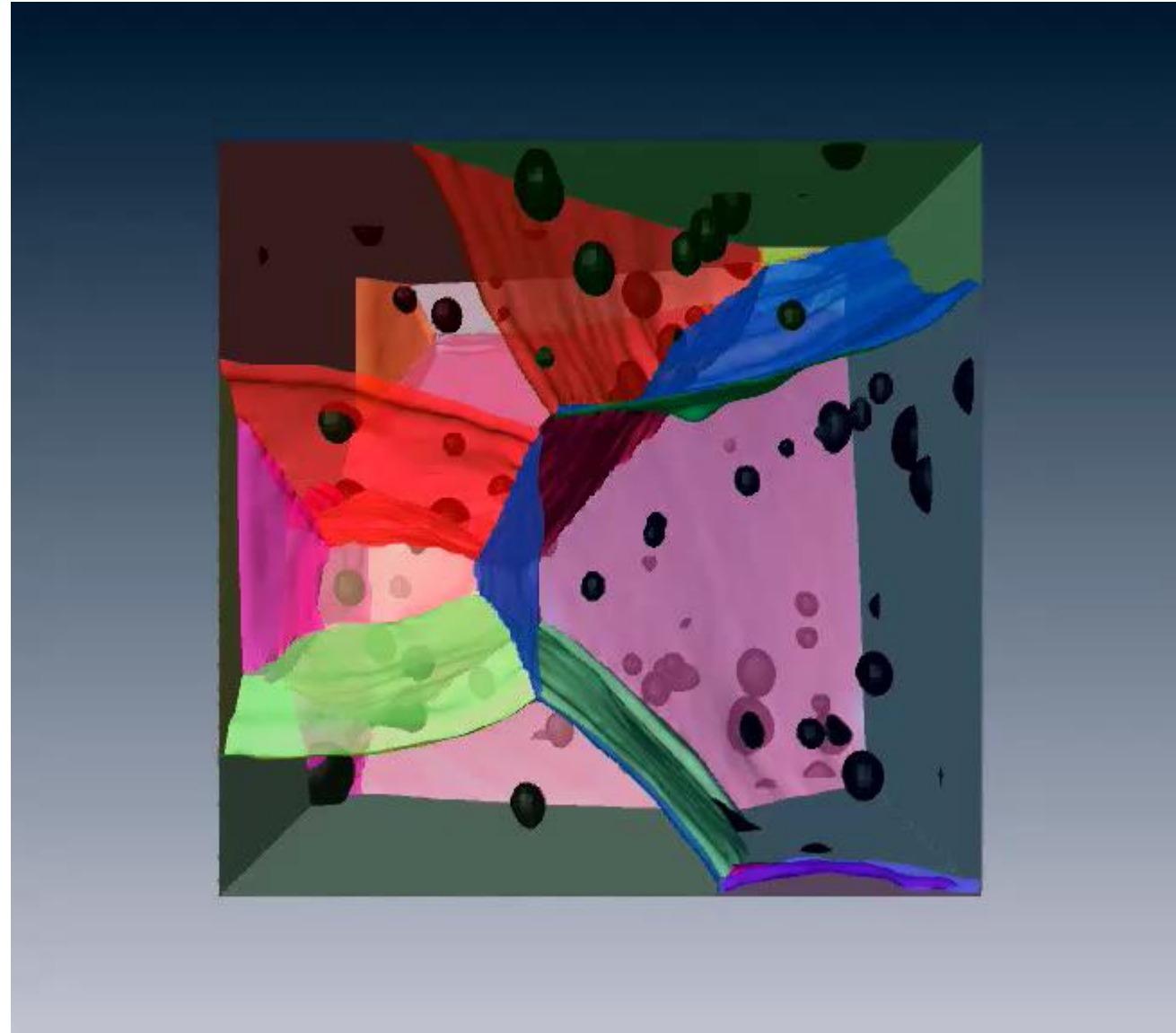
International interdisciplinary PhD Studies in Materials Science with English as the language of instruction

Project co-financed by the European Union within the European Social Funds



Serial Sectioning – Slices





Project WND-POWR.03.02.00-00-1043/16

International interdisciplinary PhD Studies in Materials Science with English as the language of instruction

Project co-financed by the European Union within the European Social Funds



6. Conclusions

- 1. A scanning electron microscope equipped with an EBSD system enables the quantitative (!) analysis of the microstructure of crystalline materials, not only metals and alloys but also non-conductive samples.**
- 2. Phase analysis of individual grains is possible.**
- 3. Deformation processes can be successfully studied.**
- 4. With a field emission scanning microscope (FEGSEM), it is possible to carry out quantitative analyses of grains/subgrains as small as ~100 nm, depending on the type of material.**



- 5. Maps of crystal orientation can be collected using EBSD. They remove any ambiguity regarding the recognition of grains and grain boundaries in the sample.**
- 6. The grains in polycrystalline material are usually not randomly oriented and crystallographic texturing can confer special properties on materials. Thus, EBSD is as an important technique for texture analysis allowing the relation between texture and microstructure to be studied.**
- 7. Boundaries formed between grains with particular orientation relationships to one another can have desirable properties. EBSD can characterize these boundaries and measure the distribution of various boundary types in a sample.**